

University of Windsor

## Scholarship at UWindor

---

Electronic Theses and Dissertations

Theses, Dissertations, and Major Papers

---

7-7-2020

# Design and Development of a Soft Robotic Gripper for Fabric Material Handling

Bowen Wang  
*University of Windsor*

Follow this and additional works at: <https://scholar.uwindsor.ca/etd>

---

### Recommended Citation

Wang, Bowen, "Design and Development of a Soft Robotic Gripper for Fabric Material Handling" (2020).  
*Electronic Theses and Dissertations*. 8406.  
<https://scholar.uwindsor.ca/etd/8406>

This online database contains the full-text of PhD dissertations and Masters' theses of University of Windsor students from 1954 forward. These documents are made available for personal study and research purposes only, in accordance with the Canadian Copyright Act and the Creative Commons license—CC BY-NC-ND (Attribution, Non-Commercial, No Derivative Works). Under this license, works must always be attributed to the copyright holder (original author), cannot be used for any commercial purposes, and may not be altered. Any other use would require the permission of the copyright holder. Students may inquire about withdrawing their dissertation and/or thesis from this database. For additional inquiries, please contact the repository administrator via email ([scholarship@uwindsor.ca](mailto:scholarship@uwindsor.ca)) or by telephone at 519-253-3000ext. 3208.

# **Design and Development of a Soft Robotic Gripper for Fabric Material Handling**

By

**Bowen Wang**

A Thesis

Submitted to the Faculty of Graduate Studies  
through the Department of Mechanical, Automotive & Materials Engineering  
in Partial Fulfillment of the Requirements for  
the Degree of Master of Applied Science  
at the University of Windsor

Windsor, Ontario, Canada

2020

© 2020 Bowen Wang

# **Design and Development of a Soft Robotic Gripper for Fabric Material Handling**

by

**Bowen Wang**

APPROVED BY:

---

A. Azab

Department of Mechanical, Automotive & Materials Engineering

---

B. P. Minaker

Department of Mechanical, Automotive & Materials Engineering

---

R. J. Urbanic, Advisor

Department of Mechanical, Automotive & Materials Engineering

May 20, 2020

## DECLARATION OF CO-AUTHORSHIP AND PREVIOUS PUBLICATION

### I. Co-Authorship

I hereby declare that this thesis incorporates material that is the result of joint research, as follows:

Chapter 1-4 of this thesis contain information co-authored by Morteza Alebooyeh and Dr. Jill Urbanic. Section 4.1 contain expansions of previous research co-authored by Morteza Alebooyeh, Dr. Jill Urbanic, Dr. Ana Djuric, and Hamed Kalami. Section 4.2 contain expansions of previous research co-authored by Morteza Alebooyeh and Dr. Jill Urbanic. The research is performed under the supervision of Dr. Jill Urbanic. In all cases, application and adaptation of previous research contents to this thesis is done by the author, under the supervision of Dr. Jill Urbanic.

I am aware of the University of Windsor Senate Policy on Authorship and I certify that I have properly acknowledged the contribution of other researchers to my thesis, and have obtained written permission from each of the co-author(s) to include the above material(s) in my thesis.

I certify that, with the above qualification, this thesis, and the research to which it refers, is the product of my own work.

### II. Previous Publication

This thesis includes 2 original papers that have been previously published/submitted for publication in peer reviewed journals, as follows:

Chapter	Publication title/full citation	Publication status
Chapter 4.1	Alebooyeh, M., Wang, B., Urbanic, R. J., Djuric, A., & Kalami, H. (2019). <i>Investigating Collaborative Robot Gripper Configurations for Simple Fabric Pick and Place Tasks</i> (No. 2019-01-0699). SAE Technical Paper.	Published
Chapter 4.2	Alebooyeh, M., Wang, B., & Urbanic, R. J. (2020). <i>Performance Study of an Innovative Collaborative Robot Gripper Design on Different Fabric Pick and Place Scenarios</i> (No. 2020-01-1304). SAE Technical Paper.	In Press

I certify that I have obtained a written permission from the copyright owner(s) to include the above published material(s) in my thesis. I certify that the above material describes work completed during my registration as a graduate student at the University of Windsor.

I declare that, to the best of my knowledge, my thesis does not infringe upon anyone's copyright nor violate any proprietary rights and that any ideas, techniques, quotations, or any other material from the work of other people included in my thesis, published or otherwise, are fully acknowledged in accordance with the standard referencing practices. Furthermore, to the extent that I have included copyrighted material that surpasses the bounds of fair dealing within the meaning of the Canada Copyright Act, I certify that I have obtained a written permission from the copyright owner(s) to include such material(s) in my thesis.

I declare that this is a true copy of my thesis, including any final revisions, as approved by my thesis committee and the Graduate Studies office, and that this thesis has not been submitted for a higher degree to any other University or Institution.

## ABSTRACT

Fabric and textile materials are widely used in many industrial applications, especially in automotive, aviation and consumer goods. Currently, there is no semi-automatic or automatic solution for rapid, effective, and reconfigurable pick and place activities for limp, air permeable flexible components in industry. The production of these light-weight flexible textile or composite fiber products highly rely on manual operations, which lead to high production costs, workplace safety issues, and process bottlenecks. As a bio-inspired novel technology, soft robotic grippers provide new opportunities for the automation of fabric handling tasks. In this research, the characteristics of fabric pick and place tasks using the clamping grippers are quantitatively investigated. Experiments on a carbon fiber fabric are performed with a collaborative robot to explore the damage, slippage, draping, and wrinkling during basic pick and place operations. Based on the experimental results, multiple soft robotic gripper configurations are developed, including a compliant glove set that can improve the performance of traditional rigid grippers, an elastomer-based soft gripper, and a linkage-based underactuated gripper. The gripper designs are analyzed and refined based on finite element simulation. Prototypes of the grippers are fabricated using a rapid tooling solution for an overmolding strategy to verify their functionality. Through the research, it is proven feasible to reliably perform flexible fabric handling operations using soft grippers with appropriate toolpath planning. Finite element simulation and additive manufacturing have shown to be useful tools during the gripper design and development procedure, and the methodologies developed and applied in this work should be expanded for more flexible material handling challenges.

## ACKNOWLEDGEMENTS

I would like to express my gratitude to those who provided help and support to this research. Sincere appreciation to my supervisor Dr. Jill Urbanic. Her advice and knowledge have guided me through the whole period of M.A.Sc studying. Sincere appreciation to my committee members Dr. Bruce Minaker and Dr. Ahmed Azab, who have provided important insights and suggestions to this research. I would also thank my classmates and colleagues who have offered help and assistance during this research, especially Morteza Alebooyeh, Hamed Kalami, and Dora Strelkova. Thank you for spending your own time on helping me with the project. Special thanks to Dr. Mehrdad Saif for providing the access to the YUMI robot. Appreciation to Dr. Eunsik Kim for providing gauge tools. Appreciation to Mr. Kevin Taylor from Kelcom for the technical support on prototyping. Finally, I would like to express my deepest gratitude to my parents for supporting and encouraging me all the time.

## TABLE OF CONTENTS

DECLARATION OF CO-AUTHORSHIP AND PREVIOUS PUBLICATION .....	iii
ABSTRACT .....	v
ACKNOWLEDGEMENTS .....	vi
LIST OF FIGURES .....	ix
LIST OF TABLES .....	xii
LIST OF ABBREVIATIONS .....	xiii
CHAPTER 1 INTRODUCTION .....	1
1.1 Fabric Materials in Industrial Applications.....	1
1.2 Problem Statement .....	3
1.3 Research Objectives.....	4
1.4 Thesis Outline .....	5
CHAPTER 2 LITERATURE REVIEW .....	7
2.1 Characteristics of Fabric Materials .....	7
2.2 Contemporary Fabric Material Handling Solutions.....	13
2.3 Soft Robotic Grippers .....	17
2.4 State of the Art .....	24
CHAPTER 3 METHODOLOGY .....	26
3.1 Classification of Fabric Materials .....	26
3.2 Pick and Place Tasks Based on Collaborative Robots .....	29
3.3 Gripper Design.....	32
3.4 Prototyping.....	35
3.5 Simulation .....	39
3.5.1 Simulation of the Underactuated Mechanism.....	39
3.5.2 Simulation of Fabric Materials .....	47
CHAPTER 4 INVESTIGATION OF PICK AND PLACE TASKS WITH CLAMPING GRIPPERS.....	50
4.1 Simple Pick and Place Tasks with One Gripper .....	51
4.1.1 Experimental Setup.....	52
4.1.2 Results and Discussion .....	59



4.2 Pick and Place Tasks Using Multiple Grippers.....	62
4.2.1 Measurement of Displacement and Wrinkling .....	63
4.2.2 Experimental Setup.....	65
4.2.3 Results and Discussion .....	69
CHAPTER 5 DEVELOPMENT OF AN UNDERACTUATED GRIPPER.....	74
5.1 An Elastomer-Based Gripper .....	74
5.1.1 Development of the Gripper Configuration.....	75
5.1.2 Gripping Simulation.....	89
5.1.3 Prototyping and Experiments.....	91
5.2 A Linkage-Based Gripper .....	97
5.2.1 Gripper Configuration and Simulation .....	97
5.2.2 Prototyping and Experiments.....	104
CHAPTER 6 CONCLUSIONS AND FUTURE WORK .....	108
6.1 Conclusions.....	108
6.2 Limitations and Future Work .....	110
REFERENCES .....	112
APPENDICES .....	121
Appendix A: Engineering Drawing of the YUMI Robot Arm.....	121
Appendix B: Experimental Data for Pick and Place Tests.....	122
VITA AUCTORIS.....	126

## LIST OF FIGURES

Figure 1.1 Supply chain of fabric materials in the automotive industry.....	1
Figure 1.2 Stages of composites manufacturing .....	2
Figure 2.1 Fabric structures .....	8
Figure 2.2 Different common weave styles .....	8
Figure 2.3 Different common knitted styles .....	9
Figure 2.4 Fiber mats with complex geometrical shapes.....	9
Figure 2.5 Master models and laminated molds .....	10
Figure 2.6 Friction Test.....	11
Figure 2.7 Peirce’s cantilever method.....	12
Figure 2.8 Mechanically actuated soft grippers.....	21
Figure 2.9 Pneumatic or hydraulic actuation .....	22
Figure 2.10 Gripping by changing stiffness.....	23
Figure 3.1 OPITZ classification code .....	27
Figure 3.2 YUMI dual arm collaborative robot .....	30
Figure 3.3 YUMI DH configurations and DH parameters.....	31
Figure 3.4 Manual picking.....	33
Figure 3.5 Cable actuated gripper configuration .....	34
Figure 3.6 Postures of a conceptual gripper configuration .....	35
Figure 3.7 Overmolding illustration .....	38
Figure 3.8 Dumbbell-shape sample .....	44
Figure 3.9 Fitting result.....	45
Figure 3.10 Modified fitting result.....	45
Figure 3.11 FE model of the sample .....	46
Figure 3.12 Comparison between FEA result and the test data .....	47
Figure 3.13 Microscopic modelling of fabrics.....	47
Figure 3.14 Draping result of the simplified fabric model .....	49
Figure 4.1 Picking locations on a square ply .....	50
Figure 4.2 Picking locations on a rectangular ply.....	51
Figure 4.3 Gripping position and home position .....	54
Figure 4.4 Moving sequence for the one arm testing.....	54

Figure 4.5 Damaged fabric .....	55
Figure 4.6 CAD design of the soft glove .....	55
Figure 4.7 Mold set.....	56
Figure 4.8 Silicone glove.....	56
Figure 4.9 CAD model of the second-generation Silicone gloves.....	57
Figure 4.10 Second generation Silicone gloves.....	57
Figure 4.11 Friction test.....	58
Figure 4.12 Sequence of the experiment.....	59
Figure 4.13 Gripper equipped with the silicone gloves .....	60
Figure 4.14 Slippage results.....	60
Figure 4.15 Wrinkling results .....	61
Figure 4.16 Displacement Measurement .....	64
Figure 4.17 Winkling measurement.....	65
Figure 4.18 Experiment setup .....	66
Figure 4.19 Draping along the midline.....	67
Figure 4.20 Pre-folded picking strategy.....	67
Figure 4.21 Toolpath of the auto-jamming strategy.....	68
Figure 4.22 Side picking test .....	69
Figure 4.23 Wrinkling results .....	69
Figure 4.24 Displacement results.....	70
Figure 4.25 Comparison of different picking strategies .....	71
Figure 4.26 Fabric after placing by different strategies.....	72
Figure 5.1 Conceptual design of an elastomer finger .....	75
Figure 5.2 Bending magnitude and gap size.....	76
Figure 5.3 FE model of a unit section.....	77
Figure 5.4 Sample results.....	78
Figure 5.5 Maximal bending magnitude of different thickness.....	79
Figure 5.6 Maximal driving force for different thickness.....	79
Figure 5.7 FE model of the elastomer finger .....	80
Figure 5.8 Deformation results of different configurations .....	82
Figure 5.9 Displacement-force results of different configurations.....	82
Figure 5.10 FE model for gripping simulation .....	83
Figure 5.11 Different gripping conditions .....	84

Figure 5.12 Inclined fingertip .....	85
Figure 5.13 Gripping force of different fingertip angles .....	85
Figure 5.14 CAD model of the gripper .....	86
Figure 5.15 Fingertip reference point .....	87
Figure 5.16 String tip displacement .....	87
Figure 5.17 Fingertip displacement in vertical direction .....	88
Figure 5.18 Fingertip trajectory .....	88
Figure 5.19 FE model for gripping simulation .....	89
Figure 5.20 Gripping simulation .....	90
Figure 5.21 Gripping simulation on a curved surface .....	91
Figure 5.22 Mold set .....	91
Figure 5.23 Gripper prototype .....	92
Figure 5.24 Geometry measurement .....	93
Figure 5.25 Manual tests .....	95
Figure 5.26 Comparison between experimental data and simulation data .....	95
Figure 5.27 CAD design of the driving mechanism .....	96
Figure 5.28 Gripper prototype with driving mechanism .....	97
Figure 5.29 CAD model of the linkage-based finger .....	98
Figure 5.30 FE model of the linkage-based finger .....	99
Figure 5.31 Deformation result .....	100
Figure 5.32 String tip displacement .....	101
Figure 5.33 Fingertip displacement .....	101
Figure 5.34 Fingertip trajectory .....	102
Figure 5.35 Gripping simulation .....	103
Figure 5.36 Structure to limit the rotary motion on certain direction .....	103
Figure 5.37 Mold set .....	104
Figure 5.38 Gripper prototype .....	105
Figure 5.39 Comparison between experimental data and simulation data .....	106
Figure A.1 Engineering drawing of the YUMI robot arm .....	121

## LIST OF TABLES

Table 1.1 Evidence for causal relationship between risk factors and musculoskeletal disorders.....	3
Table 2.1 Different fiber materials specifications.....	7
Table 2.2 Classification of conventional fabric handling methods.....	14
Table 2.3 Characteristics of conventional fabric handling methods.....	16
Table 2.4 Soft robotic grippers and their characteristics (part 1).....	19
Table 2.5 Soft robotic grippers and their characteristics (part 2).....	20
Table 2.6 Characteristics of typical actuation strategies.....	23
Table 2.7 Relevant literature .....	24
Table 3.1 Fabric structure .....	28
Table 3.2 Material properties .....	28
Table 3.3 Geometric and mold properties.....	29
Table 3.4 Characteristics of YUMI dual arm collaborative robot.....	31
Table 3.5 Technical data of Mold Star 15 SLOW .....	38
Table 5.1 Fabrication time .....	93
Table 5.2 Geometrical data .....	94
Table 5.3 Fabrication time .....	105
Table 5.4 Geometrical data .....	106
Table B.1 Data for plain picking.....	122
Table B.2 Data for pre folded picking .....	123
Table B.3 Data for auto-jammed picking.....	124
Table B.4 Data for pick and place operations with spatial transferring.....	125

## LIST OF ABBREVIATIONS

FE	Finite Element
FEA	Finite Element Analysis
CAD	Computer-Aided Design
AM	Additive Manufacturing
SDM	Shape Deposition Manufacturing
FDM	Fused Deposition Modeling
STL	Stereolithography
PC	Polycarbonates
ABS	Acrylonitrile Butadiene Styrene
DOF	Degree of Freedom
TCP	Tool Center Point
SSE	Sum of Squared Errors
RMSE	Root Mean Squared Error
CC	Correlation Coefficient

# CHAPTER 1

## INTRODUCTION

### *1.1 Fabric Materials in Industrial Applications*

Fabric and textile materials are widely used in many industrial applications, especially in automotive, aviation and consumer goods. The automotive industry, which represents the most significant global market for technical textiles, has a large demand for advanced fabric structures with better performance properties and improved design. The applications of technical textiles and fiber composite components in the automotive industry cover a wide range, including upholstery and seating, floor and door covering, trunk liners, pre-assembled interior components, safety devices, filters and engine compartment items, etc. [1,2] Figure 1.1 demonstrates the typical supply chain of fabric materials in the automotive industry.

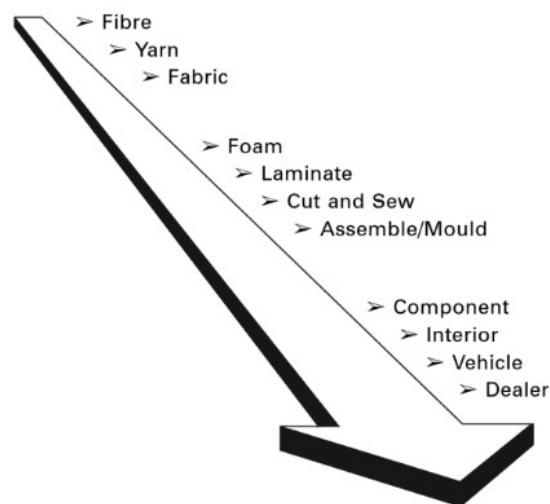


Figure 1.1 Supply chain of fabric materials in the automotive industry (taken from [1])

Introducing light-weighting material solutions to reduce vehicle mass is driving innovative materials research activities as polymer composites offer high specific stiffness, strength, and other advantages compared to contemporary engineering materials. Due to the light-weighting potentials, a higher consumption of carbon fiber will be used

within the next 20 years [3]. The aeronautical industry also requires a weight reduction of 30% and a cost reduction of 40% compared to the metallic light-weight structures [4]. The optimization and automation of novel composite components manufacturing are essential to these requirements.

There is a wide variety of technologies applied for fiber-reinforcement composites manufacturing, such as filament winding, pultrusion, hand lay-up, wet lay-up etc. The manufacturing processes start with semi-finished fiber or fabric materials. These materials are transferred to the mold, preformed, and processed into the final products. Though accomplished in different ways, all composites manufacturing processes involve four basic steps: impregnation, lay-up, consolidation, and solidification [5,6]. During impregnation, fibers and resins are mixed together to form a lamina in order to make sure that the resin flows entirely around all fibers. In the lay-up step, composite laminates are formed by placing prepregs at desired locations and angles, where the desired composite thickness and shapes are achieved by the number of layers and the structure of molds. Then, the consolidation step creates intimate contact between each layer to ensure the removal of entrapped air between layers. The final step is solidification, which may take less than a minute or up to two hours depending on the curing method. Figure 1.2 shows the main stages of composites manufacturing.

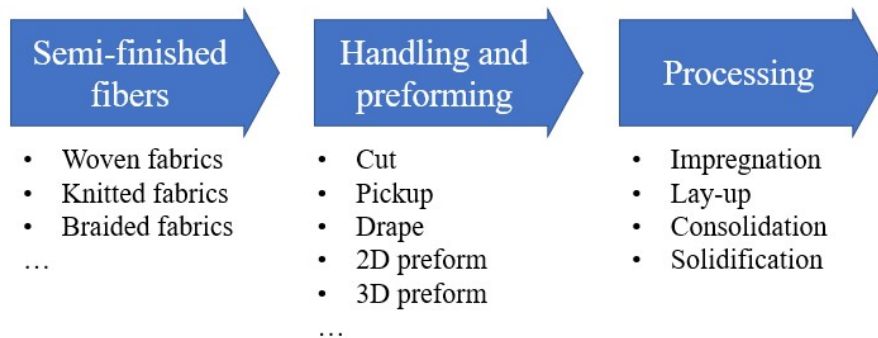


Figure 1.2 Stages of composites manufacturing

The potential of significant mass reduction strategies that can be presented using composite fiber solutions are offset by the high labor intensity and long manufacturing cycle times. Improvements to the resin transfer molding (and similar injection / compression processes) can reduce molding cycle times. However, at this time, there is



no semi-automatic or automatic solution for rapid, effective, and reconfigurable pick and place activities for limp, air permeable flexible components in the automotive domain (i.e., textile mats used for the seat manufacturing foam injection process) that can be transferred into the composite fiber manufacturing domain. Traditional principles applied for fabric material handling include needle, clamping, vacuum, adhesion, etc. Though efficient under some circumstances, all these methods have their own limitations [7].

## 1.2 Problem Statement

Presently, most of the pick and place operations for flexible components such as fiber mats are still done manually in the industry, which influences the throughput and production costs. Due to the basic characteristics of manual tasks, this also leads to workplace safety issues, as well as introducing variable process bottlenecks. Lower back disorders are related to manual material handling tasks and lifting tasks [22], as shown in Table 1.1, where the most problematic activities are highlighted. These repetitive tasks are highly probable to lead to work related issues and diseases in the long term. From an investigation done by the Association of Workers' Compensation Boards of Canada, 241,508 lost time claims were made in Canada [8]. It is clear that new solutions are required to reduce work related injuries and improve production efficiency.

Table 1.1 Evidence for causal relationship between risk factors and musculoskeletal disorders

<b>Risk Factor</b>	<b>Strong Evidence</b>	<b>Fair Evidence</b>	<b>Insufficient Evidence</b>	<b>Evidence of No Effect</b>
Lifting movement	●			
Awkward posture		◐		
Heavy physical work		◐		
Whole body vibration	●			
Static work posture			○	

The automation of material handling of flexible textile/fiber components is a process bottleneck. Robotic/automated solutions for textile/composite fiber material handling has

significant growth potential, which will be an essential component for ongoing light weighting developments, and leadership in the specialty automation fields.

Typically, it is difficult to utilize serial six-axis industrial robots with hard grippers for handling textiles without damaging the strands or introducing folds and tears. The compliance of soft robots introduces a new dimension for gripper designs for fabric material handling, where the biggest issues and challenges are related to firm picking, stable and fast transferring, precise placement and de-wrinkling, their sensitivity to process noise, and the durability of the solution.

There is also a lack of systematic studies with respect to the behavior of fabric materials during picking, transferring, and placing operations, especially quantitative studies. This lack of data in both the experimental and simulation domains makes it more difficult to carry out practical applications in industry. Therefore, academic studies expanding the knowledge base related to the fabric material behaviors during pick and place tasks would be a key breakthrough for the current technological bottleneck.

The vision of this research is to explore the possibility of developing a sophisticated solution for fabric material handling, applying a soft robotics-based technology. Although the project scope is limited, the outcomes of this project will establish a solid foundation for new automation opportunities to several manufacturing sectors. It would help employers understand the manual workloads as well as introduce new automation solutions that will benefit both robotics research and practical applications.

### ***1.3 Research Objectives***

The goal of this research was to determine ideal mechanical structures and to design a soft robotic gripper prototype that is capable of fast and effective pick and place activities. This solution should readily support quick reconfigurations. The outcome includes the theoretical concepts, CAD designs, simulation, prototyping, and testing of the soft robotic gripping solution.

The design criteria of the gripper include:

- Grasping only one ply at a time
- No slippage while in motion
- Fast transfer motions
- Minimization of wrinkling and distortion after dropping
- Avoidance of any damage to the fabric
- Compatible with different scenarios
- Cost effective

The specific research objectives include:

- Obtaining the characteristics of the fabric material during selected pick and place tasks
- Developing a general method for evaluating the performance of fabric handling
- Developing a soft gripper that meets the criteria mentioned above

#### ***1.4 Thesis Outline***

Chapter 2 presents a literature review regarding the characteristics of fabric materials, the typical fabric handling solutions that are contemporarily applied, and some necessary knowledge about soft robotic grippers.

Chapter 3 covers the methodology applied in this research. A classification system of fabric materials is proposed as a foundation for relevant research. The collaborative robot is introduced. Some important designing and prototyping tools are described. Two material models that are critical for the simulation are developed.

Chapter 4 presents the investigation of pick and place tasks with clamping grippers. A perpendicular test is performed to study the slippage and wrinkling during pick and place operations. A comprehensive experiment is performed to study the placement accuracy and wrinkling avoidance. A simple gripper design is developed in this chapter.

Chapter 5 presents the design and development of two soft robotic grippers. The first one

is an elastomer-based gripper. The second one is a linkage-based gripper. The gripper designs are evaluated through both simulation and prototyping.

Chapter 6 is the conclusion of this thesis, including the limitations and future work.

## CHAPTER 2

### LITERATURE REVIEW

#### *2.1 Characteristics of Fabric Materials*

Fabrics or textiles are flexible materials constructed by a network of yarns, which are produced by interlocking raw fiber materials. When considering mechanical properties and structures, fibers and yarns are usually treated as one-dimensional in form, while fabrics are considered two-dimensional. In the industry, fabrics are frequently made into garments, which are considered three dimensional in form. [9]

There is a wide variety of fiber materials, including glass fibers, carbon fibers, aramid fibers, polyethylene fibers, ceramic fibers, basalt fibers, metal fibers, natural fibers, etc. The mechanical characteristics of some common fibers are summarized in Table 2.1 [10].

Table 2.1 Different fiber materials specifications

	<b>Density (g/cm<sup>3</sup>)</b>	<b>Young's Modulus (GPa)</b>	<b>Tensile Strength (MPa)</b>	<b>Elongation at Break (%)</b>
<b>Glass Fibers</b>	2.45-2.90	56-115	2000-4900	1.5-5.4
<b>Carbon Fibers</b>	1.73-2.15	200-900	1750-7000	0.35-2.40
<b>Aramid Fibers</b>	1.39-1.47	58-18	2760-3620	1.9-4.4
<b>Polyethylene Fibers</b>	0.90-1.41	0.5-170	455-3100	2.7-22
<b>Ceramic Fibers</b>	2.35-4.1	150-420	1500-3600	0.4-1.1
<b>Basalt Fibers</b>	2.75	89	2000-4840	3.15
<b>Metal Fibers</b>	2.8-7.9	72-210	200-2500	1.0-2.0
<b>Natural Fibers</b>	1.3-1.5	9.4-100	568-1100	2.0-3.0

Most fabric materials can be regarded as flat sheets that are flexible and deformable. There are various types of fabric structures. In other words, fabrics can be built up from

textile fibers in many ways. Most fabrics are made from yarns and there are four main types of structures: woven fabrics, knitted fabrics, braided fabrics, and lace and net fabrics, as demonstrated in Figure 2.1.

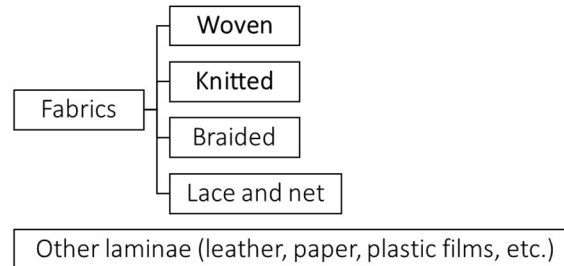


Figure 2.1 Fabric structures

Woven and knitted are the two most common structures, each contains several subclasses [11]. Figure 2.2 shows some commonly found weaving styles. Figure 2.3 shows some commonly found knitting styles. Different types of fabric structures have different properties in terms of stability, drape, porosity, smoothness, balance, symmetry, and crimp. For example, the Leno weave is more stable than that of the Satin weave, while the draping characteristic, porosity and smoothness of the Leno weave is poor in comparison to the Satin weave. There are also laminae not made of interlaced yarns but show similar properties as fabrics, such as leather, paper, plastic films, rubber sheets, etc. These sheets may also be included in the research of fabric handling.

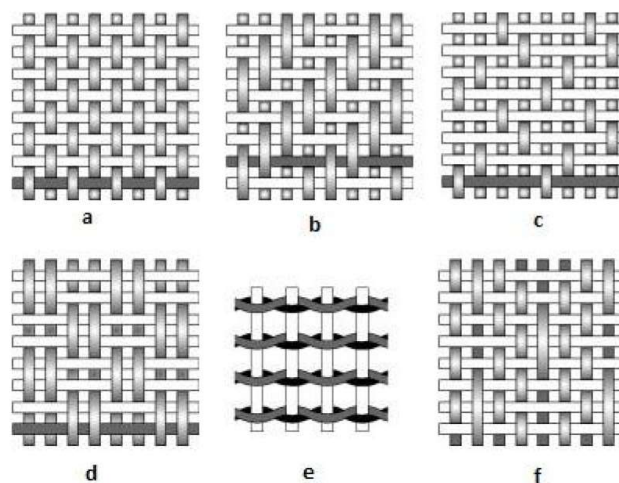


Figure 2.2 Different common weave styles (taken from [10])

a. Plain   b. Twill   c. Satin   d. Basket   e. Leno   f. Mock leno

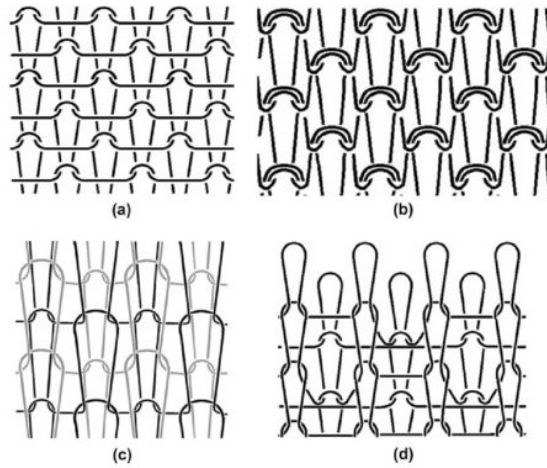


Figure 2.3 Different common knitted styles (taken from [12])

a. Plain   b. Lacoste   c. Interlock   d. Double pique

In industry, the shapes of the fabrics can be very complex, with internal slits and cut-outs as shown in Figure 2.4. Many processes require to attach these geometrically complex fabric mats onto three-dimensional mold surfaces, which makes the pick and place tasks more complicated. Figure 2.5 shows a tool shop consisting of master models and laminated molds, which are relatively complex and require manual operations.



Figure 2.4 Fiber mats with complex geometrical shapes



Figure 2.5 Master models and laminated molds (taken from [5])

There are various categories of properties that can be used to describe the performance of fabric materials. For bulk properties, there are uniaxial tension and compression, biaxial tension, compression and shear, bending behavior, torsional response, behavior under a stress concentration, dimensional stability and fatigue resistance, etc. For surface properties, there are contact behavior, roughness, attrition resistance, friction and resistance to stress concentrations, etc. For transfer properties, there are air permeability, water permeability, filtration efficiency, penetration resistance and heat transfer, etc. While performing pick and place tasks using robotic grippers, the most important properties include fabric structure, roughness, area weight, and stiffness. Aside from material properties, geometric properties of the fabric pieces such as size, thickness, shape are also important variables.

Much research has been done on obtaining the surface roughness of fabric materials, such as the Kawabata Evaluation System (KES-F), the Ring Method, the Optical Method, etc. [13,14]. In order to make quantitative comparisons, the KES-F appear to be the most qualified since it can give an accurate coefficient of friction. In the standard test, the



sample is pulled tight by applying a tension load of 20 gf/cm and a detector of 10 parallel piano wires is pressed against the fabric with a force of 50 gf (1 piano wire with 10 gf when measuring roughness). The output includes the coefficient of friction, geometric roughness, and the standard deviation of the friction coefficient [15]. There is also a simplified method to gain the coefficient of friction for the fabrics. The fabric is attached on an inclined plane with an object placed on it, where  $\theta$  is the angle of repose at which an object just starts to slide down the inclined plane. Therefore, the coefficient can simply be calculated by

$$F_f = \mu N \quad (2-1)$$

where

$F_f$  – frictional force (N),

$\mu$  – frictional coefficient,

$N$  – normal force between surfaces (N).

For an object pulled or pushed horizontally, the force is simply the gravity force or weight. Therefore,

$$F_f = \mu mg \quad (2-2)$$

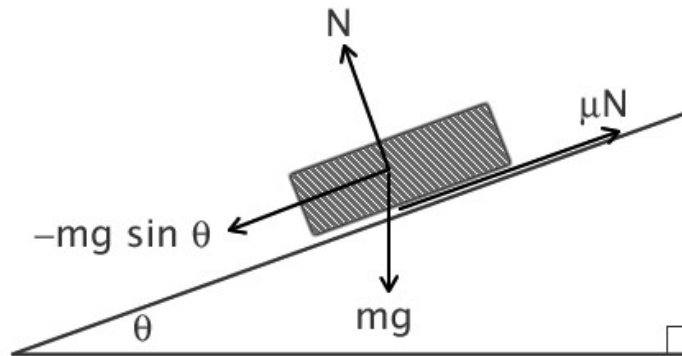


Figure 2.6 Friction Test

This method is frequently adopted by the industry [16].

The stiffness of fabrics is another important property for handling tasks. It indicates the capability of fabrics to resist bending without support. A traditional measure of fabric stiffness is the bending length, which can be measured by Peirce's cantilever method [17]. In this method, the fabric is made to deform on its own weight as a cantilever. A strip of fabric of specific size is placed on a platform and moved forward until the centerline from the edge of the platform to the leading edge of fabric makes an angle  $\theta$  to the horizontal, as shown in Figure 2.7. Then, the bending length  $c$  can be calculated by the cantilever length  $l$  and the angle  $\theta$  as

$$c = l \left( \frac{\cos(\theta/2)}{8 \tan \theta} \right)^{1/3} \quad (2-3)$$

The angle  $\theta$  is traditionally set to  $41.5^\circ$  for the ease of calculation.

Also, the bending rigidity  $B$  can be calculated by the bending length  $c$  and the fabric mass per unit  $w$  as follows

$$B = wc^3 \quad (2-4)$$

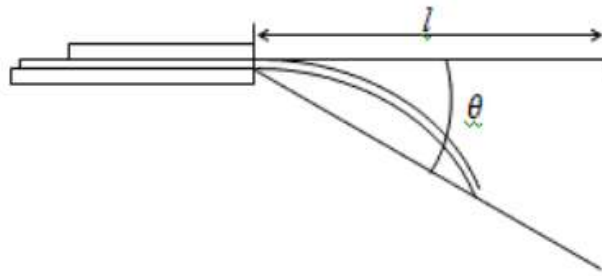


Figure 2.7 Peirce's cantilever method

Another parameter used to express fabric stiffness is the drape coefficient, which is the ratio of the projected area of the fabric sample to its undraped area, in which the area of the supporting disk is deduced. It is usually measured by the Cusick drape test. Much

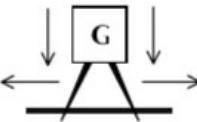
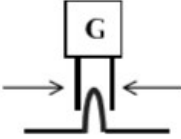
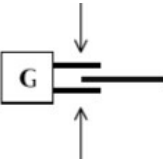
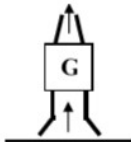


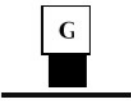
research has been done on applying this coefficient using digital image analysis. [18,19]

## ***2.2 Contemporary Fabric Material Handling Solutions***

There are various approaches for fabric material handling in manufacturing industries, where different methods for gripping, handling, and automation are being applied. Early research focusing on gripping technologies for flexible materials started at the end of last century, and several experimental gripping systems have been developed during the 1990s, many of which applied mechanical principles with elementary control. Since the middle of the 1990s, researchers began to explore new methods for fabric handling, considering various characteristics of the fabric materials. In 1990, P. Taylor et al. [20] investigated automated fabric handling techniques and the problems researchers were facing. In 1995, Taylor [21] concluded some common gripping systems for flexible materials at the time. G. Monkman [96] did a study on robotic grippers for use with fibrous materials, especially carbon fiber composites. By compiling previous research, P. Koustoumpardis and N. Aspragathos [7] derived a classification system based on the gripping principles and handling techniques.

Since handling techniques and the gripping principle are correspondent to each other, traditional principles applied for gripping and handling can be classified together into four main categories: needle, clamping, vacuum, and adhesion. There are also few other methods such as air-flow or electrostatic, which are usually restrained for materials with special properties. Table 2.2 summarizes common methods traditionally applied for fabric handling and relevant references.

Table 2.2 Classification of conventional fabric handling methods

Principle		Sketch	Reference
Needle			[23][24][25][26][28][28]
Clamping	Vertical picking		[29][30][31][32][33][34]
	Side picking		[35][36][32][37][38]
Vacuum			[39][40][26][41][42][43]
Adhesion			[26][23][44][45][43]
Others	Air-flow		[46][47]
	Electrostatic		[48][49][50]

The needle is the most commonly applied method in the industry. The typical design uses two or more tilted needles to penetrate the fabrics, then adds tension to hold the fabrics firmly. Another type of needle gripper, which was originally designed at Durham, places needles around a cylinder that rotates onto the fabrics to be attached [27]. A needle-based gripper can grip most types of fabric stably and move quickly, but it causes inevitable damage to the fabrics when puncturing, hence it cannot be applied for delicate fabrics.

The clamping method uses a pair of rigid jaws to grip the fabrics. Based on the picking style, these grippers can be subclassified as vertical picking (pinching) and side picking.

For vertical picking, the jaws are moved perpendicularly until the tips touch the surface of the fabrics, and then are brought together to pinch the fabrics. This type of gripper is very effective and reliable during picking and handling, but usually introduces folds or wrinkles when placing. The mechanism and controls of the rigid clamping grippers are very simple; hence the application is limited by the lack of adjustable movements.

The side picking method is mainly useful for picking up a fabric panel that is already placed on a plane where the edges of the fabric are approachable. Compared to vertical picking, side picking efficiently prevents the occurrence of folds or wrinkles, but the flexibility is further limited. The commercially available Walton Picker [34] is a very simple clamping gripper specially designed for simple tasks. More recent research on clamping grippers seeks to mimic the movement of human hand. The research team of Ono et al. [30,31] has presented a gripper that combines vertical picking and side picking approaches and operates as a human hand. This gripper has a highly complex mechanism equipped with a touch sensor and a force sensor.

Using a vacuum is also a well-studied method. Vacuum grippers cause minimal harm or distortion to the fabric materials. Kolluru et al. [40] have developed a vacuum gripper that has a flat bottom surface constituting a matrix of holes for suction purposes. A variety of modified configurations have been developed based on it, with intelligent control integrated [41,43]. More recent studies have developed various types of reconfigurable suction systems that are capable of adjusting to different and complex geometry shapes [39]. The biggest limitation for a vacuum gripper is due to the air permeability of fabric materials since a vacuum can only pick up dense materials. Using a vacuum is also expensive, complex, and its gripping force is weak and cannot move fast compared to mechanical grippers.

Adhesion grippers also apply surface attraction to grip and hold fabrics. These grippers are able to pick up most types of materials, as well as consistently acquire a single piece at a time, but they require an extra mechanism to release the material. Usually, adhesion grippers are constituted of a set of movable mechanism such as rollers or stripes covered with the adhesive agent. The most common adhesive is glue, and researchers are also investigating using Cryo Freeze as the adhesive agent [45]. Adhesives remaining on the

fabric may cause an undesired impact, especially during composite manufacturing, so the adhesion grippers are mainly applied in the clothing industry [23].

Table 2.3 summarizes the characteristics of the four main types of conventional fabric handling methods.

Table 2.3 Characteristics of conventional fabric handling methods

Method	Holding Force	Damage Avoidance	Ease of Release	Ply Separation	Stack Picking	Energy Efficiency
Needle	●	○	◐	◐	●	◐
Clamping	●	◐	◐	◐	◐	◐
Vacuum	◐	◐	●	●	◐	○
Adhesion	●	◐	◐	●	◐	◐

New types of grippers have been developed (sensor based Coanda gripper [51]) independently or based on existing grippers modified, e.g., by the integration of sensors to increase the material handling efficiency [52]. There are some cases where a hybrid approach is taken, i.e., combining different picking strategies. T. Le, M Jilich, et al. [38] developed a specialized gripper that can accomplish garment handling with low requirements for avoiding distortion.

Though not common, soft robotic grippers and underactuated hands have been studied in some specific cases. Z. Doulgeri and N. Fahantidis [29] developed a rigid robotic gripper with soft-tipped fingers to pick up fabric material pieces. P. Koustoumpardis, K. Nastos, and N. Aspragathos [53] performed a research on an underactuated robotic gripper that can successfully grasp, transfer, and de-wrinkle for simple fabric materials. K. Murakami and T. Hasegawa [54] have presented a gripper with a human-like fingertip and a quite complex mechanism. Their research also investigated the detection of contact conditions using a hard nail structure attached to the soft skin. A long-standing research project carried out in Japan by E. Ono et al. [30,31] has developed a clamping gripper with complex mechanism that can separate fabric plies. They managed to avoid introducing bending to the fabric by side picking strategies and studied the interaction between fabric plies when the upper layer was picked up.

In addition to a single gripper, researchers have developed gripper frames that combine multiple gripping units to accomplish more complex tasks. S. Costo, et al. [55] have developed a gripper frame with three vacuum end effectors, each can be repositioned with two DOF. S. Ragnathan and L. Karunamoorthy [56] have done a similar design with four end effectors. P. Zimmer [57] has invented a rectangular frame that can stretch the fabric to hold it firmly. Research done by S. Flixeder, T. Glück, and A. Kugi [58] has integrated a de-wrinkling roller on a Coanda-effect gripper frame. M. Tarsha Kordi, M. Hüsing, and B. Corves [59] have developed a more complex configuration with eight movable vacuum end effectors arranged on a flexible frame.

Most contemporary handling solutions can be applied utilizing a 6-axis robot. The biggest advantage of 6-axis robots is that they can be highly automated by proper programming. Also, they can be easily customized, and they occupy relatively a small area while reaching a large workspace. Traditionally, there are some non-robotic solutions, but they are less applied in the modern industry compared to 6-axis robotic solutions. Most of these non-robotic solutions apply gantry systems, which are simple but lack flexibility. Some special purpose machines have also been designed. These devices are often highly efficient but not expandable.

### ***2.3 Soft Robotic Grippers***

Soft robots are bio-inspired machines that are more flexible than traditional rigid-bodied robotic machines, making them available for more complex tasks. Conventional, rigid-bodied robots are commonly applied in manufacturing and are specifically programmed to perform a single task efficiently, but usually with limited adaptability. In comparison, soft robots have bodies made of intrinsically soft and/or extensible materials. These robots have a continuously deformable structure with muscle-like actuation system that emulates biological systems and have a relatively large number of degrees of freedom. Hence, they are able to perform more complex and flexible tasks. Since many soft robots have deformable surfaces and are under-actuated, they are also capable of handling and manipulating fragile or highly deformable objects. [60-63]

Currently, most of the fabric handling operations in industry are performed manually. However, there are only a limited variety of human hand motions are used during these operations, such as rubbing, pinching, and gipping. Since soft robotic grippers are bio-inspired grippers that can mimic human hands movements, they have great potentials to accomplish typical fabric picking tasks by mimicking manual operations. Though not common, there are some cases where grasping and clamping operations performed by soft robotic grippers are applied for fabric handling solutions. Some of the techniques mentioned in the previous section contain features of soft robotics [30-53].

The application of soft robotic grippers in fabric handling tasks has two important advantages. Since soft robotic grippers are mostly underactuated, they can automatically adjust to the geometry of the objects to be picked. Therefore, the complexity of the geometric shapes of fabric materials would not be a challenge during picking. An underactuated gripper has the potential to pick up deformable fabric materials from curved or inclined surfaces and perform certain processing with relatively complex gestures. Secondly, those grippers usually have contact surfaces made from soft and deformable materials such as rubbers or soft plastic, which can provide a firm gripping condition while not damaging the fabric material.

In the research domain, there are many different types of soft robotic grippers being developed, applying different configurations and actuation methods.

Soft robotic technology and underactuated grippers have been widely studied during past decades. L. Birglen, et al. [64] have presented a comprehensive review on underactuated gripper hands in 2008. S. Kim, C. Laschi, and B. Tripmer [62] did a similar review upon bio-inspired soft robotics in 2013. In 2018, J. Shintake, et al [65] have carried out a thorough introduction of soft robotic technology that covered most of the temporary soft robotic grippers. These papers have also discussed the fabrication and control strategies for soft robotic grippers. Table 2.4 and Table 2.5 shows some relevant soft robotic grippers and their characteristics.



Table 2.4 Soft robotic grippers and their characteristics (part 1)

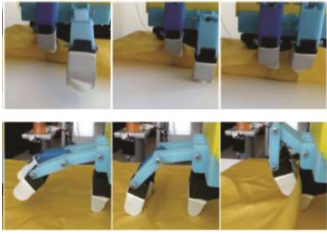
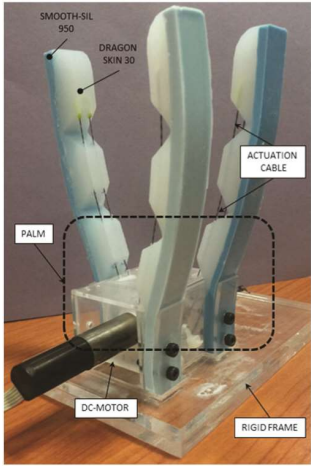

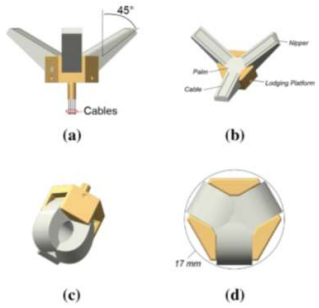
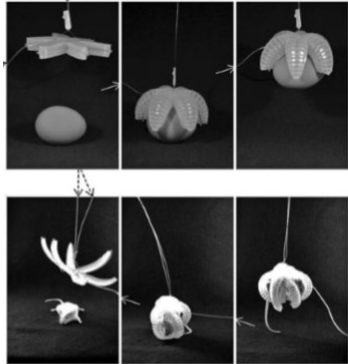
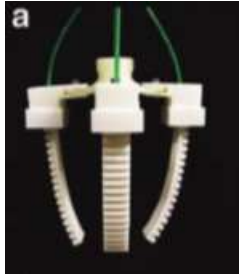
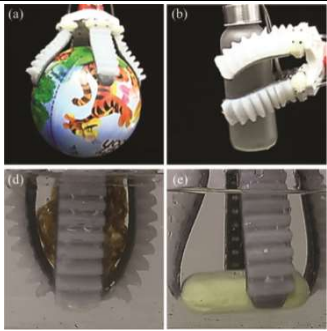
	Features	Comment	Picture
[53]	<ul style="list-style-type: none"> <li>Linkage-based fingers</li> <li>Soft tips</li> <li>Cable actuation</li> </ul>	A gripper for fabric handling inspired by human hands. It is capable of grasping, transferring, and de-wrinkling for simple fabric materials.	
[66]	<ul style="list-style-type: none"> <li>Gapped elastomer fingers</li> <li>Cable actuation</li> </ul>	A simple gripper inspired by the structure of human hands.	
[67]	<ul style="list-style-type: none"> <li>Linkage-based fingers</li> <li>Soft skin</li> <li>Cable and pneumatic actuation</li> </ul>	A gripper inspired by the structure of human hands. Different fingers are actuated separately and hence are capable of complex gestures.	
[68]	<ul style="list-style-type: none"> <li>Elastomer fingers</li> <li>Cable actuation</li> </ul>	The structure is simple. Easy to manufacture and assemble but cannot complete complex movements.	

Table 2.5 Soft robotic grippers and their characteristics (part 2)

	Features	Comment	Picture
[69]	<ul style="list-style-type: none"> <li>Fluidic elastomer actuator</li> <li>Pneumatic</li> </ul>	A gripper based on fluidic elastomer that is adaptive to different shapes and provides good surface contact.	
[70]	<ul style="list-style-type: none"> <li>Fluidic elastomer actuator</li> <li>Pneumatic</li> </ul>	A pneumatic soft robotic gripper that provides high force and large curvature. The maximum payload-to-weight ratio of is 1805%.	
[71]	<ul style="list-style-type: none"> <li>Fluidic elastomer fingers</li> <li>Pneumatic</li> </ul>	A pneumatic soft robotic gripper that is capable of grasping various types of object.	

The most common soft robotic gripper configuration is based on compliant structures being deformed by external or integrated actuators. Objects can hence be gripped through impactive prehension. There are various ways of actuation that have been studied by researchers.

As traditional rigid grippers can be driven by rotary or linear motions, one efficient way to achieve actuation force for soft grippers is to drive passive structures by external motors. Based on the location of the actuation, the working principles can be distinguished as contact-driving deformation and tendon actuation. For contact-driving deformation grippers, the actuator only drives the finger to linearly enclose such as rigid grippers, and

the gripper material adjusts to the target object by passive deformation. The tendon-driven grippers have driving cables embedded inside the gripper structure to transmit the actuation force. These grippers are mostly made by articulate elastomer fingers connected to a rigid palm. The fingers can also be hinge-connected linkages confined by elastomer skin or other elastic components. Figure 2.8 illustrates the working principles of such types of soft grippers.

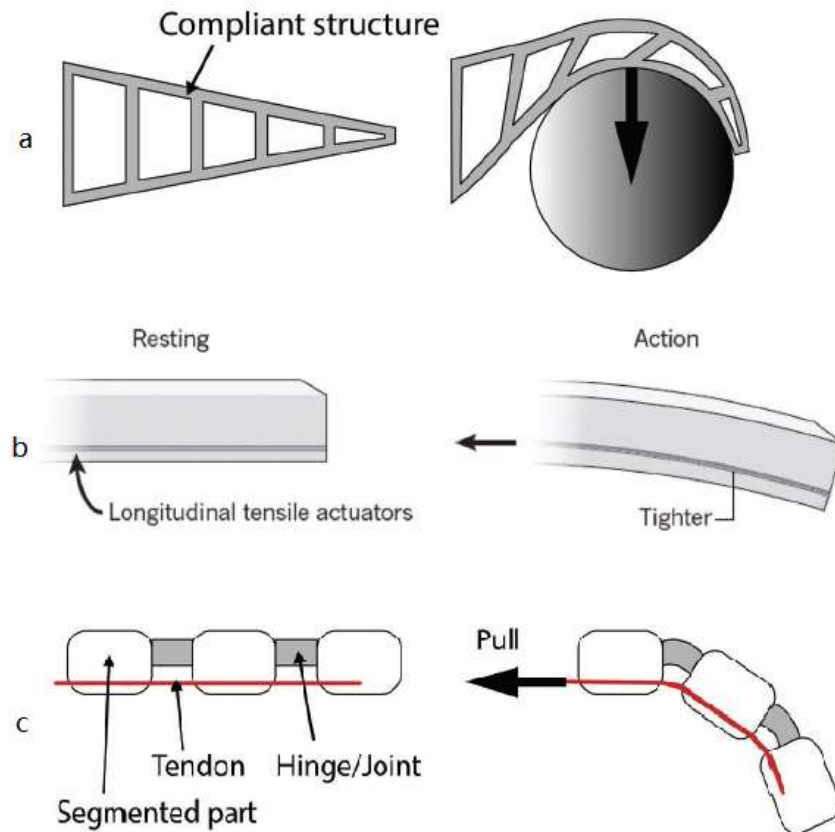


Figure 2.8 Mechanically actuated soft grippers (taken from [65])

a. Compliant structure   b. Cable actuation   c. Linkage-based cable actuation

In Table 2.4, there is a typical tendon-driven gripper molded by silicone rubber [66]. There is also a linkage-based gripper confined by elastic springs and driven by an electromagnetic motor [53]. Due to the simplicity of the mechanical structures and the fast reaction speed, these types of soft grippers are popular in industrial applications. They can be designed for a wide range of purposes.

Another popular design of actuation is to apply pneumatic or hydraulic power. Fluidic elastomer actuators, also known as soft pneumatic actuators, are one of the oldest designs for soft robotics, yet they are still widely applied in both academic studies and industrial applications. The actuation is achieved by feeding gaseous or liquid fluid into a chamber made of highly elastic materials. The inflation of the chamber then bends the gripping structure, which is usually asymmetrical or uses anisotropic materials. Some gripper configurations in table 2.5 are all based on fluidic elastomer actuators [69-71]. These grippers usually have a large bending capacity. The actuation time may vary drastically based on the details of the designs. As a simplified configuration, the pneumatic power can be directly led to a hollowed elastomer finger to create bending or elongation. Figure 2.9 shows the working principles of typical pressure-based soft grippers. It is also possible to combine pneumatic power and cable actuation [67].

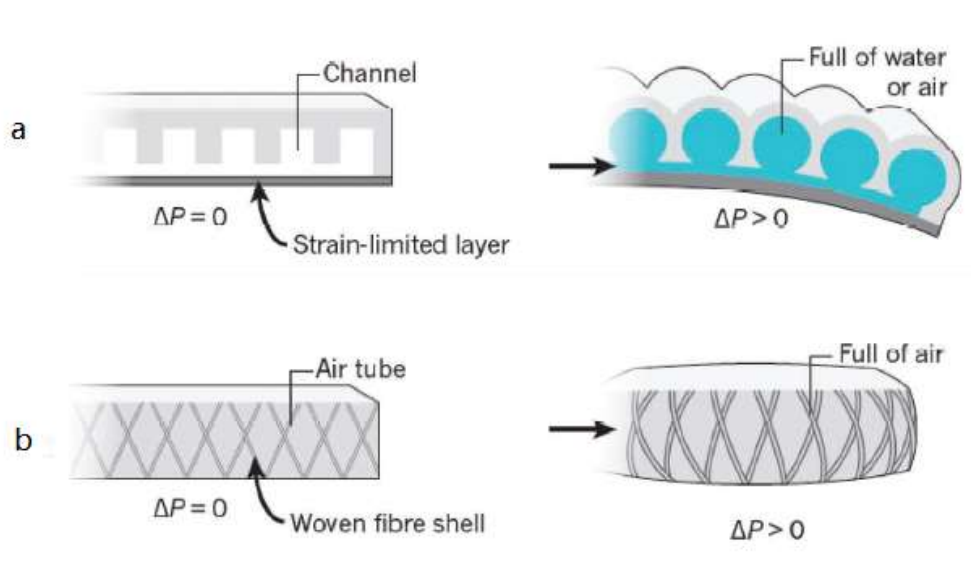


Figure 2.9 Pneumatic or hydraulic actuation (taken from [65])

a. Fluidic elastomer actuation    b. Air tube actuation

Some characteristics of these mentioned configurations are summarized and compared in Table 2.6.

Table 2.6 Characteristics of typical actuation strategies

Style	Complexity	Actuation speed	Gripping force
Compliant structure	☐	●	☐
Tendon actuation	◐	●	◐
Pneumatic actuation	●	◐	●

To actuate passive structures, there are many other novel approaches as well, including dielectric elastomer actuators, ionic polymer-metal composites, shape memory materials, etc. Aside from actuating passive structures, soft and adjustable gripping can also be achieved by varying the stiffness of the gripping structure, as shown in Figure 2.10 [72].

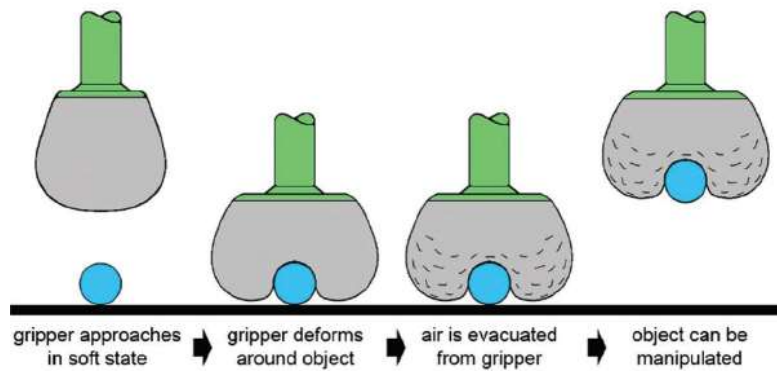


Figure 2.10 Gripping by changing stiffness (taken from [72])

Currently, most of existing soft robotic systems are applying conventional, rigid electronic sensors for automation. These sensing devices include visual sensors, contact sensors, pressure sensors, distance sensors, optimal sensors, etc. The sensors can either be attached to the frame of the robots or be inserted inside the structure of soft gripper. For the latter case, the electronic devices are usual micro and highly sensitive. Their missions are typically related to contact or force sensing, which appear to be essential in fabric handling tasks. Aside from conventional sensors, there are also much research recently being done on flexible and stretchable electronic devices [73-75]. These new technological achievements may enable new sensing and controlling strategies that are more accurate and effective.

## 2.4 State of the Art

As reviewed in previous sections, the literature related to this research is summarized in Table 2.7.

Table 2.7 Relevant literature

	Fabric handling	Clamping strategy	Vacuum strategy	Underactuated configuration	Linkage-based configuration	Integrated configuration	Soft structure	Multi-task	Wrinking avoidance	Automation	Reliability	Efficiency
[58]	•		•			•		•	•	•		
[55]	•		•			•		•				
[42]	•		•								•	•
[56]	•		•			•		•				
[59]	•		•			•		•		•		
[76]	•		•			•		•	•	•		•
[30]	•	•			•			•		•	•	•
[31]	•	•			•			•		•	•	•
[29]	•	•					•			•	•	•
[38]	•	•								•	•	
[53]	•	•		•	•		•	•		•		
[104]	•							•	•	•	•	
[66]		•			•		•					
[68]		•			•		•	•				
[77]	•	•					•		•		•	•
This research	•	•		•	•		•	•	•	•	•	•

It can be observed that most of the recent research on fabric handling tasks explored the integrated frames that use vacuum grippers as end effectors. As discussed in the previous sections, this approach is proved effective but is limited to a relatively small range of material types.

There is research that applied the clamping strategy. Some of the gripper designs in these studies contain features of soft robotic, such as soft gripper tip or skin. However, only one had developed a strictly defined soft robotic gripper that has an underactuated mechanism, and its investigation on the gripper structure is very simple. There is also a lack of quantitative study on the interaction between the gripper and the fabrics. This makes the avoidance of wrinkling and gripping reliability an unexplored problem when it comes to clamping grippers. Aside from fabric picking, there are some studies on soft robotic grippers for other tasks that can provide insights for this research.

Therefore, it is necessary to fill the research gaps on clamping grippers for fabric handling. Preliminary results of this research showed the factors that affect the gripper performance quantitatively [77]. More detailed investigation following those results is presented in this thesis. This research also covers the design and analysis of soft robotic grippers for fabric handling, as mentioned in the research objectives.

## CHAPTER 3

### METHODOLOGY

#### *3.1 Classification of Fabric Materials*

Different types of fabric materials show drastically different behaviors during the picking, transferring, and placing operations. In order to standardize the setup of experiments and analyze them respectively, it is necessary to have a classification system considering the important properties of the fabrics. The classification system should be consistent, complete, and compatible with existing databases. These properties should also be summarized in a searchable manner so that the classification system can be easily applied during experiments and analysis.

The OPITZ classification code system, shown in Figure 3.1, is a typical example of searchable classification systems in group technology in the manufacturing domain [78]. It uses a 9-digit code to characterize a manufacturing strategy. The first five digits describe the geometrical form of the part to be manufactured, including whether the part is rotational or not, external shape, internal shape, machining requirements, and auxiliary features. Then, there are four secondary digits that summarize the dimensions, work material, the original shape of raw material, and accuracy requirements.



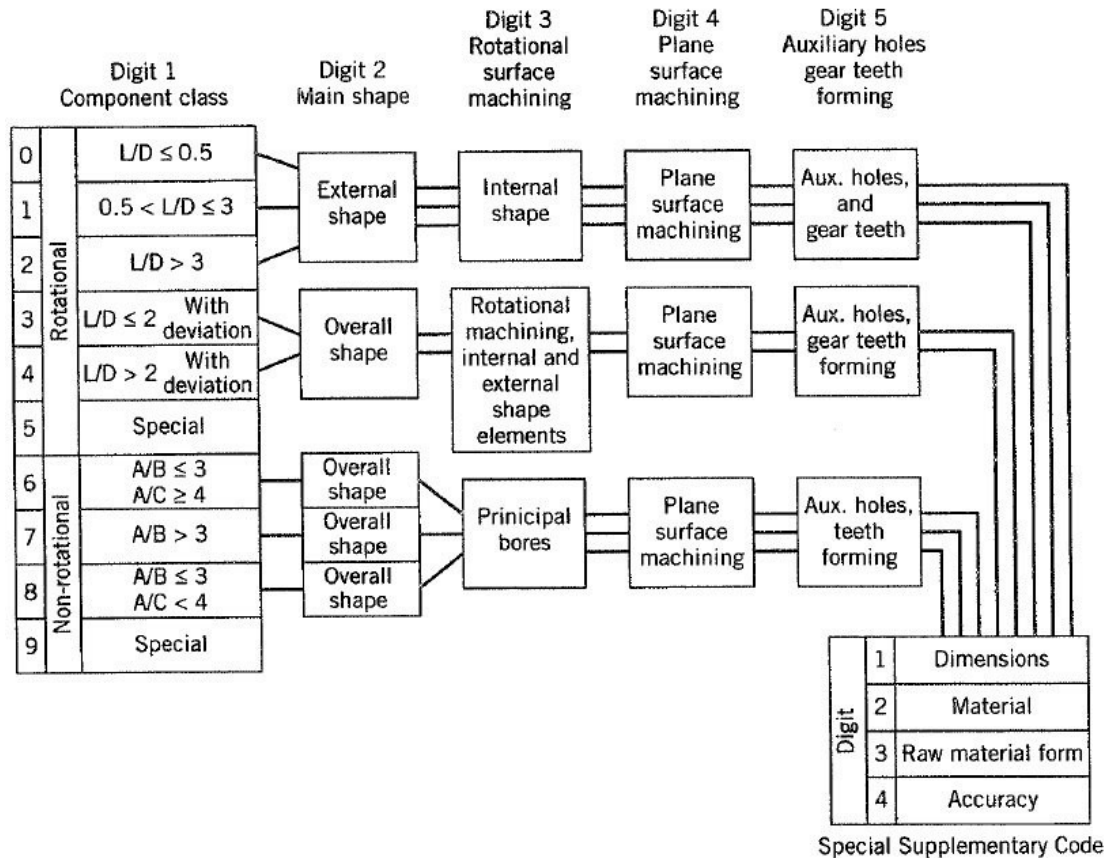


Figure 3.1 OPITZ classification code (taken from [78])

By using a similar strategy, a digit-based classification code system for fabric materials is developed. While performing pick and place tasks using robotic grippers, the most important properties include fabric structure, roughness, area weight, and stiffness. Each of these properties can be characterized by a digit number, hence the first four digits would summarize the relevant material properties of the fabrics. Additionally, the behaviors of a fabric piece are also determined by its geometrical characteristics, including the size, thickness, external shape, and internal shape of the fabric piece. Finally, the mold surface on which the fabric pieces are to be placed is also a critical condition. Therefore, by using a 10-digit code, the important characteristics of fabrics during handling operations can be effectively summarized in a standard and searchable manner. Table 3.1 to 3.3 show the digital-expressed fabric structure, material properties, and geometric and mold properties respectively for the classification system.

Table 3.1 Fabric structure

<b>Fabric structure</b>				
<b>1. woven</b>	<b>2. knitted</b>	<b>3. braided</b>	<b>4. lace and net</b>	<b>5. others</b>
1. plain	1. plane			1. paper
2. twill	2. lacoste			2. leather
3. satin	3. interlock			3. foam
4. basket	4. double pique			4. plastic
5. leno	5. others			
6. mock leno				
7. others				

Table 3.2 Material properties

<b>Material properties</b>		
<b>Roughness (coefficient of friction)</b>	<b>Area weight (g/m<sup>2</sup>)</b>	<b>Stiffness (bending length, mm)</b>
1. <0.3	1. <50	1. <5
2. 0.3-0.4	2. 50-100	2. 5-10
3. 0.4-0.5	3. 100-150	3. 10-15
4. 0.5-0.6	4. 150-200	4. 15-20
5. 0.6-0.7	5. 200-250	5. 20-25
6. 0.7-0.8	6. >250	6. >25
7. >0.8		

Table 3.3 Geometric and mold properties

Geometric properties				Mold surface
Size (m <sup>2</sup> )	Thickness (mm)	External shape	Internal shape	
1. <0.2	1. <0.2	1. rectangular	1. continuous	1. flat
2. 0.2-0.5	2. 0.2-0.4	2. round	2. few small holes	2. lightly wavy
3. 0.5-1.0	3. 0.4-0.6	3. polygonal	3. many small holes	3. heavily wavy
4. 1.0-1.5	4. 0.6-0.8	4. irregular	4. large circular holes	4. irregular with mild bulges or hollows
5. 1.5-2.0	5. 0.8-1.0	5. extremely irregular	5. large non-circular holes	5. irregular with large bulges or hollows
6. >2.0	6. >1.0			

For the ease of application, the whole classification code can be separated into four sections, connected by dashes. Therefore, the characteristics of a specific piece of fabric can be expressed using a 10-digit code “x.x-xxx-xxxx-x”. The first section represents the fabric structure, where the first digit is the upper class and the second digit after dot is the subclass. The subclass digit may be neglected when there is no necessity for this information. The second section represents the material properties of the fabric. The third section represents the geometric properties of the fabric. The last section, which contains only one digit, represents the mold shape. Under circumstances where the mold shape is uncertain, the last section can be neglected.

### ***3.2 Pick and Place Tasks Based on Collaborative Robots***

Cobots, or collaborative robots, are robots intended to interact with humans in a shared space and to collaborate safely in close distances. A collaborative robot provides advanced automation platform designed to interact with personnel [79]. Compared to traditional industrial robots which are designed to work autonomously with safety insured

by isolating human contact, the typical working range associated with industrial robotic solutions is altered to allow human-machine engagement in the working range [80,81]. These traits are usually achieved through accurate sensing, fast response, light weight, round-edged structures, etc. Existing cobots share a highly identical architecture design, generally with a six or seven axis with one arm configuration or dual arm configuration. Their payload ranges from 1 kg to 5 kg. This architecture displays the highest level of dexterity available today with the maximum of simplicity. This type of arm can position and orient the gripper through a combination of a complete cylindrical and spherical workspace with an infinite range of arm poses.

Because of the lack of automation for fabric material handling, human-robot interaction and tool path design would be critical for relevant research. The advantages of cobots, including close human-robot interaction and their potentiality for complex movements, would be greatly beneficial for carrying out various experiments.

In this research, the YUMI ABB 14000 dual arm robot shown in Figure 3.2 was applied for pick and place experiments. It is a dual arm collaborative robot with seven DOFs for each arm. This robot has a vision system, controllable dexterous grippers (speed and gripper position), sensitive force control feedback, flexible software and built-in safety features that collectively allow for programming through teaching rather than coding. The design and performance characteristics are summarized in Table 3.4.



Figure 3.2 YUMI dual arm collaborative robot

Table 3.4 Characteristics of YUMI dual arm collaborative robot

Feature	Value
Degrees of freedom	7 (rotational joints) per side
Working range	559 mm
Linear speed of gripping operation	0.25 mm/s
Max force	20 N
Max payload	500 g
Max TCP velocity	1.5 m/s
Width, length, height	399*497*571
Weight	38 kg

The robot has a compact frame and fourteen axes, seven for each arm. The structure representations and the DH parameters of both arms are presented in Figures 3.3 [77].

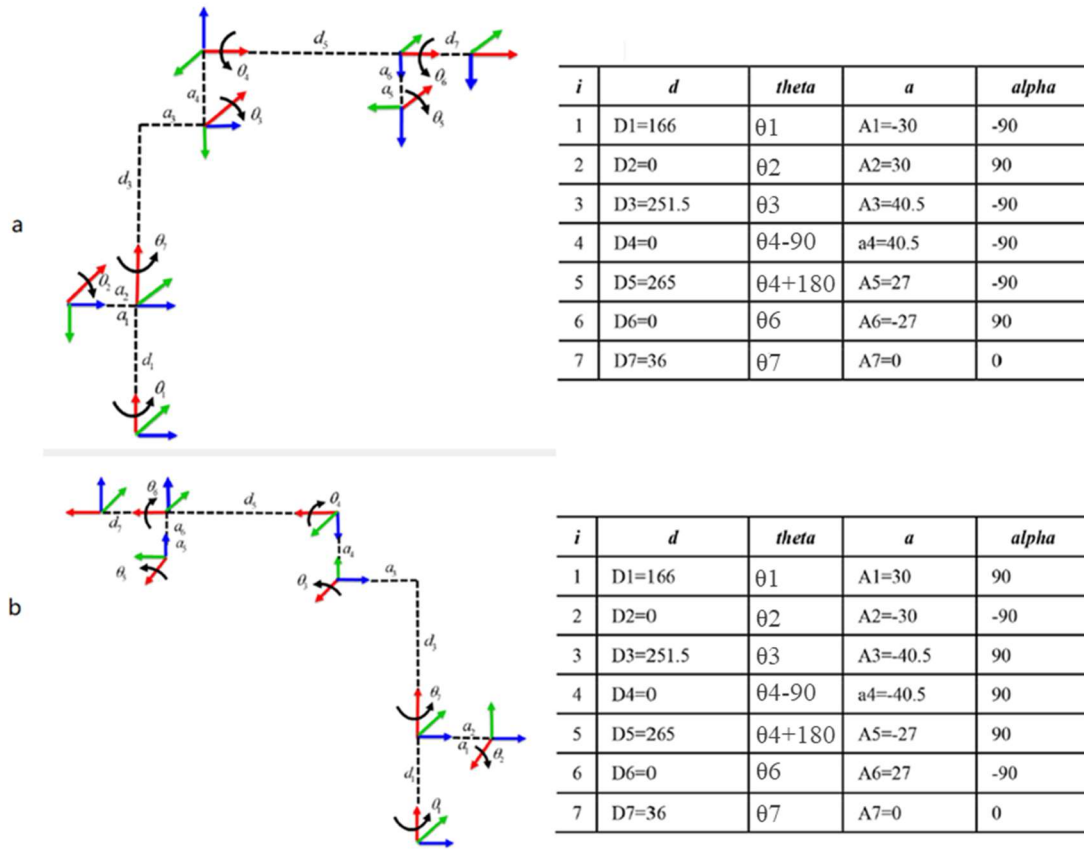


Figure 3.3 YUMI DH configurations and DH parameters

a. Left arm   b. Right arm

### ***3.3 Gripper Design***

There are three important characteristics to consider for fabric handling operations: the fabric's light weight, high deformability, and complex geometry. Compared to other objects manipulated in industry (i.e. rigid metal components), common fabric materials such as carbon fiber fabric or glass fiber fabric have a much lighter density, making them easier to carry. Hence, the demand for the gripping force is necessary but not very high. Fabric materials are highly deformable, causing draping and shifting during the pick and place operations. Deformability also causes many types of fabrics vulnerable to hard contact, making grasping more challenging. The geometrical complexity is related to various mold shapes mentioned in the previous chapter. During application, the gripper might need to pick or place fabric plies with respect to curved or cornered surfaces. Deformation of the fabrics also increases the geometrical complexity. Aside from these three characteristics, efficiency and motion speed are also required as for any other pick and place operations.

Though traditional grippers might be able to perform fabric picking operations for simple scenarios as past literature suggests, they can hardly remain feasible to deal with the increasing complexity in many applications. In order to perform more complex pick and place movements rather than linear motion, a soft robotic gripper is designed, simulated, and tested. Multiple gripper design strategies are investigated for this project to derive a broad solution set.

Soft robotic grippers are the product of bio-inspired engineering. In order to develop a soft gripper adjustable to various scenarios, it is wise to observe the motion of human hands. When manually picking up a ply of fabric, the index finger and thumb are typically applied. As shown in Figure 3.4, at the beginning of the picking movement, the index finger and the thumb would open wide so that the finger pulps become parallel the fabric surface. Then, the finger pulps are pushed toward the fabric to create a firm contact condition. While picking up, the hand would lift upward while pinching the fabric up through friction force. After the movement is finished, the fabric would be firmly clamped between the two fingers.



Figure 3.4 Manual picking

According to the literature review, finger-based gripper designs with cable actuation appeared to be the most suitable configuration for fabric handling tasks because of their high actuation speed, steady and reliable gripping force, and structural simplicity. They are capable of rapid movements, providing firm gripping conditions, and complex gestures for various operations. This type of gripper is also compatible with novel grasping, smoothing, and hybrid lifting strategies, which would be investigated under specific situations. Fluidic elastomer actuators are another competitive candidate, as they also provide high gripping capability, but are not favored due to their mechanical complexity and relatively lower actuation speed.

For the purposes of this research, it is required that the gripper should have a large and controllable opening magnitude. It should be able to adjust itself to the working surface when picking or placing while providing enough gripping force. When fully enclosed,



there should be enough contact area between the fabric and the gripper tip to prevent slippage. That means the gripping fingers should be able to bend in double directions and the bending magnitude being controlled by a simple input, which is the pulling force for cable actuation. A typical cable actuated gripper configuration is based on elastomer fingers with gaps on the bending sides and driving tendons inserted through the gaps. To achieve controllable double-direction bending, there should be gaps on both sides of the finger. Figure 3.5 illustrates a conceptual version of such design.

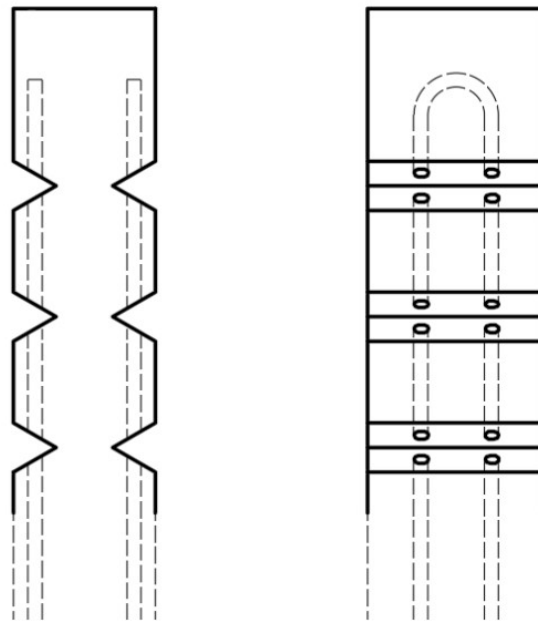


Figure 3.5 Cable actuated gripper configuration

As shown in the drawing, multiple triangular gaps are distributed on the bending side of the finger, separating the elastomer bar into multiple sections. Two slots are present at the gapped edge for the driving tendons to go through. At the top section, there are U-shaped slots strengthened by a stiffer material to hold the tendons. These underactuated fingers would be attached to a rigid ‘palm’ structure. When the driving force pulls the tendons from the bottom, the gripper would open or enclose due to the pulled sides. When touching the working surface while enclosing, the gesture of the fingers would be confined by its elasticity behavior, hence adjusting itself to the target geometry. Figure 3.6 illustrates the resting, opening, and gripping positions of a conceptual gripper



configuration. The potentiality of complex gestures also allows flexible touching areas for various gripping and smoothening requirements.

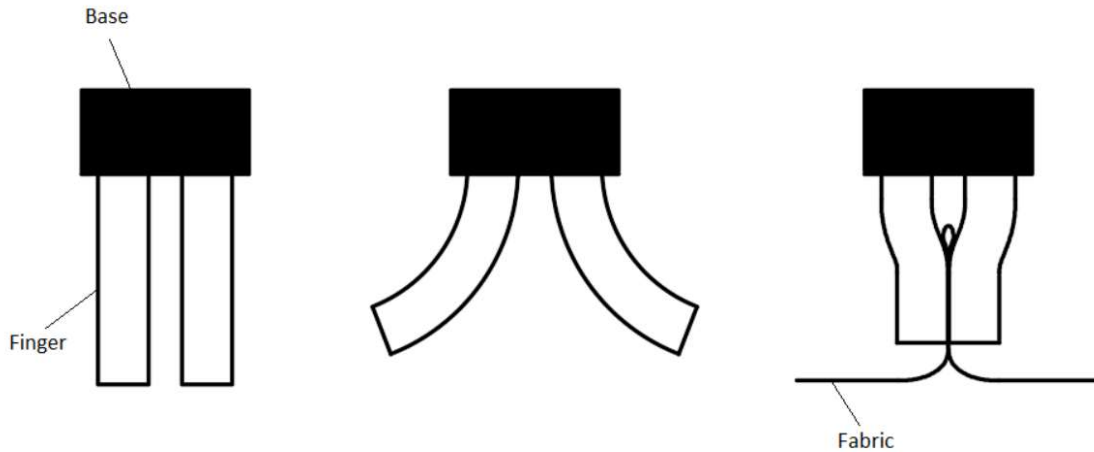


Figure 3.6 Postures of a conceptual gripper configuration

The elastomer could include one-side bending or two-side bending depending on the applications. There could be multiple gaps on each side of such a finger. The distribution of gaps and other geometrical characteristics both affect the behavior of the gripper. Aside from elastomer fingers made of a single material, it is also possible to apply other actuating principles, such as linkage-based grippers with an elastomer skin, as mentioned in the previous chapter. Detailed design variations are investigated and presented in later chapters. This also includes combinations of a traditional gripper with a soft robotic glove to achieve efficient performance in simpler pick and place tasks. After a feasible design is achieved, driving and controlling components are taken into consideration during the prototyping stage.

### ***3.4 Prototyping***

Selected additive manufacturing (AM) and other related processes are utilized for prototyping.

Additive manufacturing includes various processes that create three-dimensional objects

by joining materials directly from a digital model. The materials are added together as melted powder grains or fused molecules. The processes are typically done layer by layer. One of the most important advantages of additive manufacturing is the capability to create complex geometries directly from computer-aided design (CAD) models in a fast, convenient, and low-cost manner. This property makes it a favored method for rapid prototyping while the design is in engineering development.

A great amount of progress related to the fabrication of soft robotic grippers has been enabled by the recent development of AM techniques and other related design and manufacturing tools. Researchers have created complex soft robotic grippers and systems by taking advantage of rapid and adaptable manufacturing technology [82], such as multi-material 3D printing [83], shape deposition manufacturing (SDM) [84], soft lithography [85], etc.

For the soft gripper related parts in this research, the most important AM technology is the fused deposition modeling (FDM) process. FDM is an AM technique in which a physical object is created directly from a CAD model using layer-by-layer deposition of a feedstock plastic filament material extruded through a nozzle. During printing, the nozzle travels back and forth based on the design described in a STL format file, adding materials layer by layer until the whole 3D structure is completed. With an FDM processes being utilized, rigid components such as linkage skeleton with reconfigurable feature tubing or cable channels can be quickly fabricated. Other components such as mold sets and gripper bases can also be fabricated this way.

The STL file is a file format that describes the geometry of three-dimensional objects using triangulated surfaces, and can be directly converted from a 3D model by any popular CAD software. In this research, the selected CAD software is SolidWorks for most of the modelling work. Technically, STL is a suboptimal file format because it is not possible to perfectly represent curved surfaces using triangles, especially for extremely complicated geometry. However, the components included in this research are relatively simple, so this drawback can be neglected when printing the parts. For the same reason, tool path design challenges for the FDM process are not too difficult, either.

The FDM machine used in this research is a Fortus 400mc 3D printer. It is a 3-axis AM machine that accommodates a wide range of production-grade thermoplastics and is able to provide accurate, repeatable builds. This device has a vacuum stage to fix the building sheet and an enclosed oven to provide steady building temperature.

Two different types of building materials, ULT9085 and PC30, are used to make relevant components. Because the forces withstand by rigid components in this research are significantly smaller than the capacity of these two types of materials, the differences in their physical behaviors can be ignored. UTL\_S and PC\_S were used as support materials respectively to support parts with complex geometries or overhang angles that exceed the threshold (approximately 45° depending on material types and extrusion characteristics).

Another important prototyping technique is the overmolding process. Overmolding is a molding technique where two or more different materials are combined together to create a single part. Typically, during overmolding, the substrate materials are partially or fully covered by subsequent materials referred as overmold materials. The substrate materials are usually much more rigid than the raw subsequent materials before curing. These processes include plastic over metal molding, rubber over plastic molding, rubber over metal molding, rubber over plastic molding, etc. Overmolding processes can be used to fabricate complex structures with multiple materials included. In other research, specialty, multi-stage low volume overmolding solutions have been developed for cables slots [86], and to emulate a human thorax for thoracentesis training mannequin [87]. These rapid, low cost pattern and tooling methodologies are leveraged for the soft gripper manufacturing processes.

Taking the elastomer finger in Figure 3.5 as an example (three-gap version), the part can be overmolded using a mold set with movable components. The plastic U-shape tube is the substrate material, and silicone rubber is the subsequent material. As illustrated in Figure 3.7 (only half of the mold set is shown here), the basic geometry of the gapped elastomer finger can be directly created from the mold shape, and two removable tubes are inserted into the cavity to create the cable slot. The U-shape tube is held by the extractable tubes. After the subsequent material cures, the extractable tubes would be removed, leaving the U-shape tube inside the elastomer structure as part of the finger.

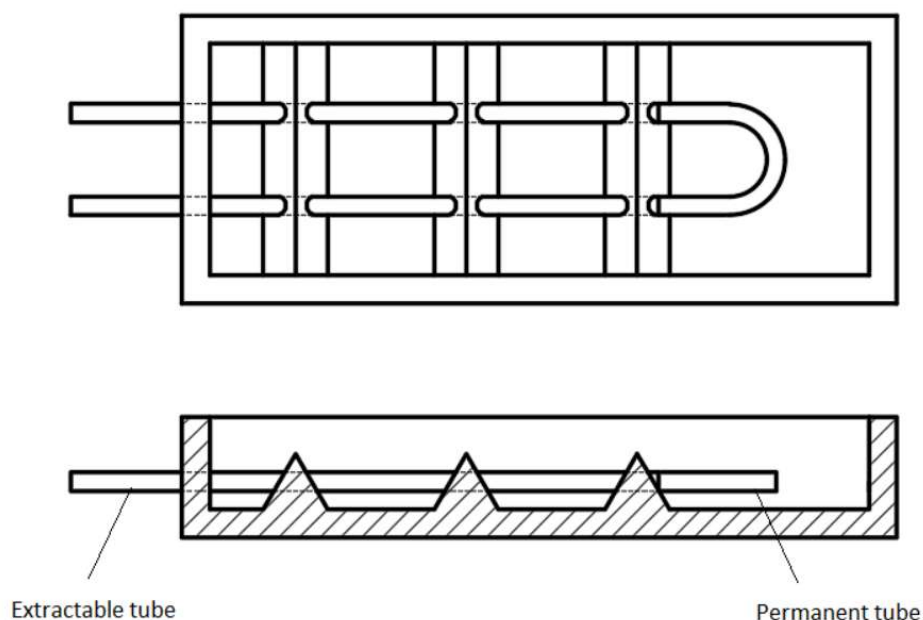


Figure 3.7 Overmolding illustration

The elastomer material used in this research is Mold Star 15 SLOW silicone rubber, a mediate hard, strong rubber material that is tear resistant and exhibits very low long-term shrinkage. The raw materials should be mixed 1A:1B by volume when molding. The curing time is four hours at room temperature and can be accelerated by heating up. Table 3.5 shows some technical data of Mold Star 15 SLOW.

Table 3.5 Technical data of Mold Star 15 SLOW

A:B Mix Ratio	1:1
Mixed Viscosity (ASTM D-2393)	12,500 cps
Specific Gravity (g/cc) (ASTM D-1475)	1.18
Specific Volume (cu. in./lb.) (ASTM D-1475)	23.5
Pot Life (ASTM D-2471)	50 min
Shore A Hardness (ASTM D-2240)	15A
Tensile Strength (ASTM D-412)	400 psi
100% Modulus (ASTM D-412)	55 psi
Elongation at Break % (ASTM D-412)	440%
Die B Tear Strength (ASTM D-624)	88 pli

The U-shape tubes are made by heat-shrink plastic tubes. Other components include cotton strings, nylon strings, plastic, and metal components.

### ***3.5 Simulation***

Compared to the computational analysis of traditional rigid body systems, design and simulation tools are limited for soft materials, including fabrics and elastomer materials that are essential to soft robot grippers. While the position and movement of rigid objects can be sufficiently described by six degrees of freedom (three transitional coordinates and three rotational coordinates), soft bodies cannot be confined to simple and discrete planar motions. Soft materials are elastic (sometimes elastoplastic), and can be highly bent, twisted, stretched, compressed wrinkled, etc. Therefore, the analysis and simulation for soft bodies are much more complicated than rigid bodies.

In order to analyze the performance of soft grippers and fabrics, special analysis approaches such as Finite Element Analysis (FEA) are applied. Various studies have applied FEA simulation among those subjects. The simulation challenges also require sophisticated modelling of the structural and dynamic configurations of the system. Abaqus is used to perform the simulation. This allows the model-based design of the gripper configurations.

#### ***3.5.1 Simulation of the Underactuated Mechanism***

The most critical part regarding the simulation of soft robotic grippers is the modelling of the elastomer fingers and similar structures. For this task, hyperelastic material models are necessary to capture the nonlinear material properties of the rubber-like materials.

For rubber-like materials such as elastomers or bio tissues, a large strain occurs when a small stress is applied. Traditional linear theories of elasticity represented by Hooke's law fail to adequately predict their mechanical behaviors. During the past decades, researchers represented by Mooney and Rivlin have introduced a nonlinear theory of elasticity that leads to hyperelastic material models using strain-energy functions to

describe the mechanical properties of rubber-like materials [88-91]. There are also various researches that applied hyperelastic theories and models in mechanical and biomechanical domains [92,93]. Specifically, hyperelastic models are ideal for characterizing silicone rubber materials in industrial applications [94,95].

In the hyperelastic theory, the materials are assumed to be isotropic and incompressible. This is generally valid for rubber-like materials, especially when they are not strictly confined. A hyperelastic material model relies on the strain-energy function  $\Psi$ , which is obtained from symmetry, thermodynamic and energetic considerations.

If the material is isotropic, the strain-energy function depends on the strain invariants. That is

$$\Psi_{isotropic} = \Psi(I_1, I_2, I_3) \quad (3-1)$$

where the strain invariants

$$I_1 = \sum_{i=1}^3 \lambda_i^2 \quad (3-2)$$

$$I_2 = \sum_{i,j=1}^3 \lambda_i^2 \lambda_j^2, i \neq j \quad (3-3)$$

$$I_3 = \prod_{i=1}^3 \lambda_i^2 \quad (3-4)$$

$\lambda_1$ ,  $\lambda_2$ , and  $\lambda_3$  are the principle stretches [95].

If given the assumption that the material is incompressible ( $I_3 = 1$ ), Equation 3-1 becomes

$$\Psi_I = \Psi(I_1, I_2) \quad (3-5)$$

Since the strain invariants directly depend on the principal stretches as mentioned in Equations 3-2 to 3-4, the strain-energy functions can also be expressed as a function of the principle stretches:

$$\Psi_I = \Psi(\lambda_1, \lambda_2, \lambda_3) \quad (3-6)$$

In the more complicated cases such as biomechanics where anisotropic characteristics are present, an anisotropic contribution can be added to compensate for the anisotropic nature of those materials. Hence, the full expression of  $\Psi$  becomes

$$\Psi = \Psi_{isotropic} + \Psi_{anisotropic} \quad (3-7)$$

An example of such cases is the Martins material model. There are some cases where this expression is applied [90,91]. However, such complicated cases are not within the domain of this project.

Multiple models have been established by researchers, such as the Neo-Hookean material model, the Mooney–Rivlin material model, the Yeoh material model, the Ogden material model, etc. The majority of these models are based on one or more quantities among the principle stretches  $\lambda_1, \lambda_2, \lambda_3$  and the Cauchy–Green tensor invariants  $I_1, I_2, I_3$ . The four mentioned models are all available in the Abaqus software.

The Neo-Hookean material model is the simplest hyperelastic model and one of the most popular models. It was first established by the study of vulcanized rubber using statistical theory [91]. In this approach, the rubber material is considered as a three-dimensional network of long chain molecules connected by few points. One coefficient is needed to establish the strain-energy function:

$$\Psi = c_1(I_1 - 3) \quad (3-8)$$

Another famous and commonly applied hyperelastic model is the Mooney-Rivlin material model. It is one of the earliest developed hyperelastic models and is well known

for its high accuracy in describing the mechanical behaviors of isotropic rubber-like materials. The strain-energy is expressed as

$$\Psi = c_1(I_1 - 3) - c_2(I_2 - 3) \quad (3-9)$$

The Yeoh material model, first presented in 1990, for incompressible materials established the strain-energy function using three coefficient and only the first strain invariant  $I_1$ :

$$\Psi = \sum_{i=1}^3 c_i(I_1 - 3)^i \quad (3-10)$$

Another example, the Ogden material model is based on Ogden's phenomenological theory of elasticity [90]. Its strain-energy function has a complex general form

$$\Psi = \sum_{i=1}^N \frac{c_{2i-1}}{c_{2i}} (\lambda_1^{c_{2i}} + \lambda_2^{c_{2i}} + \lambda_3^{c_{2i}} - 3) \quad (3-11)$$

For technical applications, including the settings in Abaqus, the number  $N$  is typically set to 3 to achieve optimal convergence between theoretical and experimental results. That makes the function dependent on six coefficients.

Relevant studies have shown that in cases where the deformations are moderate (<100%), simple models like the Neo-Hookean model would suffice. The Mooney Rivlin model potentially remains accurate until the deformations reach approximately 200%. The Yeoh model and the Ogden model can provide accurate results under large deformations, but the complexity of these models leads to high computational costs. [94,104]

In the study of soft robotic grippers, the deformations of the elastomer materials are significantly smaller than the capacities of the simpler models mentioned above. Therefore, by balancing the accuracy and computational efficiency, the Mooney-Rivlin was initially selected as the hyperelastic model for elastomer materials in the research.



For the prototyping material, Mold Star 15 SLOW silicone rubber, there were no data regarding hyperelastic models available on the internet. Thus, a tension experiment was designed and performed to obtain the Mooney-Rivlin coefficients.

For the case of incompressible Mooney–Rivlin materials under uniaxial elongation,

$$\lambda_1 = \lambda \quad (3-12)$$

$$\lambda_2 = \lambda_3 = \frac{1}{\sqrt{\lambda}} \quad (3-13)$$

The strain-stress equation can be written as

$$\sigma_{11} = \left(2c_1 + \frac{2c_2}{\lambda}\right) \left(\lambda^2 - \frac{1}{\lambda}\right) \quad (3-14)$$

where

$\sigma_{11}$  – the true stress (Cauchy stress) (MPa)

$\lambda$  – the principal stretch

With the Cauchy stress and stretch data collected, the coefficients can be calculated using a least square fit procedure [104]. Given  $n$  measured stress-strain pairs, the best set of constants is the one that minimizes the error

$$E = \sum_{i=1}^n \left(1 - \frac{S_i^{th}}{S_i^{test}}\right)^2 \quad (3-15)$$

where

$S_i^{th}$  – theoretical stress calculated from the stress-strain equation

$S_i^{test}$  – experimental stress

The goodness of the fitting can be evaluated by the sum of squared errors (SSE), the coefficient of determination (denoted by R-squared), adjusted R-squared, and the root

mean squared error (RMSE). SSE is the sum of the squared differences between each observation and its group's mean. R-squared is the proportion of the variance in the dependent variable that is predictable from the independent variable. The adjusted R-squared compares the descriptive power of regression models—two or more variables—that include a diverse number of independent variables—known as a predictor. RMSE is the standard deviation of the residuals, which measure how far from the regression line data points are. These methods are available in the MATLAB curve fitting toolbox.

The uniaxial tensile test followed the ISO 572-2 standard. A dumbbell-shape sample was designed as shown in Figure 3.8.

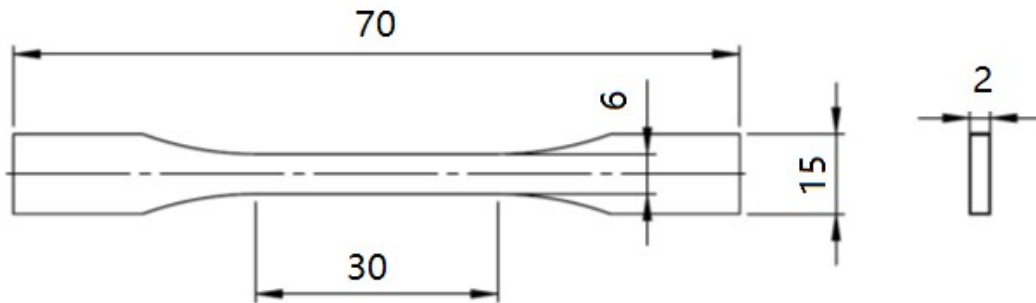


Figure 3.8 Dumbbell-shape sample

During the test, the sample underwent an increasing uniaxial load until the deformation reached 100%. The test was performed with unfixed tension gauge, so the deviation was high. In order to ensure the validity, the test was performed multiple times. After the data was collected. The coefficients  $c_1$  and  $c_2$  were obtained using the curve fitting toolbox in MATLAB. The results were  $c_1 = 0.08412$  and  $c_2 = -0.04687$ . Figure 3.9 shows the fitting result compared with the experimental data.

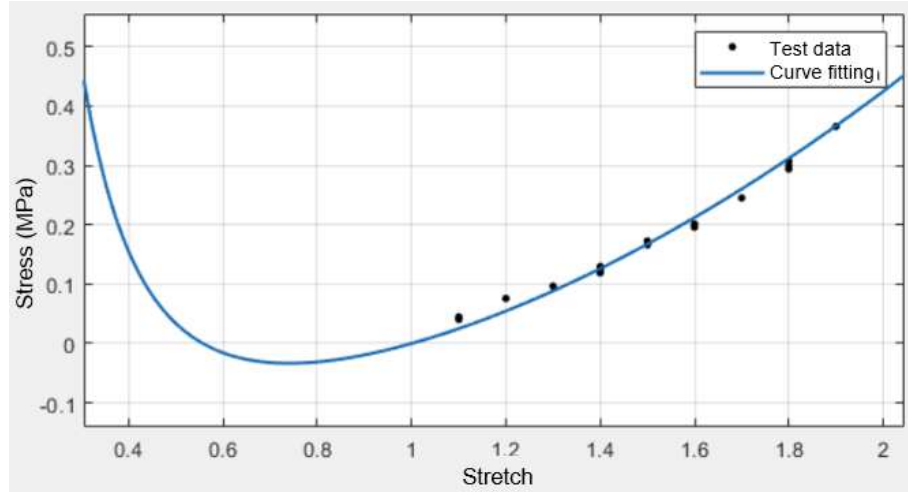


Figure 3.9 Fitting result

The SSE was 0.005717. The R-squared was 0.9878. The adjusted R-squared was 0.9874. The RMSE was 0.01429. According to the figure, there was good fit between the material model and the experimental data. However, when the stretched a certain level in the compression region, this model predicted unrealistic behaviors. This could lead to convergence problems during simulations.

A suggested way to solve this problem is to force  $c_2$  to be positive [97]. With this extra constraint introduced, the result became  $c_1 = 0.05773$  and  $c_2 = 0$ . The material model hence became identical to a Neo-Hookean model. Figure 3.10 shows the adjusted fitting result.

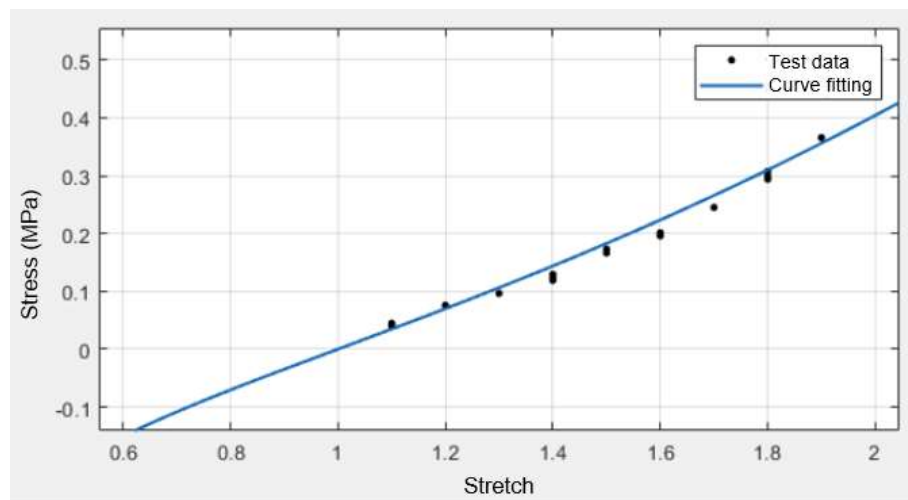


Figure 3.10 Modified fitting result

The SSE is 0.01141. The R-squared is 0.9757. The adjusted R-squared is 0.9749. The RMSE is 0.02019. Though the fitting goodness is slightly lower than the first model, this model remained accurate.

Based on these results, a finite element (FE) model of the test sample is established in Abaqus, as shown in Figure 3.11. The quality of an FE model can be evaluated by the correlation coefficients (CC) between experimental and simulation data, which can be given by:

$$Correl(X, Y) = \frac{\sum(x - \bar{x})(y - \bar{y})}{\sqrt{\sum(x - \bar{x})^2 \sum(y - \bar{y})^2}} \quad (3-16)$$

where  $X$  and  $Y$  are the experimental and simulation data respectively.  $\bar{x}$  and  $\bar{y}$  are the average of corresponding data.

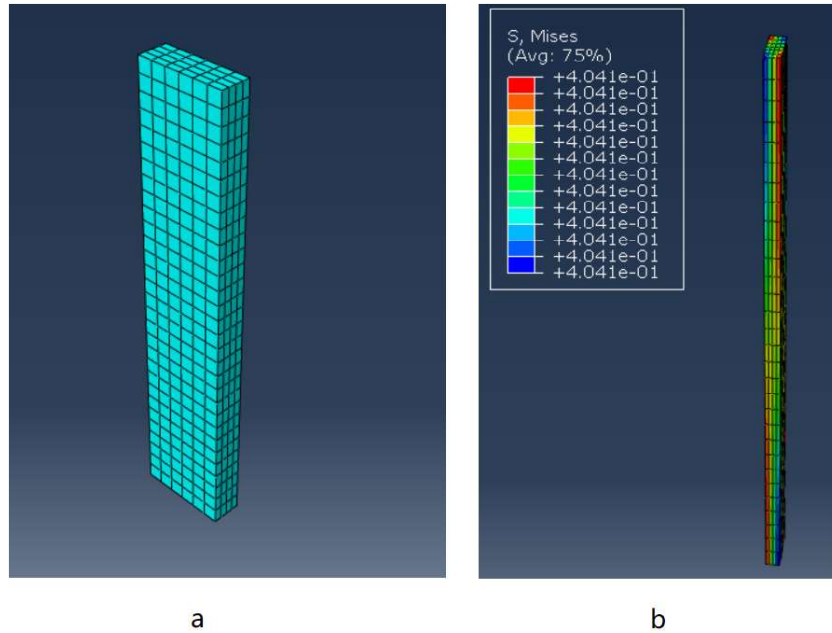


Figure 3.11 FE model of the sample  
a. Meshed model   b. Simulation result

Figure 3.12 shows the comparison between FEA result and the test data that validated the material model. The CC of this model was 0.9896, proving its validity.

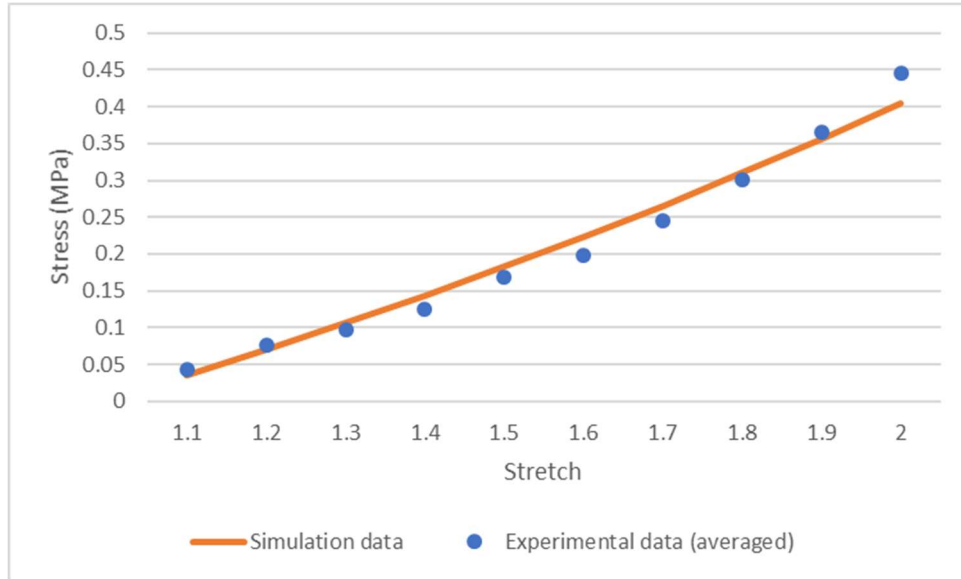


Figure 3.12 Comparison between FEA result and the test data

### 3.5.2 Simulation of Fabric Materials

The simulation of fabric materials under large deformation is a challenging problem in relevant research. In Abaqus, the “lamina” type of elasticity is available for describing the orthotropic behaviors of fabric materials. This elastic model is characterized by six parameters: Young’s modulus  $E_1$  and  $E_2$ , Poisson’s ratio  $\nu_{12}$ , and shear modulus  $G_{12}$ ,  $G_{13}$ ,  $G_{23}$ . Researchers have also developed algorithms and subroutines to accurately capture the anisotropic behaviors of fabric by modelling the microscopic interaction between each yarn that constitutes the fabric ply [98-100]. Figure 3.13 illustrates an example of the microscopic modelling strategy.

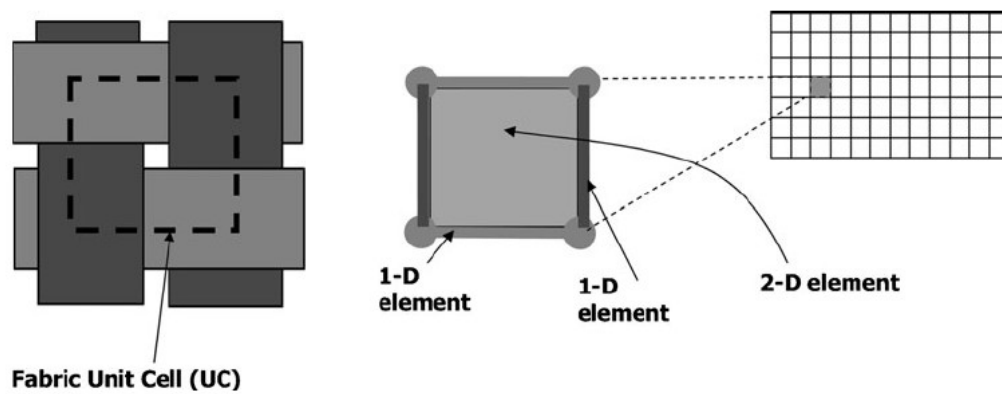


Figure 3.13 Microscopic modelling of fabrics (taken from [98])

Though proved reliable to simulate the deformation of fabric materials with high accuracy, these methods are not favored in this research because of the high computational expense and the difficulty to calibrate the parameters. In this research, the purpose of fabric simulation is to verify the capability of the gripper design to pick up fabric materials. The accurate stress and strain distributions of the fabrics are not needed. Therefore, it would be possible to model the fabric as an isotropic ply, where only two parameters (Young's modulus  $E$  and Poisson's ratio  $\nu$ ) are needed. Researchers have applied such simplified approach for simulating the wrinkling and draping behaviors of flexible fabric plies and other laminae [101,102].

As mentioned in section 2.1, the most important properties of fabric materials during gripping motions are roughness and stiffness. While roughness can be simply characterized by the coefficient of friction, stiffness should be calibrated based on experimental draping behavior. The fabric sample used in this research is plain woven carbon fiber fabric. The thickness of the fabric ply is 0.2 mm. The density is  $1.15 \times 10^{-3}$  g/mm<sup>3</sup>.

A cantilever experiment is performed following the method described in section 2.1 and 3.1. As demonstrated in Figure 2.7, a 5 cm wide strip of the fabric is placed on a platform and moved forward until the centerline from the edge of the platform to the leading edge of fabric makes a 41.5° angle to the horizontal plane. The bending length  $c$  is measured to be 4.28 cm. The length  $l$  of the hanged section of the fabric strip before bending is 8.40 cm.

In order to ensure the validity of the isotropic FE model, an equivalent pair of parameters should be found so that the model would result in the same bending length. A 50 mm by 84 mm rectangular shell part is modelled in Abaqus and meshed using S4R elements. A 9800 N/ton gravity field is applied. The encastre boundary condition is applied to one short edge of the ply to simulate its bending under self-weight as the end section of a long flat strip. It is found that with the equivalent parameters  $E$  set to 240 MPa and  $\nu$  set to 0.1, the simulation result (shown in Figure 3.14) shows the same draping behavior as the experiment.

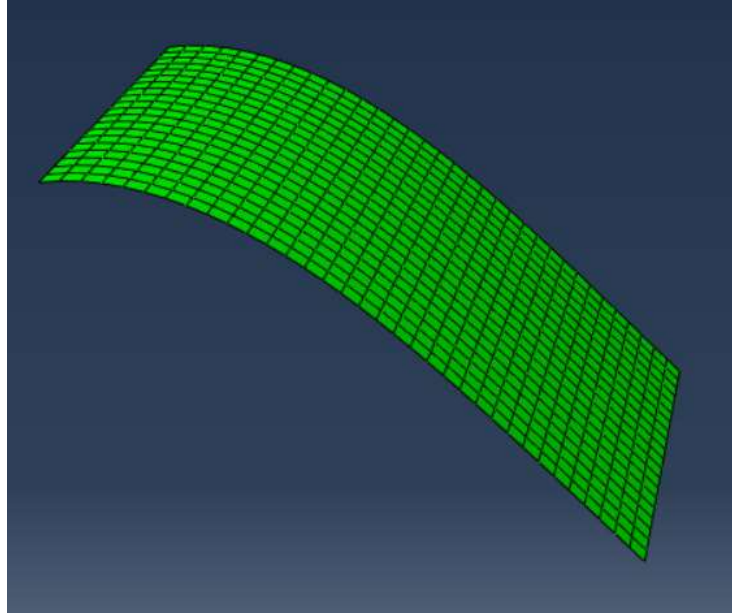


Figure 3.14 Draping result of the simplified fabric model

## CHAPTER 4

### INVESTIGATION OF PICK AND PLACE TASKS WITH CLAMPING GRIPPERS

Because of the complexity of fabric and mold geometry, there are various picking and handling strategies in industrial applications, making it an unsolved problem for the industry. All these pick and place are based on a most simplified scenario, which is picking a rectangular fabric ply from a plain surface and placing it to another plain surface. This research would focus on such simple conditions to build a firm base for fabric picking research.

There are multiple approaches to pick up a fabric ply. If the workpiece is square or nearly square, i.e., the width of the workpiece is close to the length of the workpiece, there are typically three pick positions: center picking, side picking, and corner picking. If a corner of the fabric ply is folded upward, side picking and corner picking could be used to unfold the ply. Figures 4.1 and 4.2 illustrate these scenarios.

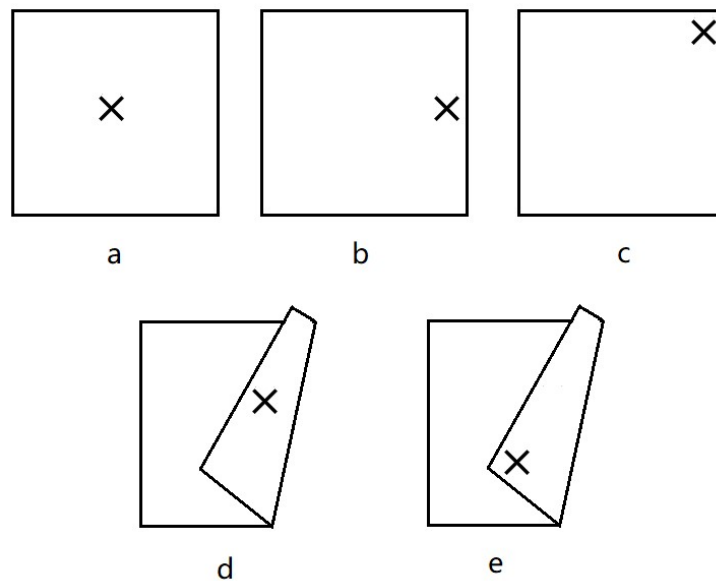


Figure 4.1 Picking locations on a square ply

- a. Center picking   b. Side picking   c. Corner picking   d. Side picking for unfolding  
e. Corner picking for unfolding



For workpieces with a larger size or higher length-width ratio, multiple picking position may be needed. As shown in Figure 4.2, side picking and midline picking approaches can be applied with doubled picking locations. Even when side-picking strategies are not applied, the distances from the picking positions to the edges may also matter.

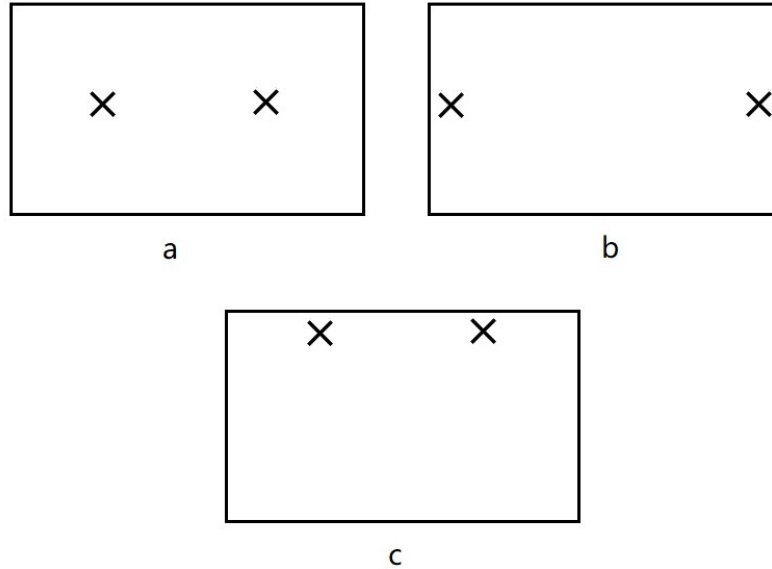


Figure 4.2 Picking locations on a rectangular ply  
a. Midline picking   b. Midline picking (closer to edges)   c. Side picking

This chapter focuses on some basic pick and place tasks and presents the achieved quantitative results to characterize the behaviors of fabric materials during these tasks. The investigated characteristics include slippage, draping, wrinkling/folding, and placing accuracy. The experiments are applied using the YUMI robot mentioned in section 3.2. The purpose is to prove the feasibility of accomplishing fabric pick and place tasks using clamping approaches and to quantitatively demonstrate the potentiality of novel gripper designs. This would also set up a firm foundation for further studies.

#### ***4.1 Simple Pick and Place Tasks with One Gripper***

For pick and place tasks with a clamping method approach, the slippage between the gripper and fabrics is one of the biggest concerns. Low slippage during gripping, lifting,

and moving leads to a firm gripping condition, making it possible to perform rapid transportation. Low slippage increases the controllability and reliability of the gripper performance. The slippage during picking and handling reduces location accuracy and increases the wrinkling after dropping, which are not desired. If the slippage is too large, the fabric may even drop off while moving. In this section, factors that affect the slippage condition were investigated using one robot gripper. Some of the preliminary research results for this project have been published [77].

#### ***4.1.1 Experimental Setup***

For this experiment set, one arm of the YuMi robot was used. The fabric workpiece that was employed are plain weave carbon fiber mats, with a 10 mm wide fiber skein. A plain surface made of hard plastic served as both the workplace where the fabric is picked from and the target area where the fabric would be placed on. This type of carbon fiber fabric is one of the most commonly applied fabric materials in industrial applications. Its draping and friction characteristics make this material challenging. Therefore, it would serve as a representative specimen for relevant researches. By the classification code mentioned in section 3.1, the code of this fabric workpiece would be “1.1-251-2211-1”.

In order to observe and measure the slippage condition, a painter correction pen was used to mark readable orthogonal reference lines onto the material. The fabric workpiece was marked by two perpendicular lines at four fabric sides, each containing a horizontal and vertical distance of 15 cm from the edges of the fabric for measuring slippage while gripping and moving. Four different sides were chosen due to concerns related to potential fabric damage introduced by the pick and place operations, which may adversely affect the repeatability and validity of the experiments.

Since the fabric piece was placed on a plastic working surface that is planar and parallel to the ground, the coefficient of friction for the materials can be determined as a controlled variable. Interior and edge region tests were performed with standard and modified grippers. The force, velocity, slippage, and wrinkling data were collected.

For fabric pick and place tasks, the most severe slippage occurs during vertical

movements due to the weight of the fabric aligning up with the inertia. The faster the lifting speed, the worse slippage situation there will be. Therefore, this experiment specifically focused on vertical pick and place tasks. These tasks can be characterized by three basic motions:

Pick: the gripper touches the fabric and grips it by friction force.

Move: the gripper moves perpendicularly with a high speed.

Place: the gripper steadily lowers down to a certain height and drapes the material onto the given surface.

The robot was programmed so that each test includes three linear pick and place motions to determine how the material shifted during these movements. Based on the targeted movements, three reference locations of the tool center point (TCP) were programmed as follow:

Gripping position: the position where the TCP touched the marked picking point.

Home position: the position where the TCP stayed before the motion started, which is 18 cm above the gripping position.

Middle position: 9 cm above the gripping position.

Placing position: 1.5 cm above the gripping position.

At the start of program, the tip of the gripper would move downward from the home position until it touches the fabric (shown in Figure 4.3). The gripper would close and pick the fabric up to the home position, and then move to the middle position. The robot would then repeat that motion to go to the home position and once again return to the middle position. Here, the gripper would be fixed at this position for 20 seconds so that the slippage result can be measured. Finally, the TCP would travel to the placing position, release the fabric, and head back to the home position to prepare for the next round. The entire moving sequence is illustrated in Figure 4.4.

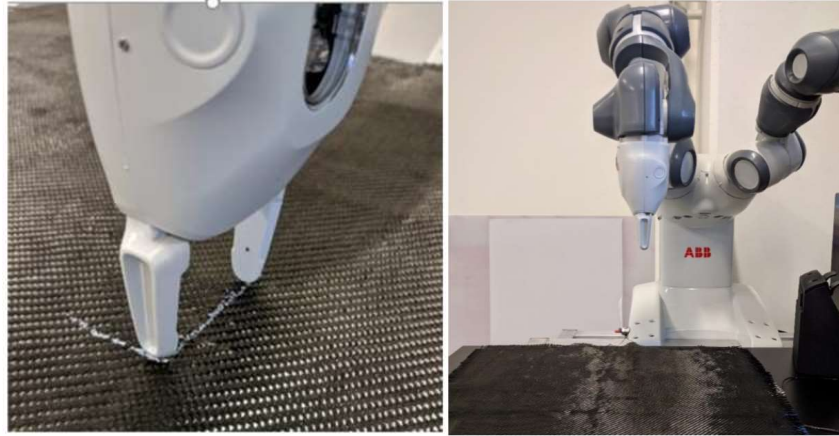


Figure 4.3 Gripping position and home position

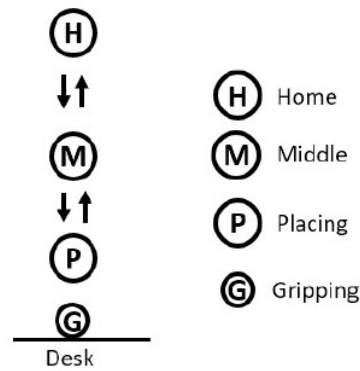


Figure 4.4 Moving sequence for the one arm testing

As shown in the picture, the original gripper attached on the YuMi robot is made of hard plastic and is only capable of simple clapping movement. Primary research had shown that the fabric material would be significantly damaged by the hard gripper even under the low velocity, low force configuration, which is the mildest case. This disqualified the hard-plastic grippers from any applications regarding similar materials. Figure 4.5 shows the damaged fabric workpiece. In order to solve the problem, a novel glove set that would act as a soft skin, a feature of soft robotics, was designed and fabricated to improve the performance of the gripper.



Figure 4.5 Damaged fabric

By reverse-engineering the gripper finger of the YuMi cobot, the soft glove that can be attach to the hard gripper was designed in SolidWorks, as shown in Figure 4.6.

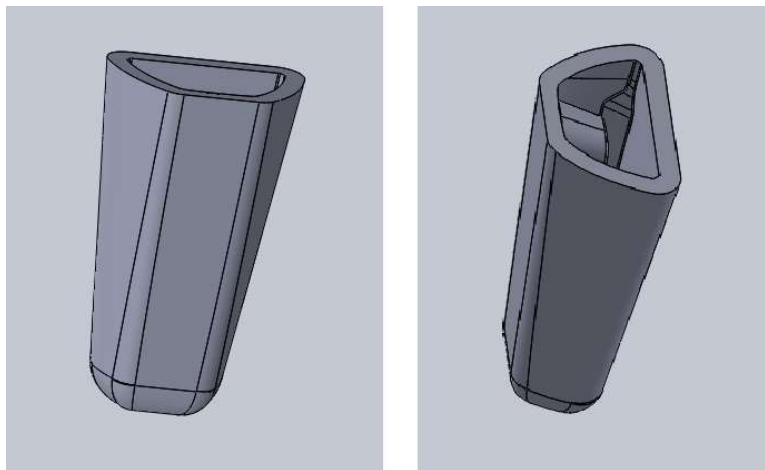


Figure 4.6 CAD design of the soft glove

Based on the CAD model, a multi-component specialty mold set was designed and fabricated through FDM process. Therefore, pairs of elastomer gloves can be quickly and repeated fabricated by silicone molding. The material used to make the gloves is Mold

Star 15 SLOW silicone rubber, as mentioned in section 3.4. The mold set is shown in Figure 4.7. The gloves are shown in Figure 4.8.

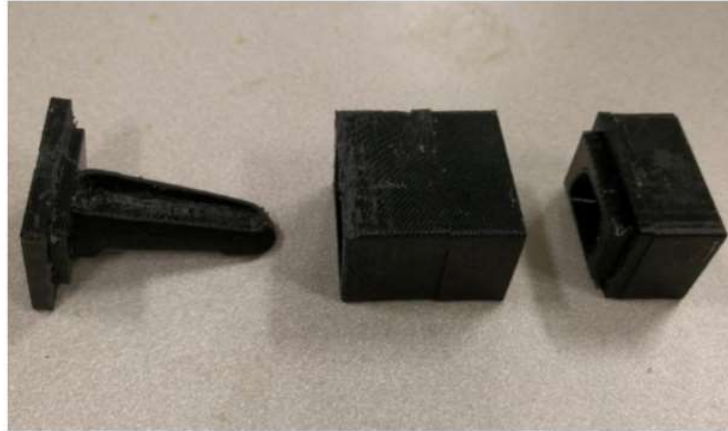


Figure 4.7 Mold set



Figure 4.8 Silicone glove

With the silicone gloves attached, the gripper would be able to provide firmer gripping condition while cause less negative impact to the fabric materials. The soft skin serves as a compliant structure as introduced in section 2.3. When applying load onto the fabric ply, the elastic nature of elastomer would cause the surface of the gripper to deform, hence adjusting to the structure of the fabric to prevent any damage.

As revealed by these initial tests, with the application of the silicon glove, the gripping condition was significantly improved. There was no material fiber damage for any force or velocity settings. The observed wrinkling condition was also improved. Following the pursuit for firm gripping, a modified configuration of the silicone gloves was also designed. Figure 4.9 shows the conceptual model of the second-generation gripper design.

It was hypothesized that by introducing a curved gripping surface, the contact condition can be improved, hence providing better performance than the first-generation design.

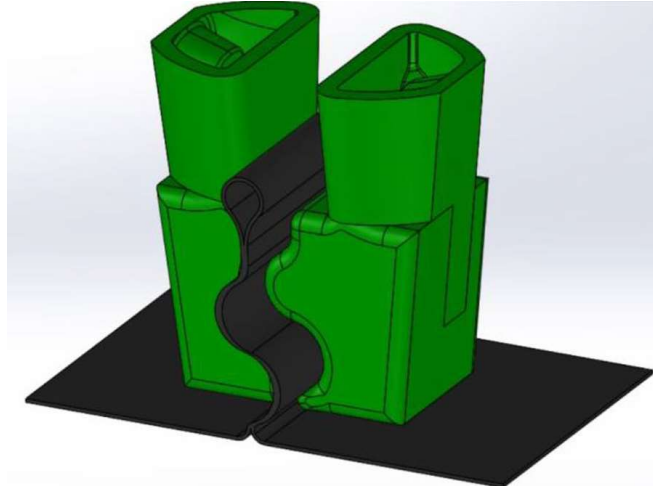


Figure 4.9 CAD model of the second-generation Silicone gloves

The second-generation gripper was designed and fabricated using the same procedure as the first-generation configuration. Figure 4.10 shows the mold set and the prototyping products.



Figure 4.10 Second generation Silicone gloves

As a controlled variable, the coefficient of friction between the fabric and relevant materials were measured using the method in section 2.1. As shown in Figure 4.11, a

silicone block that has its base material used for gripper's tip was placed at an inclined surface covered by one layer of the tested fabric. The angle  $\theta$  was measured and the coefficient of friction  $\mu$  was calculated by Equation 2-1. It was found that the coefficient of friction between Mold Star 15 SLOW silicon rubber and the fabric is 0.7.



Figure 4.11 Friction test

Likewise, the coefficient of friction between the carbon fiber fabric and the working surface was determined. The angle of repose (inclination) is measured to be  $\theta=17^\circ$ . Therefore,  $\mu = \tan 17^\circ = 0.3$ . For this experiment, the frictional force between carbon fabric and work surface is:

$$F_f = \mu mg = 0.3 \times 0.087 \times 9.81 = 0.26N \quad (4-1)$$

The material of the original gripper is hard plastic and was assumed to have similar characteristics to the plastic working surface. Therefore, the frictional force between the carbon fiber fabric and the original gripper can be calculated as follow:

Low level gripping force:  $F_f = \mu N = 0.3 \times 10 = 3 \text{ N}$

High level gripping force:  $F_f = \mu N = 0.3 \times 20 = 6 \text{ N}$

Similarly, the frictional force between carbon fabric and silicon gripper is:

Low level gripping force:  $F_f = \mu N = 0.7 \times 10 = 7 \text{ N}$



High level gripping force:  $F_f = \mu N = 0.7 \times 20 = 14 \text{ N}$

#### ***4.1.2 Results and Discussion***

The sequence of events for the baseline gripper tests is shown in Figure 4.12. Figure 4.13 shows a working gripper equipped with the second-generation silicone gloves.

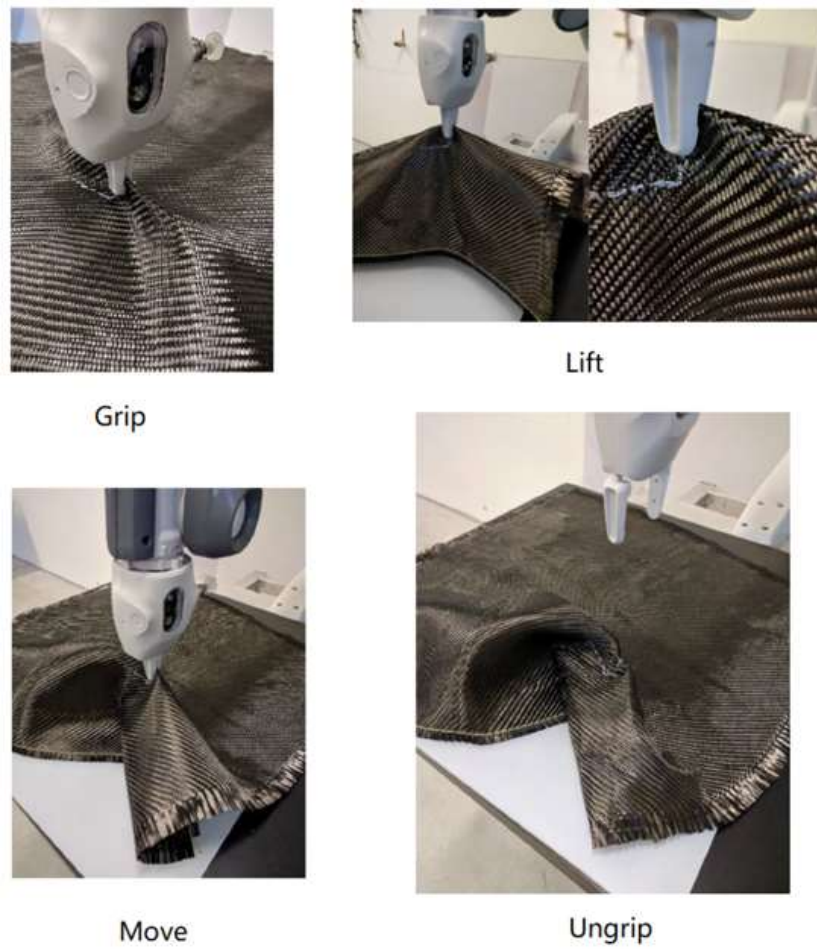


Figure 4.12 Sequence of the experiment

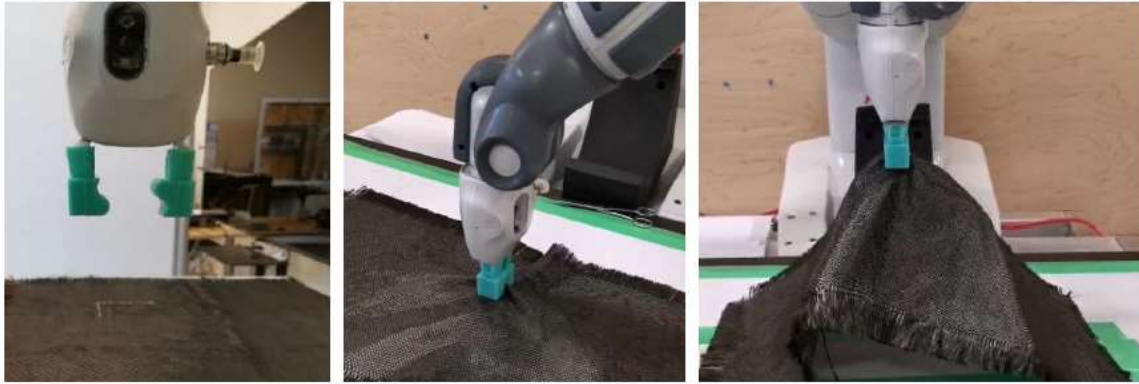


Figure 4.13 Gripper equipped with the silicone gloves

As expected, while the original gripper showed poor performance during these basic pick and place tasks, the introduction of the two types of silicone gloves to create soft-skin grippers improved the results significantly. As previously mentioned, while using the original gripper, the material was damaged at the mildest scenario. There was no damage observed with either the first-generation or the second-generation soft-skin silicone grippers. Figure 4.14 shows the slippage results of the three gripper configurations. Figure 4.15 shows the wrinkling results.

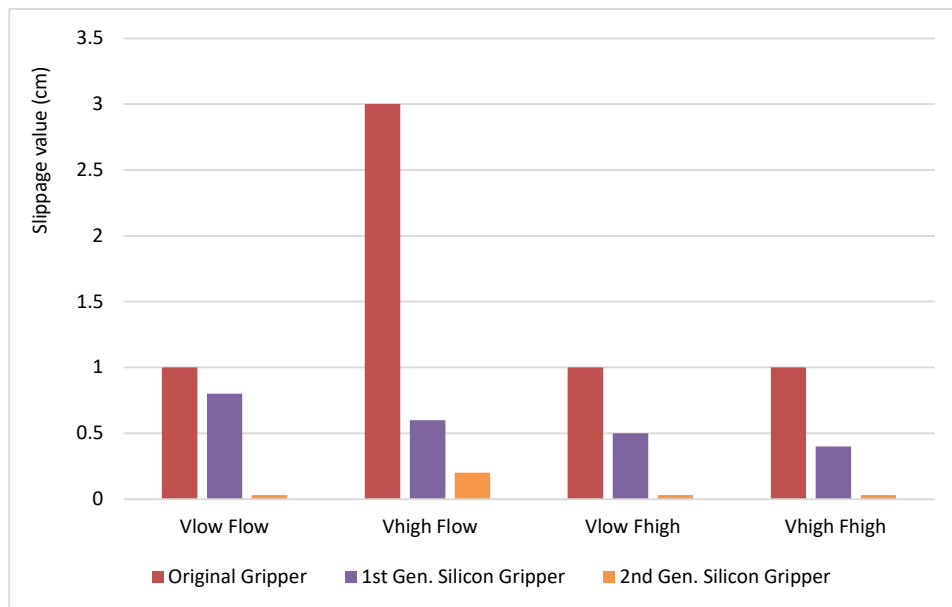


Figure 4.14 Slippage results

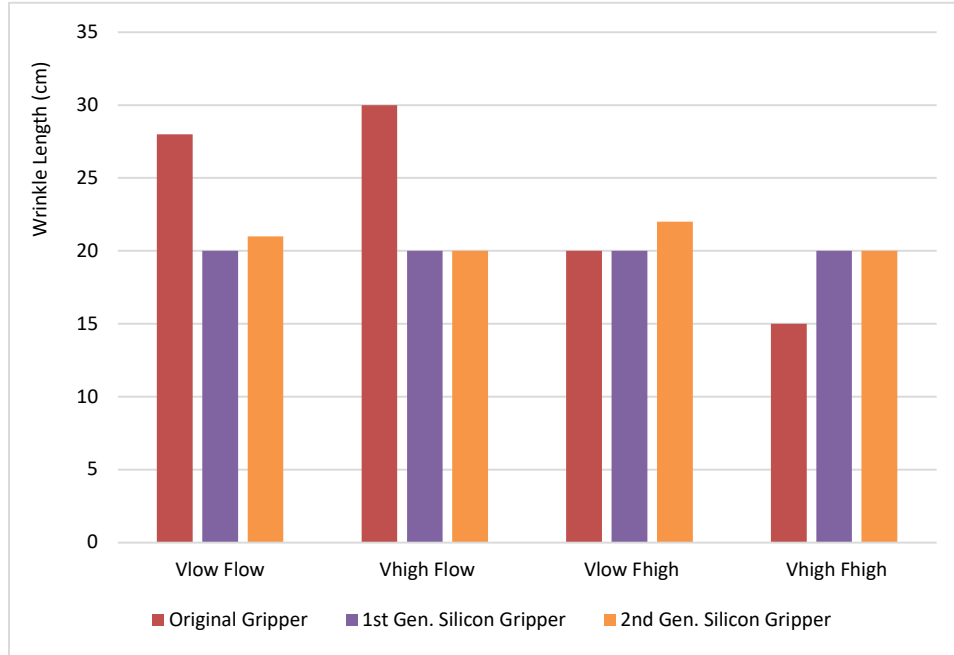


Figure 4.15 Wrinkling results

As revealed in Figure 4.14, with the original gripper, the workpiece slipped severely (3 cm) at the high velocity, low gripping force configuration. All other observed slippage values for the baseline gripper indicated a 1 cm result for the balance of the velocity-force sets. The slippage was significantly decreased when the first-generation silicone gloves were used for each scenario. With the second-generation silicone gloves, there is no slippage at all under most of the scenarios. A slight slippage less than 0.25 cm occurred under the most critical scenario. It was also shown that higher gripping force (causing high friction force between the gripper surface and the workpiece) and lower handling velocity lead to less slippage regardless of the gripper type.

Interesting results were revealed with respect to the fabric wrinkling assessments. It was observed from Figure 4.15 that the gripper configuration influenced the observed wrinkling results only under some scenarios. When the gripping force was low, the original hard gripper caused longer wrinkling lines compared to the silicone grippers, and the situation was slightly worse for high velocity than low velocity. When the gripping force was high, the wrinkling results became nearly identical regardless of the velocity and the gripper configurations. There was no noticeable difference between the first-generation and the second-generation silicone grippers and the wrinkling magnitude

remained almost constant under all scenarios.

This could be caused by the severe inability of the original gripper to provide reliable gripping conditions. When the gripping force was low, the gripping condition was least reliable, causing uncontrollable shift during the movement that led to larger wrinkling after placing. The shift became worse as the velocity increased. However, when the gripping condition was improved to a certain level, no matter by gripping force or by compliant structure, the wrinkling pattern became constant and can no longer be changed by further improving the gripping condition.

By comparing these results, it can be concluded that it is difficult to utilize industrial robots with hard grippers for handling textiles without damaging the strands or introducing large slippage and wrinkling. The situation can be highly improved by the introduction of a simple feature of soft robotic gripper, which was compliant structure in this case. This proved the potentiality of soft robotic technology in fabric pick and place operations. The compliance of soft robots introduced a new dimension for gripper design.

The gripping force and the transfer velocity are both crucial factors that influence the behavior of fabric materials during pick and place tasks. Specifically, the wrinkling results suggested that there is a limit for improving wrinkling conditions by optimizing gripper design alone. In order to further improve the wrinkling behaviors, picking strategies and toolpath need to be taken into consideration. This is investigated and presented in the next section.

The experiments also showed that novel design and fabrication technology, including CAD, AM processes, and overmolding techniques, would play an important role among gripper development in relevant domains, revealing a new perspective regarding fabric picking research. These ideas would be further pursued in chapter 5.

#### ***4.2 Pick and Place Tasks Using Multiple Grippers***

In the previous section, it was shown that clamping grippers with soft skin can provide

reliable gripping conditions, i.e. avoiding slippage and outputting constant wrinkling results under certain movements. However, picking strategies and toolpath design remained necessary to explore if applicable placing results with minimal wrinkling and folding are expected. In this section, picking, transferring, and placing operations with multiple grippers are investigated. The purpose was to further prove the capability of clamping grippers to perform reliable and accurate handling and placing for general pick and place tasks.

#### ***4.2.1 Measurement of Displacement and Wrinkling***

As the damage to workpieces and slippage during high velocity can be solved by the use of soft-skin grippers, the two most important criteria remaining to be studied for the pick and place tasks are the placement accuracy and the wrinkling condition as the fabric ply is being placed at the target location. For an ideal situation, the workpiece should be placed on exactly where it was designed to be, and no wrinkling or folding should occur. The measurement of these two indicators would be crucial for evaluating the performance of a pick and place strategy.

To measure the placement accuracy, four vertices of the rectangular fabric were used as reference points to determine the location of the fabric ply. As marked by green points in Figure 4.16, the target area can also be defined by those reference points, which should coincide with the fabric ply under the ideal situation. The location of a reference point can be expressed as a set of cartesian coordinates. After the placement was finished for each operation, new coordinates of the fabric vertices would be recorded. Hence, the displacement of each reference point (red solid lines in Figure 4.16) can be calculated by

$$d = \sqrt{(x^2 - x_{ref}^2) + (y^2 - y_{ref}^2)} \quad (4-2)$$

where

$x, y$  – coordinates of the reference points on the fabric ply

$x_{ref}, y_{ref}$  – coordinates of the reference points of the target area

Therefore, the average displacement of all reference points (four in case of rectangular fabric ply) can be used as an indicator value of placement accuracy.

In case a corner of the fabric was folded, an imaginary point can be obtained from two extension lines along the edges of the corner where the folding occurred (red dashed lines in Figure 4.16). Such an imaginary point would serve as the reference point instead of the folded vertex.



Figure 4.16 Displacement Measurement

As for the wrinkling condition, the projected area of the fabric ply on the working plane can be a useful indicator. As illustrated in Figure 4.17, when the fabric ply was placed on the working surface with wrinkling or folding, the projection of the workpiece on the working surface would form a polygon. Worse wrinkling conditions would cause a larger portion of the fabric stacking on itself, making the area of the projected polygon smaller. Therefore, the ratio of the projected area with respect to the flattened area can effectively reflect the wrinkling condition.

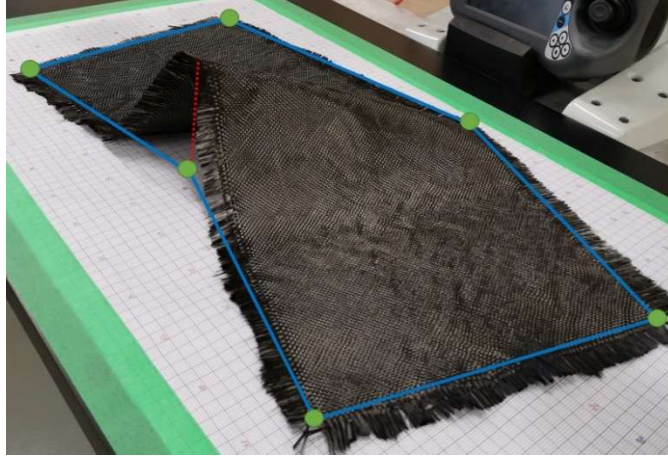


Figure 4.17 Winkling measurement

To measure the projected area of an irregularly wrinkled fabric ply, every two consecutive points of the folded fabric that made up a straight line should be considered. A hanging vertex should be vertically projected onto the working surface. Therefore, every vertex of the projected polygon on the working surface can be expressed by a set of cartesian coordinates. The projected area can then be easily calculated from the coordinates of the vertices.

#### ***4.2.2 Experimental Setup***

The tests in this section would apply both arms of the YUMI robot equipped with the second-generation silicone grippers, as shown in Figure 4.18. The working surface was planar and marked with a coordinate grid so that all reference points can be easily measured. The fabric workpiece was the same type of carbon fiber fabric as previous experiments, but the shape was changed to a rectangle approximately 55 cm by 29 cm. The accurate projection area when flattened was  $1576.1 \text{ cm}^2$ . The friction between the fabric and the working surface remain the same as previous tests.





Figure 4.18 Experiment setup

A rectangular zone was defined by four reference points, identical to the shape of the flattened workpiece. This zone would serve as both the workplace where the fabric is picked from and the target area where the fabric would be placed on. The transferring operations were performed with back and forth movements. Every test would be repeated three times to get an averaged value.

The experiments began with midline picking strategy shown in Figure 4.2. The grippers would pick the fabric on the midline at two points close to the shorter edges of the rectangular workpiece. The distance was determined from trial tests. A one-arm picking strategy from the center point of the fabric would also be performed as comparison. Both the average displacement and the projection area ratio would be recorded generally. However, if the projection area ratio was too small (less than 60% in this case), the displacement became meaningless due to too much folding and would not be measured.

During initial tests, it was discovered that severe draping would occur along the midline as shown in Figure 4.19, causing unacceptable results.





Figure 4.19 Draping along the midline

The situation can be improved by introducing a pre-folding at the centerline of the fabric ply before picking up, as shown in Figure 4.20.

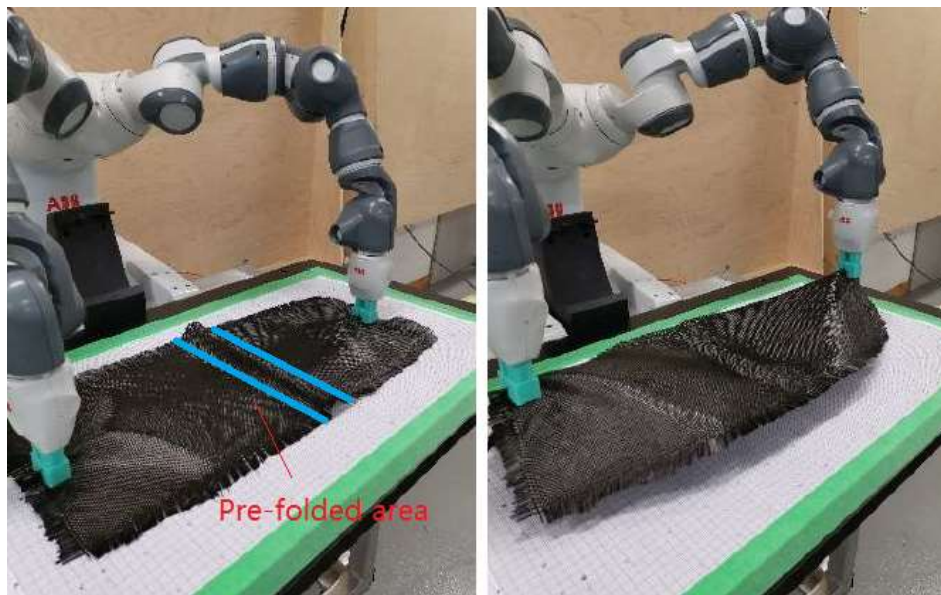


Figure 4.20 Pre-folded picking strategy

This phenomenon was explained that the pre-folded area introduced mild draping in the

center area among the folding direction, resisting the original draping that was perpendicular to it. Following this concept, an auto-jamming toolpath is designed. As illustrated in Figure 4.21, the grippers jammed toward each other after picking up the fabric, creating a draping area in the center automatically. After the movement was finished, the gripper moved away from each other to flatten the fabric before releasing.

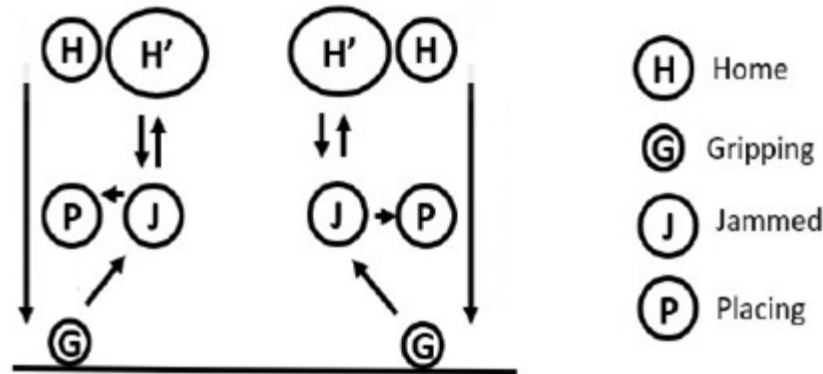


Figure 4.21 Toolpath of the auto-jamming strategy

Both the pre-folding strategy and the auto-jamming strategy are tested under different magnitudes for comparison. For the ease of discussion, both methods would be referred to as the center-folding strategy. The variable would hence be referred to as center-folding magnitude.

After the optimal strategy for midline picking was determined, spatial transferring would be introduced in the tests. Any handling operations can be characterized by a combination of multiple translational movements and rotational movements. Therefore, the special movements applied in these tests included a 10 cm linear translation and a 90° rotation, both were back and forth movements.

Finally, an extra test would perform the same movements using a side-picking strategy, as shown in Figure 4.22. The result would be compared with midline picking strategies.

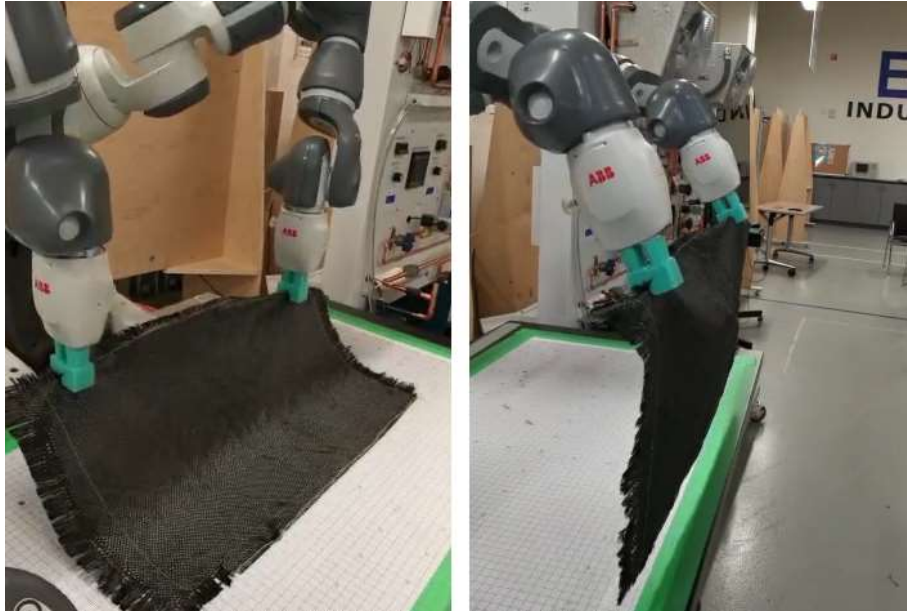


Figure 4.22 Side picking test

#### 4.2.3 Results and Discussion

Figure 4.23 shows the wrinkling results (the projection area ratio) with plain picking strategies, in which the variable is the center-folding magnitude. Figure 4.24 shows the displacement results. The result of one-arm picking scenario was also included as the “extra” result.

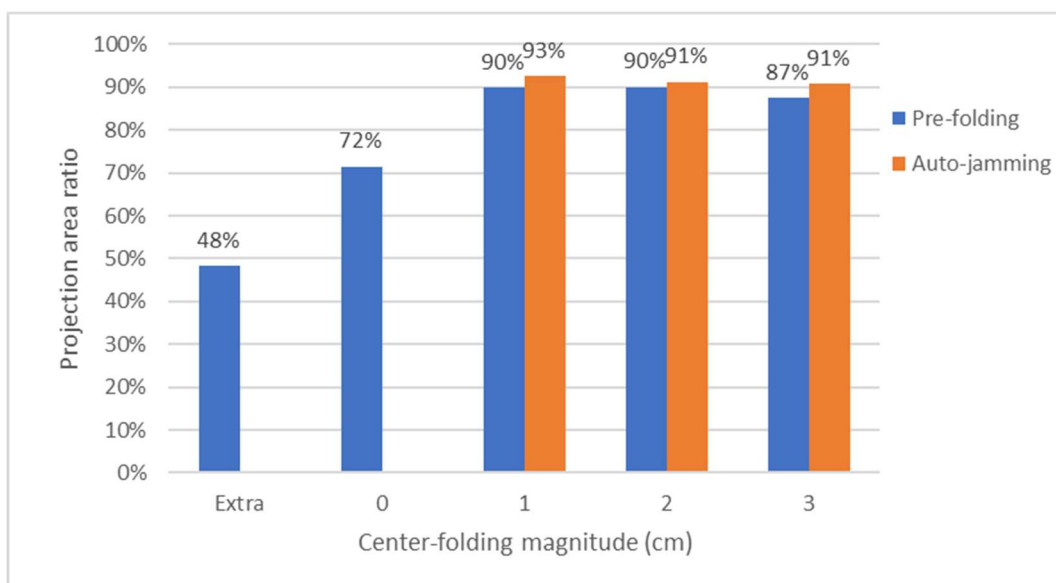


Figure 4.23 Wrinkling results

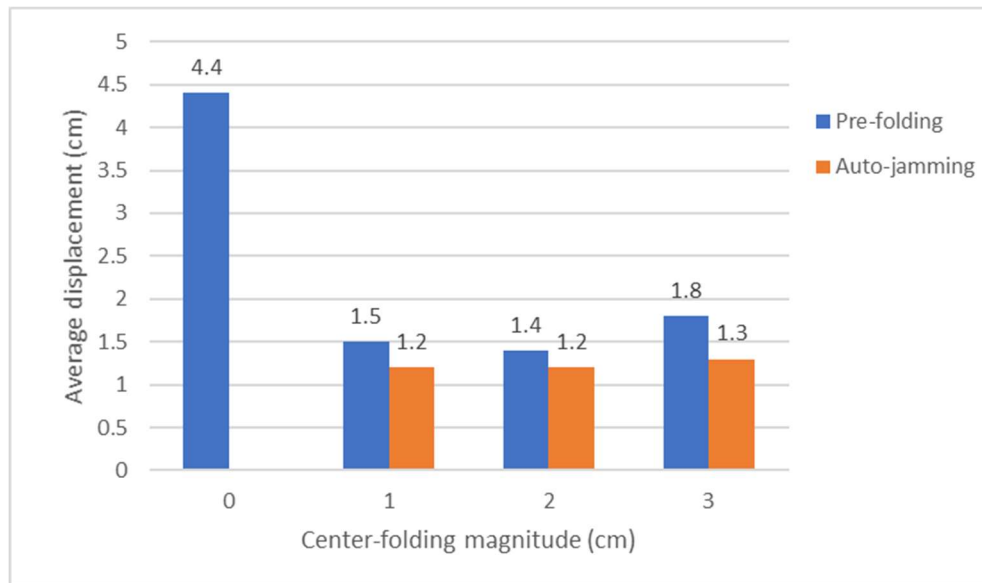


Figure 4.24 Displacement results

As is shown in the figure, the fabric is severely folded for the single arm scenario, proving its inability to provide a good solution. The displacement of this scenario was therefore not measured. When two grippers were applied, the situation was highly improved, but both the wrinkling result and the displacement result remained undesirable. Multiple folded corners had been observed during the tests.

The pre-folding and auto jamming strategies improved the situation. According to the results, the performance of the auto-jamming solution remained constant and were slightly better than the pre-folding solution regardless of the jamming magnitude. The projection area ratio of the pre-folding solution stayed close to correspondent auto-jamming results when the folding magnitude was low, but began to deteriorate when the folding magnitude reached 3 cm. The same trend occurred more clearly for displacement results. This phenomenon could be explained by the fact that the pre-folding solution lacked the ability to remove the center folding after placement. Aside from the superiority in performance, the auto-jamming solution also exceeded in the ease of automation, making it a more desirable strategy.

With the preferred strategy for midline picking, the scenarios with spatial transferring movements were tested. Figure 4.25 shows the wrinkling results and displacement results,

where the compared scenarios included:

- A. midline picking with small jamming magnitude (2 cm)
- B. midline picking with large jamming magnitude (10 cm)
- C. side-picking

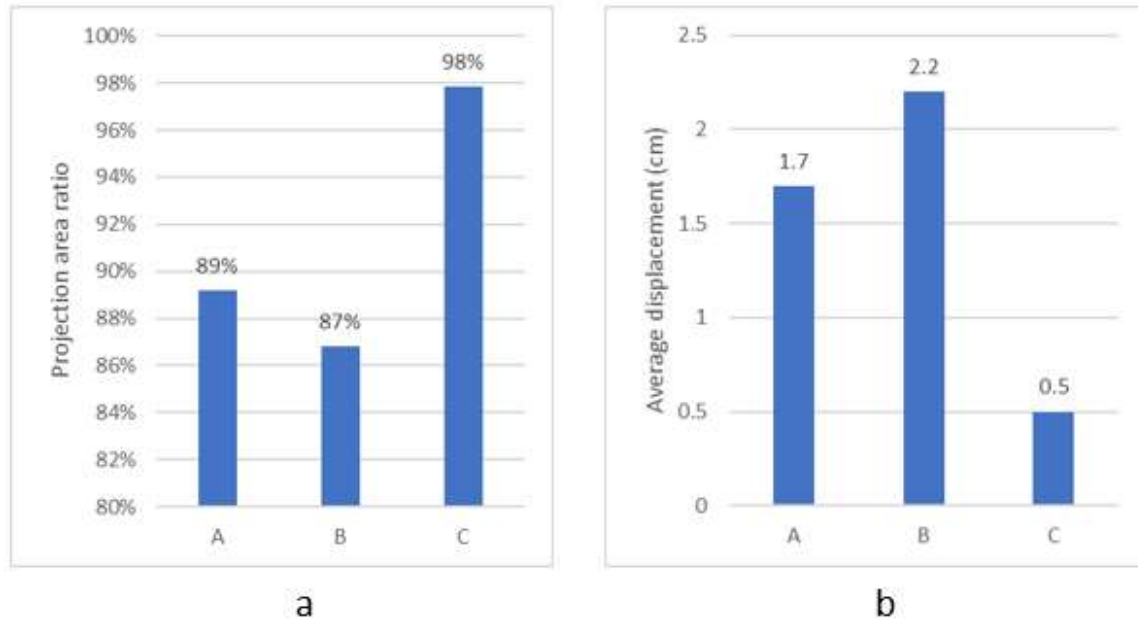


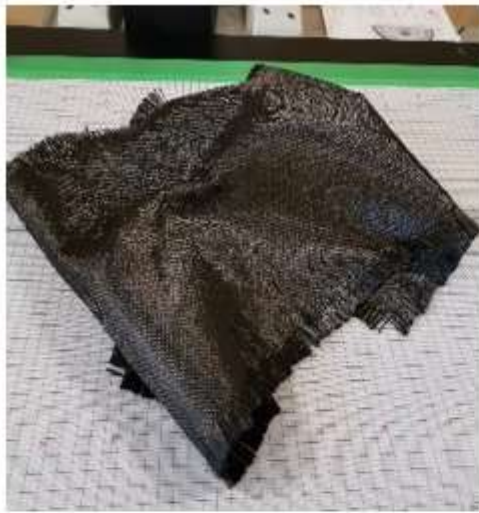
Figure 4.25 Comparison of different picking strategies

a. Wrinkling results    b. Displacement results

Comparing scenario A from the previous results, it can be concluded that spatial transferring movements, no matter whether they are translational or rotational, would not affect the performance of a pick and place strategy. Scenario B suggested that a large center-folding magnitude would slightly worsen the performance of the auto-jamming solution. However, it should be noticed that large center-folding can save space occupation and increase transferring efficiency. Thus, this drawback might be balanced depending on actual applications.

Side picking appeared to be a superior strategy. The wrinkling and displacement were almost entirely eliminated. To visually demonstrate this advantage, examples of typical placing results from previous tests are shown in Figure 4.26.





a



b



c



d

Figure 4.26 Fabric after placing by different strategies

- a. One-arm picking   b. Plain midline picking   c. Auto jammed midline picking  
d. Side picking

So far, it had been fully proved that fabric pick and place operations can be reliably performed by clamping approaches with soft-skin grippers. By appropriate toolpath planning, wrinkling and displacement caused by material deformation can be sufficiently prevented. The side picking approach showed excellent performance, while the insight of the midline picking solution can be easily expanded to more general situations. Collaborative robots appeared to be a useful tool in fabric picking research for its

flexibility and ease of training. More sophisticated toolpath design and simulation would play a critical role to deal with more complicated fabric geometry in future research.

It was noticeable that the 1-DOF gripper equipped with compliant structure can only perform picking on a flat surface. It also lacked the flexibility to perform de-wrinkling movements. A more flexible soft robotic gripper was still needed. This is discussed in next chapter.

## CHAPTER 5

### DEVELOPMENT OF AN UNDERACTUATED GRIPPER

During the previous experiments, it was proven that clamping grippers are capable of performing standard pick and place tasks efficiently for fabric materials. Soft surfaces made of silicone can provide firm gripping condition as well as prevent damaging the fabrics. By introducing multiple grippers and adjusting picking positions, folding and wrinkling can be avoided. However, the simple gripper used in the previous experiments can only perform linear in-and-out movements. Hence, it is only applicable for simple tasks on plain surfaces. The size, shape, and rigidity of the fabrics are also limited to a small variety. In order to deal with more complicated scenarios, an underactuated gripper that can automatically adjust to the working environment would be necessary.

In this chapter, two types of underactuated soft gripper configurations are studied, designed, and tested. The first model is a tendon-driven soft gripper based on silicone elastomer fingers. The second one is an underactuated gripper with silicone rubber skin and with a rigid skeleton.

#### ***5.1 An Elastomer-Based Gripper***

As described in Chapter 3, an elastomer-based finger actuated by pre-inserted tendons can efficiently mimic the motion of human fingers. By attaching two underactuated elastomer fingers onto a rigid palm, the manual picking movement can be reproduced by such a soft gripper. In this section, the mechanical structure of the elastomer finger and the gripper design would be explored.

The curved gripping surface that proved its advantage in the previous chapter is not taken into consideration in this chapter. This feature would remain compatible with the gripper designs presented in this chapter. It can be applied in any applications when needed, and can be explored in the subsequent research.



### 5.1.1 Development of the Gripper Configuration

The basic structure of a tendon-driven elastomer finger is a silicone rubber bar with gaps on the side to create bending. The bar is hence separated by the gaps into multiple sections. As illustrated in Figure 5.1, slots are pre-built within the gaped edge for the driving tendon, which is a string, to go through. A U-shaped tube on the top section constrains the driving string. As the string is pulled downward from the bottom of the finger, the gaps enclose and bend the whole elastomer bar. The magnitude of bending is correlated to the driving force. Hence, a simple linear force can be converted to self-adjusted bending movement. This design was to follow up with the configuration mentioned in Figure 3.6, completing the engineering details.

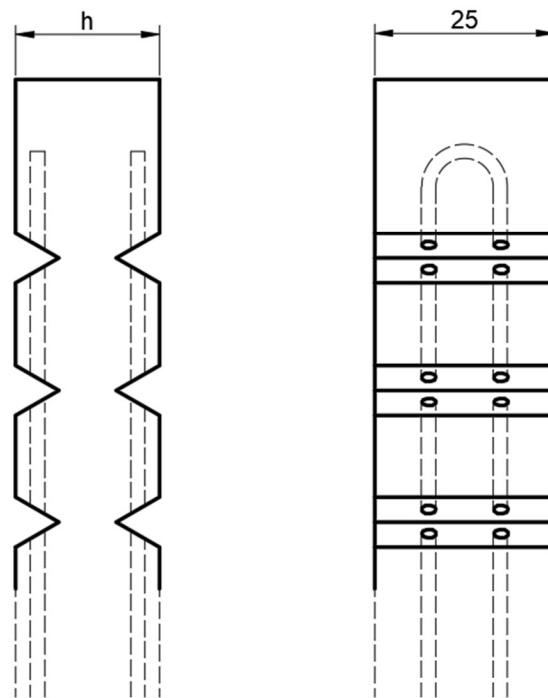


Figure 5.1 Conceptual design of an elastomer finger

The elastomer finger can be one-sided or two-sided depending on the locations of the gaps and driving slots. For fabric picking tasks, bending on both directions are needed, so this finger is designed to be two-sided. The angle of each gap is 60 degrees and the depth of the gap is 6 mm. A 1 mm fillet was designed at the inner vertex of the gap to prevent

stress concentration. The distance between two adjacent gaps is 15 mm. The width of the finger  $w$  is 25 mm. Other features and their effects on the mechanical behaviour need to be analyzed using FEA simulation. The finger is molded using Mold Star 15 SLOW silicone rubber, so the material model developed in Chapter 3 is applied.

First, the relationship between the gaps and the bending magnitude of the top section need to be studied. Ideally, if the finger is made of rigid parts that are connected by hinges and have 60-degree gaps at the edges to limit its motion, then the maximal bending magnitude at the top section can be easily given by

$$\varphi = n\theta \quad (5-1)$$

where

$\varphi$  – the angle between the centerline of the top section and the vertical line

$n$  – the number of gaps

$\theta$  – the opening angle of each gap. Here,  $\theta = 60^\circ$ .

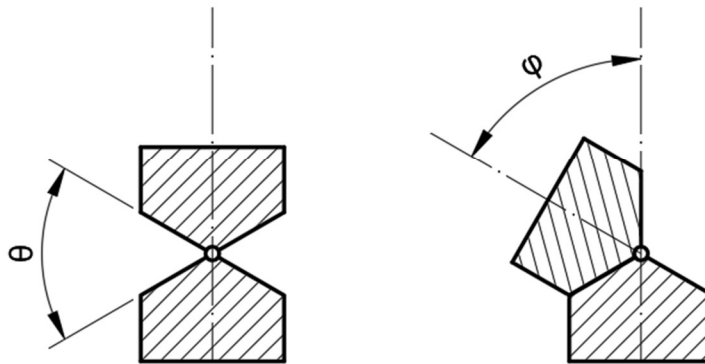


Figure 5.2 Bending magnitude and gap size

Figure 5.2 illustrated such an ideal scenario. However, for the elastomer finger, due to the thickness and the hyperelastic nature of silicone rubber, the actual maximal bending magnitude would be smaller than the hinge-based simplification. When the size of each

gap is determined, the maximal bending magnitude would be influenced by the finger thickness  $h$  shown in Figure 5.1.

Since the structure of the elastomer finger contains a linear pattern, the mechanical behavior of the whole finger is based on that of each section. An FE model is established to simulate the behavior of a single section, as shown in Figure 5.3.

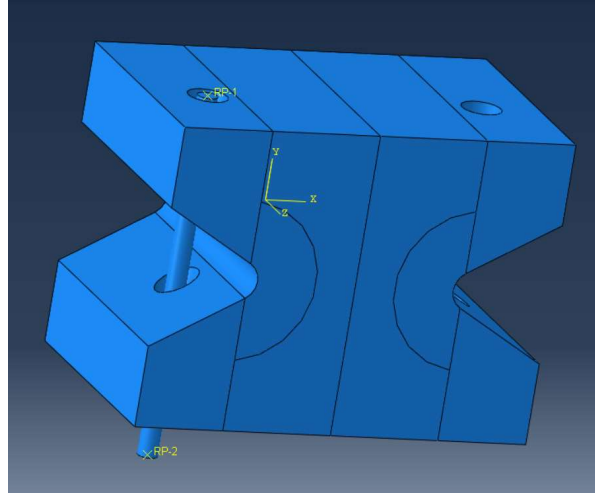


Figure 5.3 FE model of a unit section

Because the structure is symmetrical, only half of the section need to be modeled. Symmetrical boundary conditions for the Z-axis is applied to the corresponding surface. A contact relationship is established between the slot and the string surfaces. Self-contact is established on the gaped surface. This simulation is a static simulation, for this simulation focused on the mechanical behavior under relative static conditions rather than its dynamic responses. Due to the same reason, the friction between the contact pairs can be neglected.

An encastre boundary condition is applied to the bottom surface of the finger to fix it to the ground. The top surface is coupling constrained to the same control point as the upper tip of the driving string. Therefore, when the string is pulled downward, the entire top surface would rotate as a plain surface, which is the same as the behaviour of a section when the whole finger bent. The bending magnitude of one section  $\varphi_i$  equals to the angle between the top surface and the horizontal plane.

The hyperelastic material model developed in section 3.5 is applied for the rubber, while the string was modelled using elastic material. The model is segmented and meshed using C3D8RH elements. The string is meshed using C3D8R elements. A 4.8 mm displacement was applied to the bottom tip of the string. The driving force, which is the reaction force at the bottom tip of the string, is recorded as well. The simulation is run with different finger thickness.

Two typical results are shown in Figure 5.4 as examples. When the 4.8 mm displacement was accomplished, the gap became fully enclosed, and the top surface rotated to a certain degree. After the result was obtained, the model was re-meshed denser to test its validity. As the mesh was refined, the change of result was less than 5%, proving the appropriateness of the FE model.

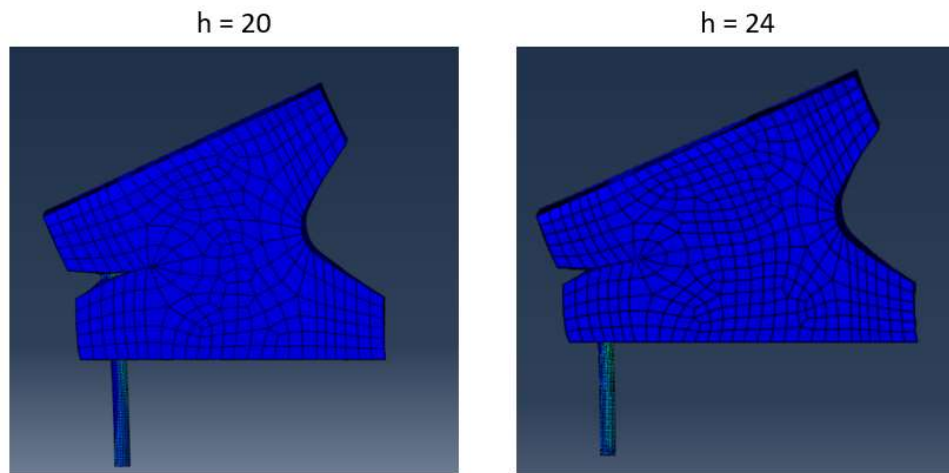


Figure 5.4 Sample results

Figure 5.5 shows the relationship between the maximal bending magnitude and the finger thickness. Figure 5.6 shows the relationship between the maximal driving force and the finger thickness.

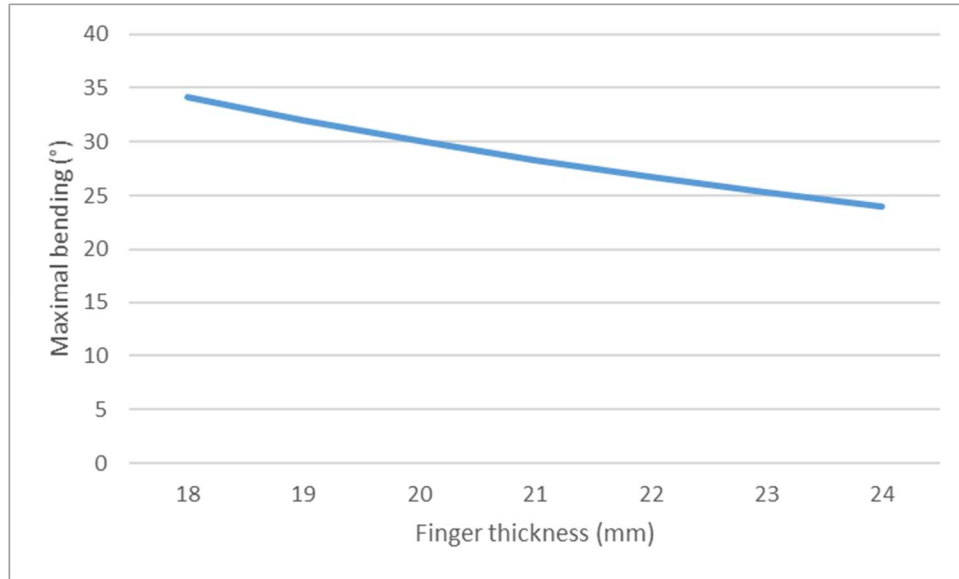


Figure 5.5 Maximal bending magnitude of different thickness

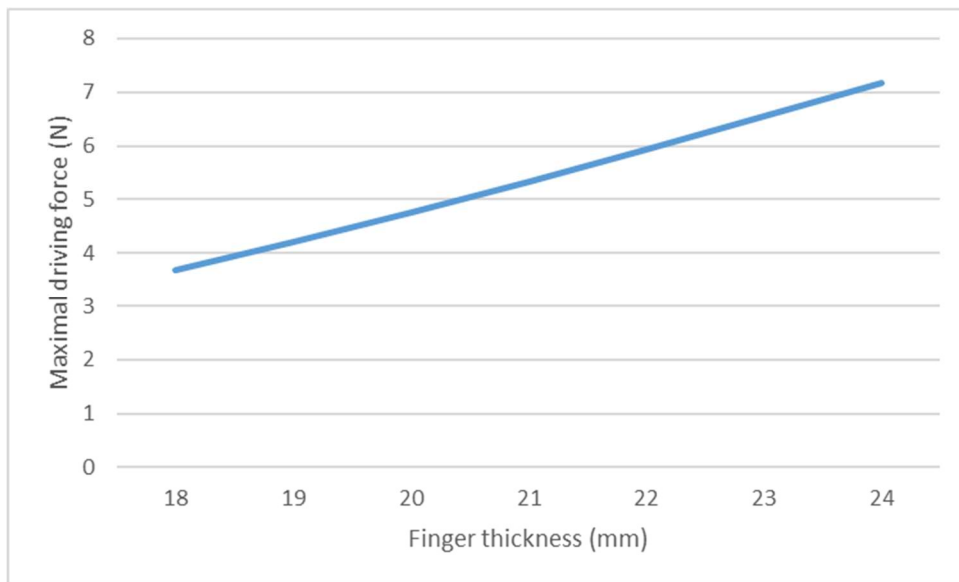


Figure 5.6 Maximal driving force for different thickness

According to the results, as the thickness of finger increases, the maximal bending magnitude decreases, and the driving force increases. Usually, larger bending magnitude and smaller driving force are preferred. However, when the thickness is too small, the stiffness of the finger would become too small, hence make it less controllable and unreliable. The actual thickness should be decided based on the size of the gripper. In this research, the thickness was chosen to be 20 mm, where the maximal bending magnitude

was close to 30 degrees.

When the maximal bending magnitude of a single section  $\varphi_i$  is known, the maximal bending magnitude of the whole finger can be given by

$$\varphi = \sum_1^n \varphi_i \quad (5-2)$$

where n is the number of gaps on the corresponding side.

For this project, the inner side of the finger, which is the gripping side, should be parallel or nearly parallel to the fabric surface when the gripper is fully opened. That means the maximal bending magnitude of the outer side of the finger should reach approximately 90 degrees. Therefore, the number of gaps on the outer side should be at least three.

A full FE model of the finger was developed to investigate the effect of the number of gaps. The model is shown in Figure 5.7a.

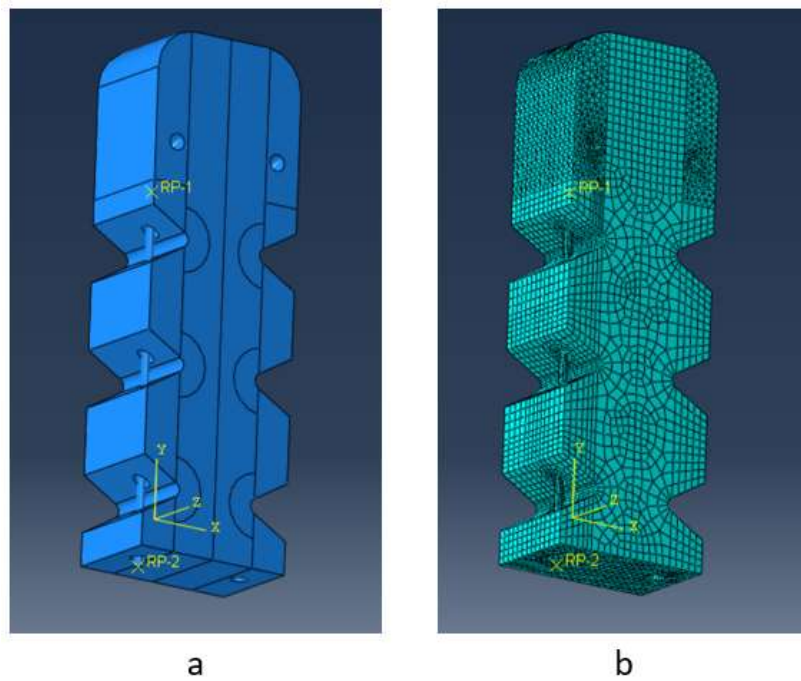


Figure 5.7 FE model of the elastomer finger

a. Assembly    b. Meshed model

Like the one-section model, this model was symmetrical along the Z-axis. Contact pairs were established. The coupling constraint was applied to the inner surface of the U-shaped tube to connect the finger and the string. The coupling constraints limited all six degrees of freedom, causing the relative position of every node on the constrained surface to remain constant to the control point. Compared to the physical finger where the U-tube may slightly deform, this simplification is not 100% realistic. However, the detailed stress and deformation on the U-tube, which is much more rigid than the silicone rubber, were not of concern. Therefore, such simplification would be acceptable.

The finger model was sectioned and meshed mainly with C3D8RH hexahedral elements. Due to the geometrical complexity, C3D4H tetrahedral elements were used at the regions where the U-shape tubes were present. Being a linear element, C3D4H does not have high integrity during analysis, but this problem can be neglected for the detailed behaviors in those regions were not of concern. The mesh around the regions where contact or large deformation would happen were created denser. The string was still meshed using C3D8R elements. Figure 5.7b shows the meshing strategy.

By changing the number of the gaps on the outer side or the inner side, there could be several variations of the finger model. A certain combination of outer and inner gaps can be represented by an abbreviation code  $O_xI_y$ , where a number  $x$  stood for the number of gaps on the outer side and a number  $y$  stood for the number of gaps on the inner sides. As an example, the configuration in Figure 5.7 can be noted by  $O3I3$ . Here, the simulated configurations included  $O2I2$ ,  $O3I1$ ,  $O3I2$ ,  $O3I3$ , and  $O4I4$ . For each configuration, a 4 N force was applied downward on the bottom tip of the string. The displacement of the bottom tip of the string and the driving force were recorded. Figure 5.8 shows the bending results. Figure 5.9 shows the displacement-force relationships for different configurations.

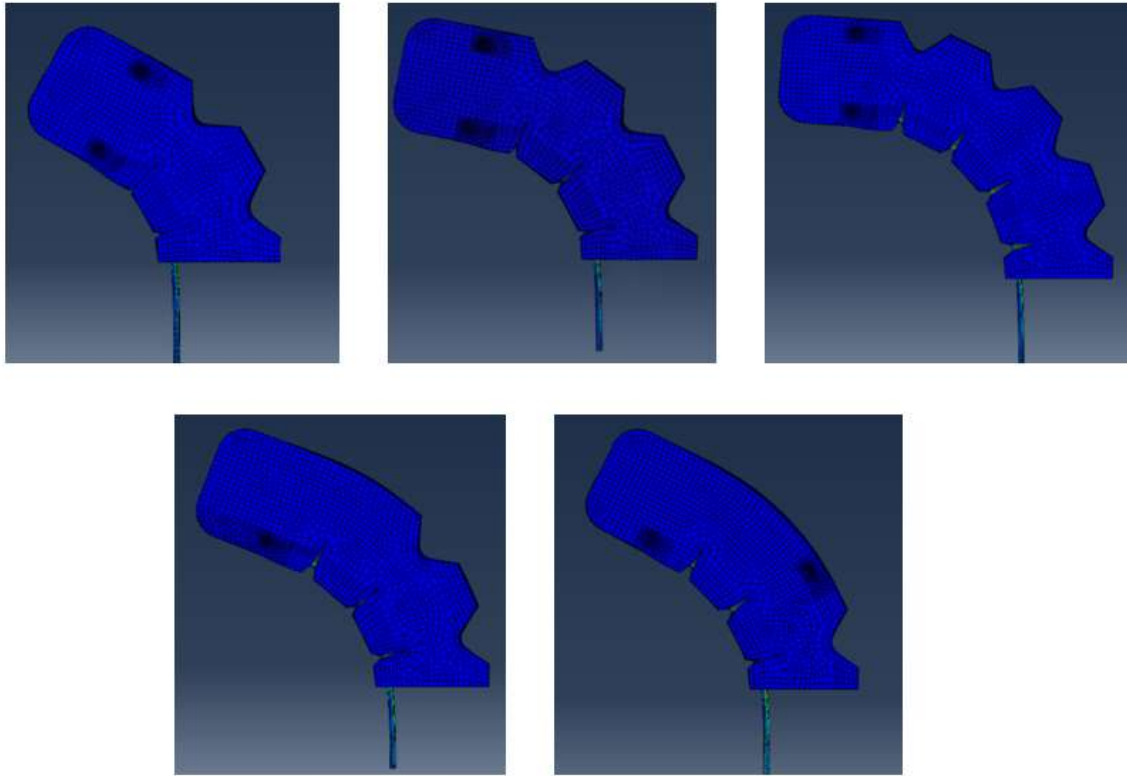


Figure 5.8 Deformation results of different configurations

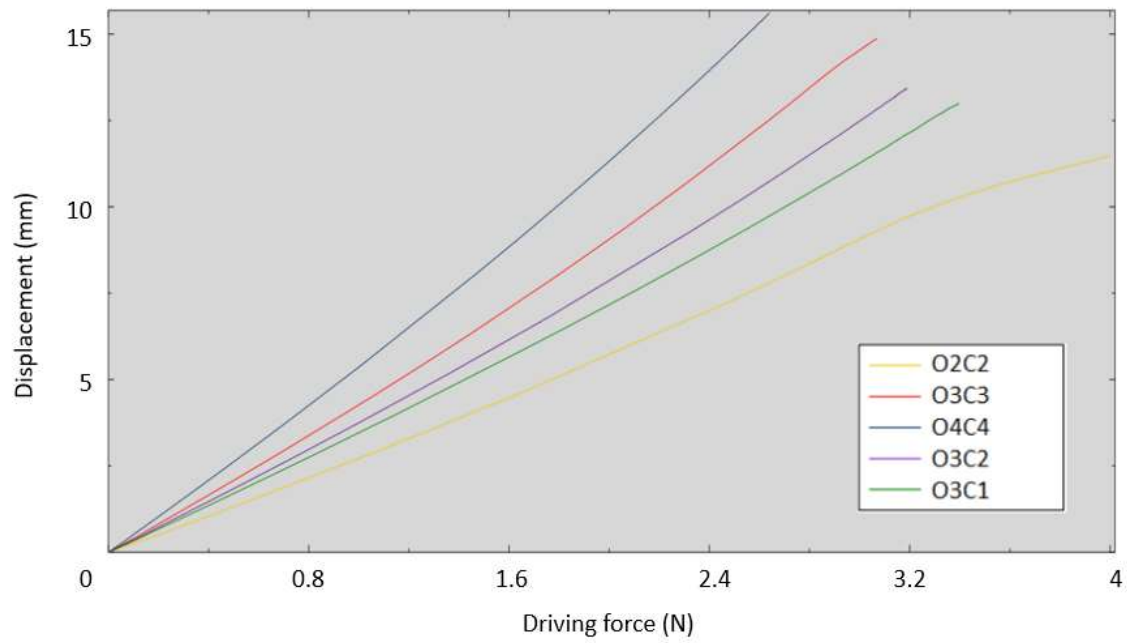


Figure 5.9 Displacement-force results of different configurations



The actuation did not reach its full capacity for some cases due to convergence difficulty, but the trend was available. It could be observed that when the gap distribution was symmetrical, more gaps/sections led to lower stiffness. That is, less force was required for the finger to bend to a certain magnitude. When the number of gaps remained constant on the outer side, decreasing the number of gaps on the inner side would increase the stiffness.

If the stiffness was too high, not only too much actuation force would be required, but the maximal bending magnitude would not be able to reach  $90^\circ$ , as in the cases of O2I2 and O3I1. Extremely low stiffness was not desired, either. The finger would become less controllable and highly sensitive to environmental disturbances. A typical example is the draping under gravity. When the gripper was aligned parallel to the ground, the maximal vertical displacement at the tip caused by self-weight was 5.97 mm for the O3I3 configuration and 14.14 mm for the O4I4 configuration.

As for the gripping movements, a similar model can be created as shown in Figure 5.10. An analytical rigid plane was fixed at the midplane of the gripper where the gripping would happen. The finger and the string were constrained and meshed using the same strategy. A 6 N driving force was applied.

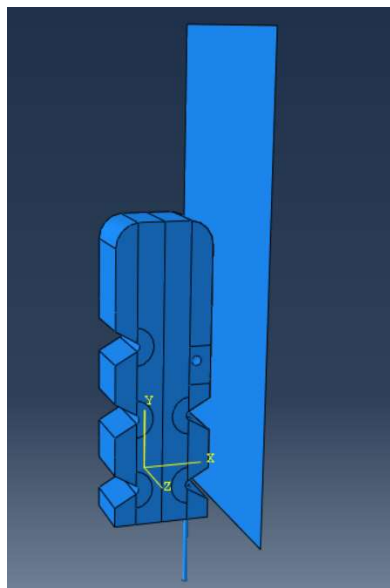


Figure 5.10 FE model for gripping simulation

It was discovered that when there were too many gaps on the inner side, the gripper tended to bend around multiple gaps, causing the tip to roll against the gripping plane, as shown in Figure 5.11a. The bending continued as the upper gaps enclosed and the bottom gap opened up. This rolling grip phenomenon would cause poor contact condition and was not desired. The problem can be solved by limiting the number of gaps on the inner side. As for the O3I2 configuration shown in Figure 5.11b, the rolling grip was stopped as the upper gap fully enclosed. The elastic nature of the elastomer material would then create firm gripping that can adjust to the object to be gripped.

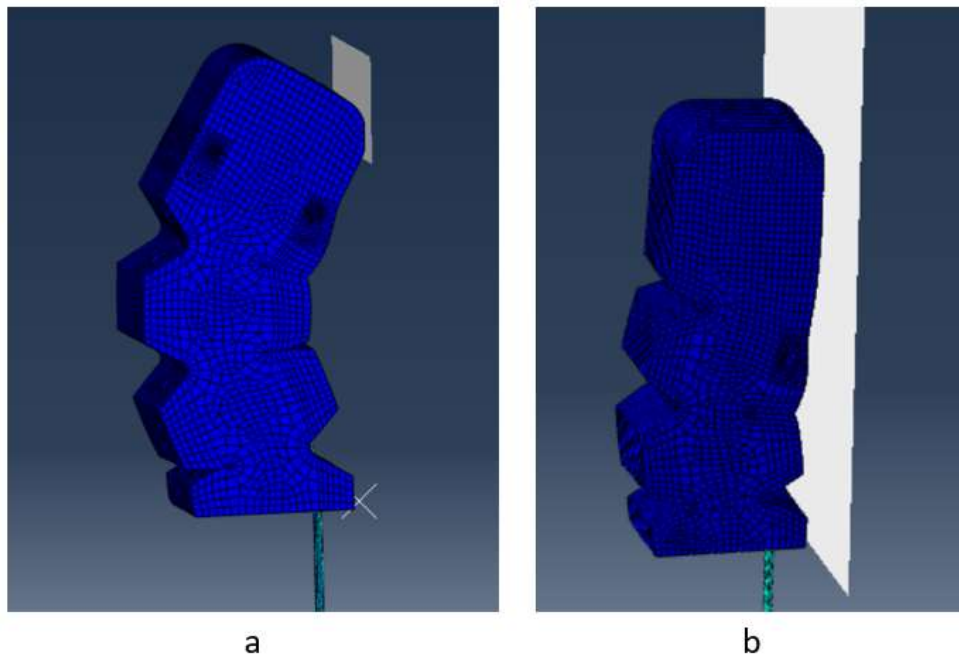


Figure 5.11 Different gripping conditions

a. Rolling grip   b. Firm grip

It was discovered that the distance from the midplane to the fingertip did not affect the gripping efficiency, which is the proportion of the gripping force to the driving force. Meanwhile, it was found that by adding an inclined surface at the fingertip as shown in Figure 5.12, the gripping efficiency can be increased.

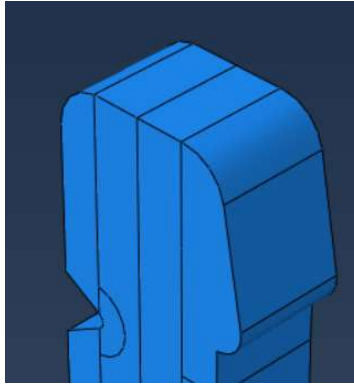


Figure 5.12 Inclined fingertip

Different fingertip angles were simulated and compared. Figure 5.13 shows the relation between gripping force and driving force for multiple scenarios.

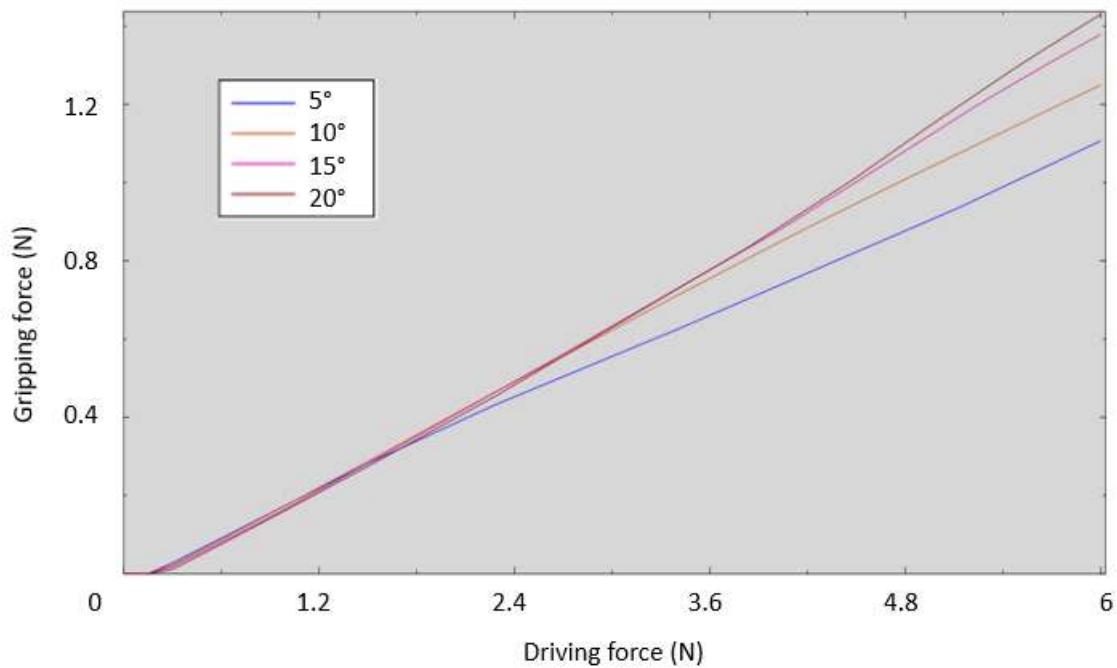


Figure 5.13 Gripping force of different fingertip angles

At the beginning of actuation, the gripping force remained zero until the fingertip touched the midplane. The gripping force then started to increase proportionally with the driving force. A larger tip angle had higher gripping efficiency, but this advantage became less

significant as the tip angle increased. A larger tip angle would also increase the size of the gripper and make it more sensitive to gravity. The actual parameter should be decided based on the application.

After balancing all previously mentioned variables, the final design was determined to be an O3I2 configuration with 20 mm finger thickness and a  $15^\circ$  fingertip. Figure 5.14 shows the CAD design of the gripper assembly.

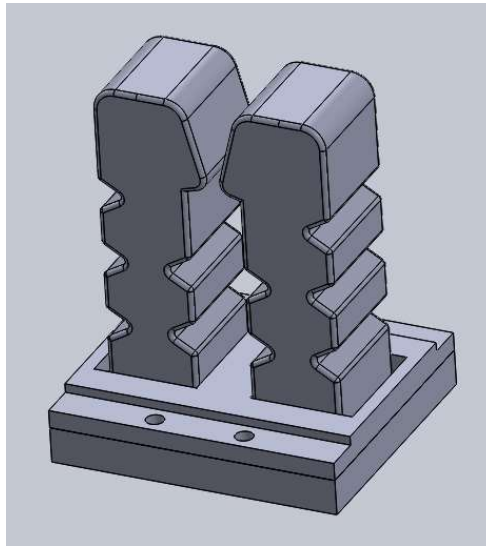


Figure 5.14 CAD model of the gripper

Based on the geometrical symmetry of the gripper design, the behavior of the full gripper can be obtained from the half-finger FE model (force multiplied by four). Because the TCP would shift as the fingers bend, the deformation of the fingers during the opening movement would be important reference data for controlling strategy. As shown in Figure 5.15, a reference point was created from the extension lines of the geometrical boundaries of the fingertip to monitor the tip displacement during the opening process.

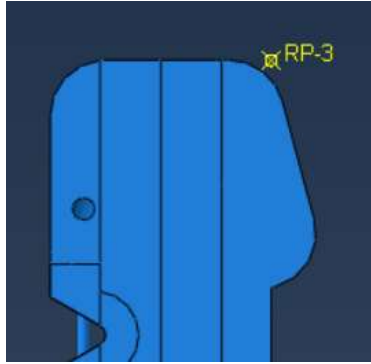


Figure 5.15 Fingertip reference point

The relationship between the string tip displacement and the driving force is shown in Figure 5.16. Figure 5.17 shows the relationship between the fingertip displacement on vertical direction and the driving force. Figure 5.18 shows the trajectory of the tip reference point for one finger (using the initial position as the origin).

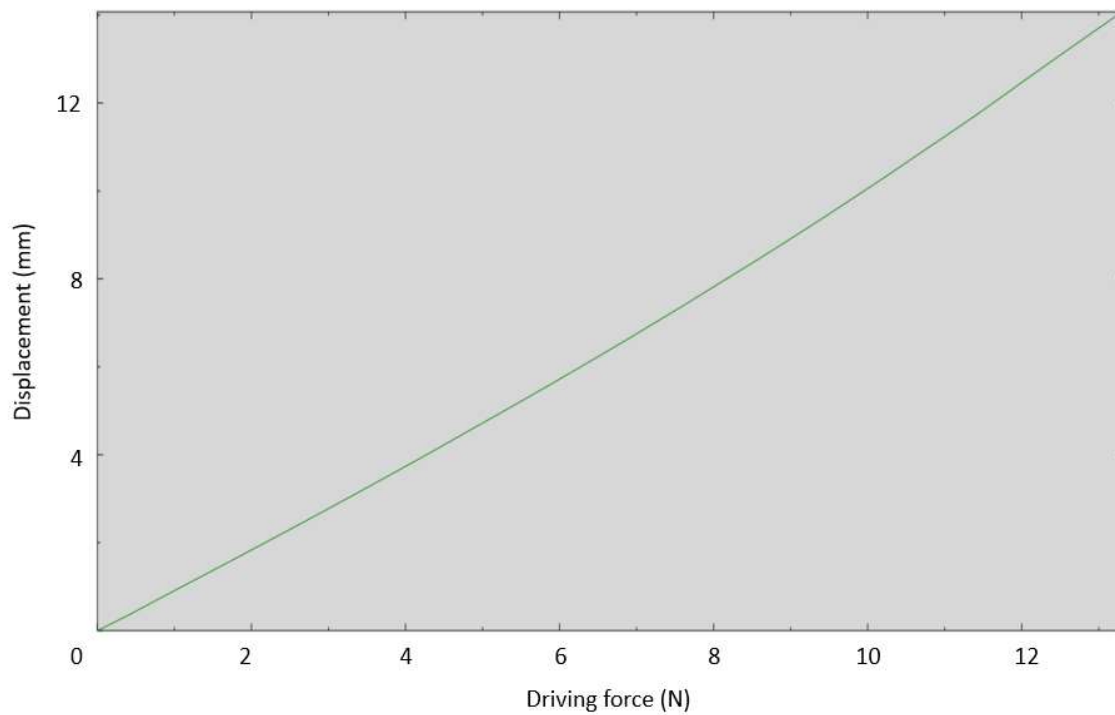


Figure 5.16 String tip displacement

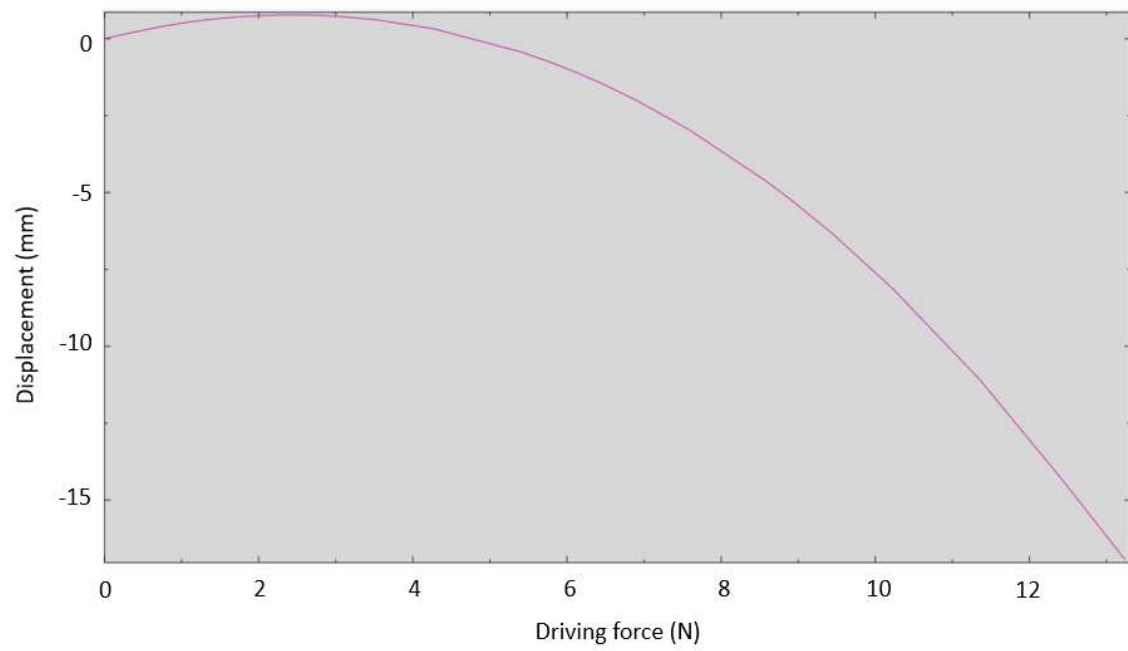


Figure 5.17 Fingertip displacement in vertical direction

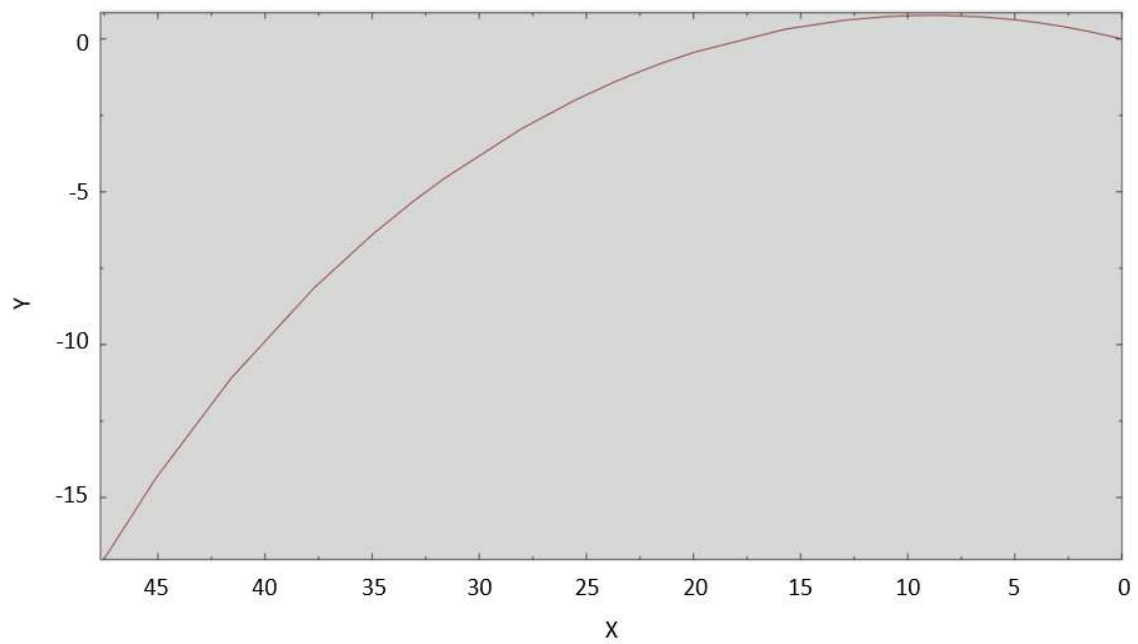


Figure 5.18 Fingertip trajectory

### 5.1.2 Gripping Simulation

A dynamic explicit simulation is established to verify the functionality of the gripper design. The property model of the fabric developed in section 3.5.2 is applied. The FE model configuration is shown in Figure 5.19. Two fingers are located symmetrically in respect of the Y-Z plane. An analytical rigid plane that serves as the working surface is placed underneath. The fabric workpiece is modelled to be a 300 mm by 100 mm rectangle and is placed on the rigid plane. Due to the geometrical symmetry, the model includes only half of the physical scenario. A symmetrical boundary condition along Z-axis is applied to the corresponding side of the fingers and the fabric ply.

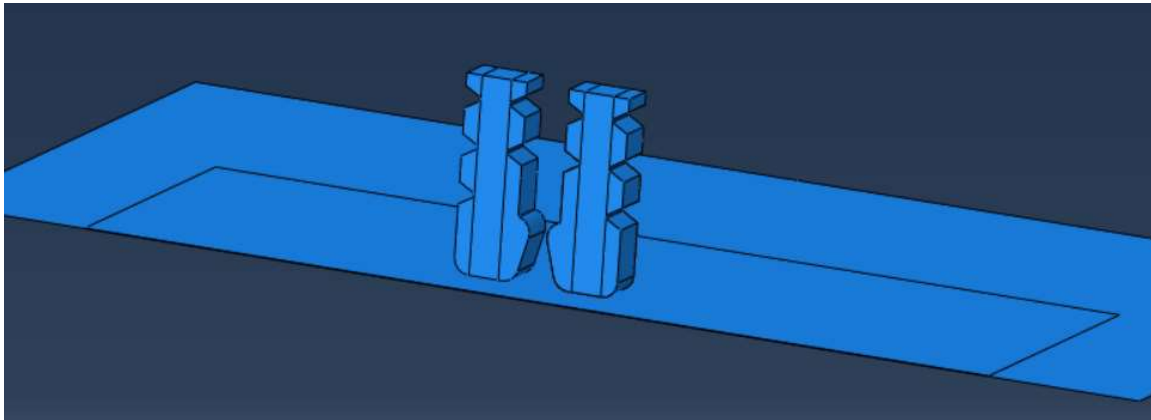


Figure 5.19 FE model for gripping simulation

The complexity of this model is much higher than the simulation of a single finger. Multiple simplification strategies are applied to save the computational expense. Since the accurate force-deformation relation of the elastomer finger is no longer of concern, the models of the actuation cables and slots are removed. Instead, the actuation is achieved by applying forces onto certain reference points that are coupling constrained with certain geometry on the finger models. The forces are adjusted so that the finger deforms in a nearly identical way as the realistic model previously studied.

The simulation includes three steps: opening, gripping, and lifting. The bottom surfaces of the two fingers are fixed at all time. Meanwhile, the rigid plane moves steadily to relatively simulate the lifting and lowering movements of the gripper during the picking

operation. According to experimental data, the friction coefficient between the fabric and the working surface is set to 0.3. The friction coefficient between the fabric and the fingertip is set to 0.7. Other contact pairs are simplified as frictionless. A 9800 N/ton gravity field is applied. At the opening stage, the rigid plane moves upward for 35 mm as the fingers bend to open the gripper. At the gripping stage, the rigid plane steadily moves back to its original position, and the modified loading condition causes the gripper to enclose and grip the fabric. Finally, the rigid plane moves downward, causing the fabric to be picked away from the working surface.

Figure 5.20 shows the whole picking process of the simulation result. The visualization of the result is mirrored in respect to the X-Y plane. It is thus verified that the gripper can successfully pick up the fabric ply and hold it firmly, as the design criteria requires.

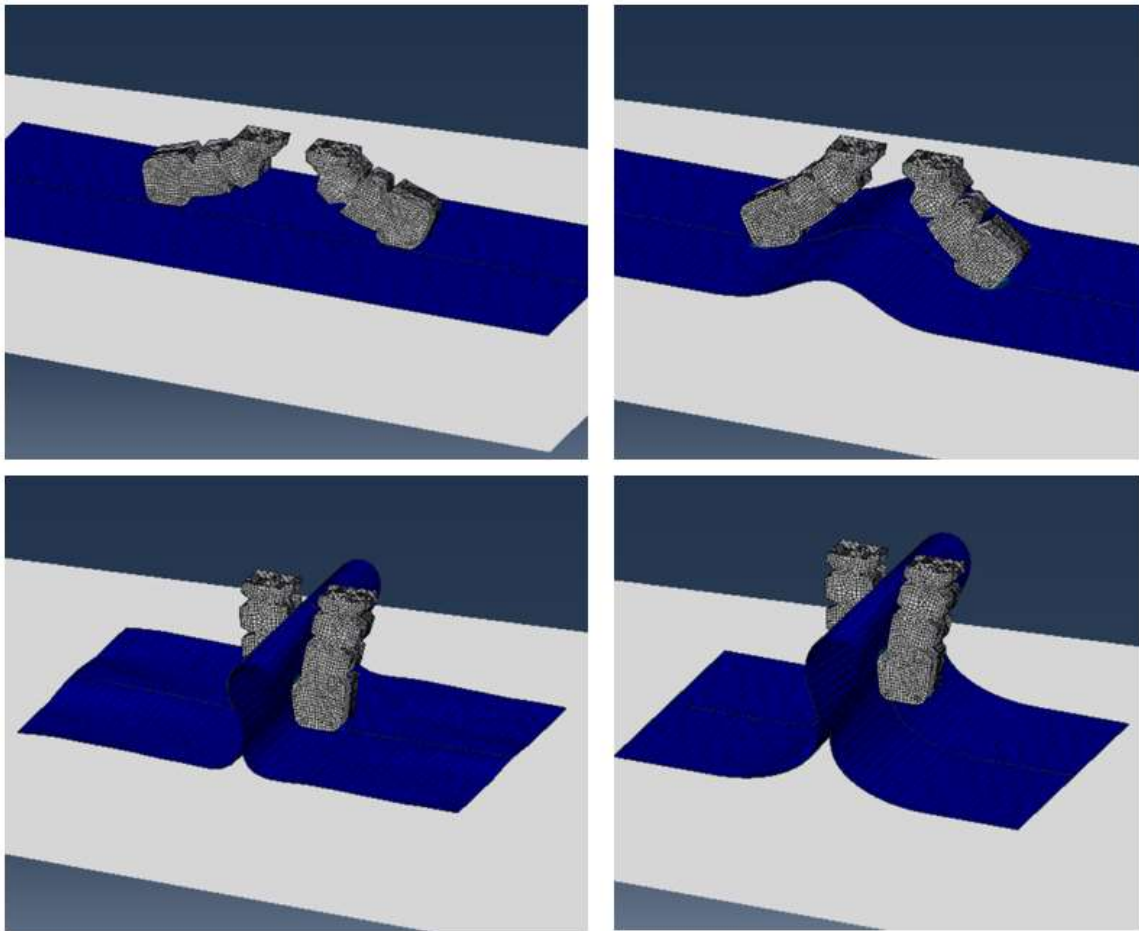


Figure 5.20 Gripping simulation



Similarly, a modified FE model shows that the gripper can also pick up the fabric ply from a curved surface, as shown in Figure 5.21.

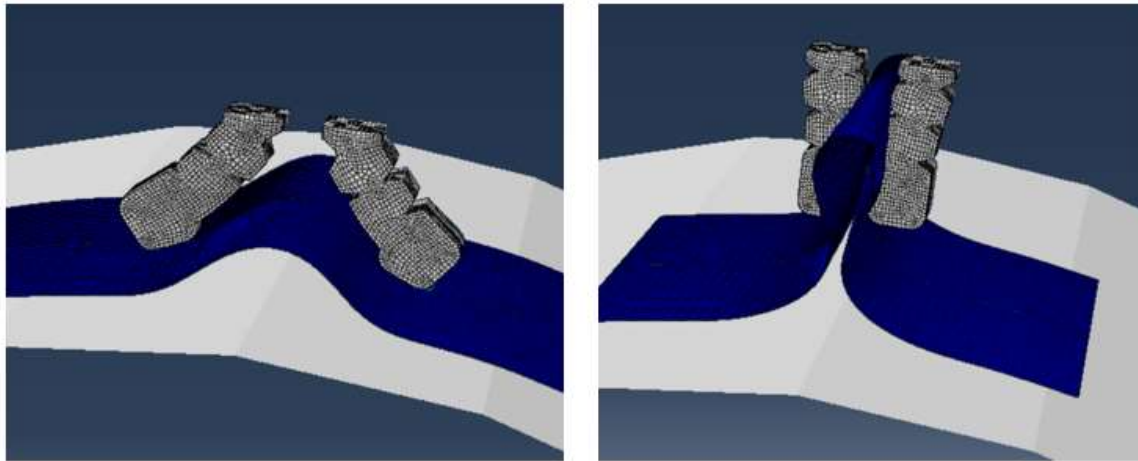


Figure 5.21 Gripping simulation on a curved surface

### 5.1.3 Prototyping and Experiments

A prototype was fabricated using the methods mentioned in section 3.4. Based on the CAD model, a mold set was created through FDM process. The mold set is shown in Figure 5.22a.

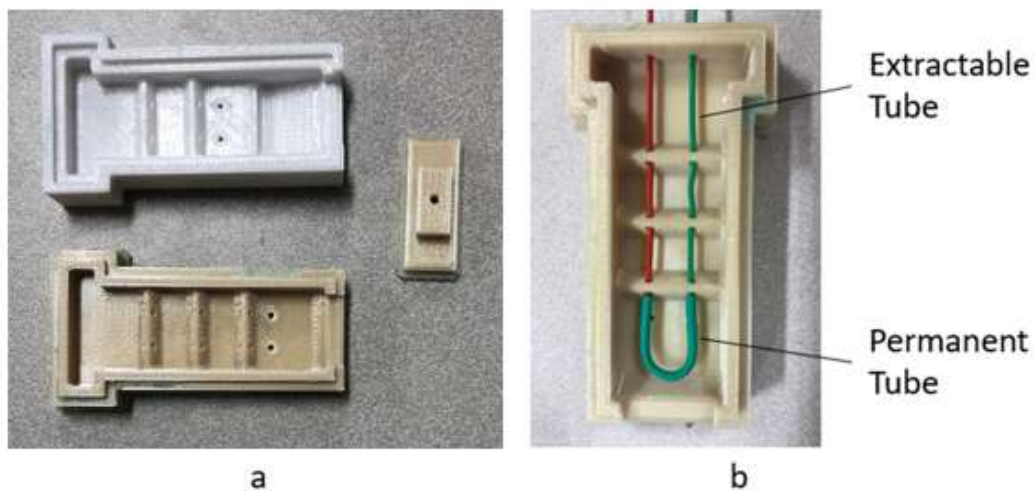


Figure 5.22 Mold set

Figure 5.22b shows the assemble strategy for overmolding. The heat-shrink plastic tube was soft when heated so it can be deformed to create the U-shape permanent tube. The rigidity of the tubes became much higher after fully shrank and cooled down. Two extractable tubes, on which the U-shape tube was attached, were inserted through pre-built holes on the mold. After the silicone cured, the sticks were removed, and the U-shape tube remained inside the finger. The driving string would then go through the U-shape tube and the slot in the finger that was formed by the extractable tubes.

The gripper base can also be directly printed though FDM process. Figure 5.23 shows an assembled gripper prototype (without driving mechanism).



Figure 5.23 Gripper prototype

It took 2 hours and 35 minutes to print the mold set and approximately 3 hours to remove the support material. The material used to make the mold set is ULT9085. The time and effort spent on removing support material may be reduced if the AM material is polycarbonate or ABS, whose support material can be removed more easily and thoroughly. With the mold set prepared, it would only take about an hour to mold one silicone finger. The gripper base was directly printed, which took an hours and 26

minutes to print and approximately 30 minutes to remove the support material. The time consumption is summarized in Table 5.1.

Table 5.1 Fabrication time

Reusable	Printing the mold set	2h35m
	Removing support material	3h
Molding silicone fingers		1h * 2
Printing the gripper base		1h26m
Removing support material		30m
<b>Total</b>		9h31m (first time) / <b>3h56m</b>

As so calculated, it would take approximately 3 hours and 56 minutes to make one gripper prototype with the mold set available, which was quite efficient.

The weight of one finger was 51 g. the weight of an assembled gripper was 127.5 g. The geometrical parameters for opened and closed gestures were measured, as illustrated in Figure 5.24. A bluing test was performed to observe the contact condition. Table 5.2 summarizes these geometrical data of the gripper prototype.

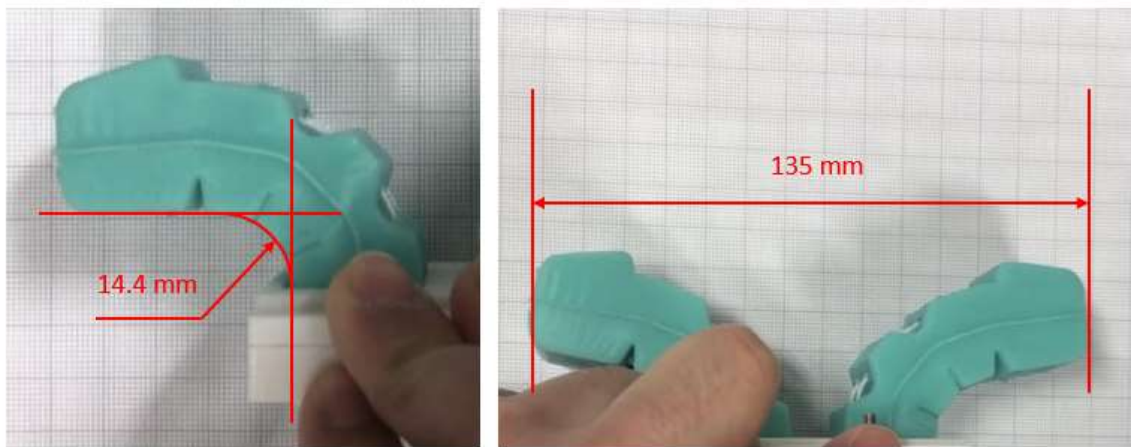


Figure 5.24 Geometry measurement

Table 5.2 Geometrical data

<b>Size (mm)</b>	Normal	Maximum open
	93 * 55 * 47	66 * 135 * 47
<b>Weight (g)</b>	Gripper	One finger
	127.5	41
<b>Maximum open angle (°)</b>	180	
<b>Maximum open length (mm)</b>	135	
<b>Maximum bending radius (mm)</b>	14.4	
<b>Maximum contact area (mm<sup>2</sup>)</b>	375	

Because the access to change the robot gripper was not obtained during the research period due to COVID-19, a manual test was performed to verify the capability of the gripper. The tests included picking up a single fabric ply, separating one ply from a stack, and the de-wrinkling process. It should be noticed that the human operations during the tests only included pulling the actuation tendons and pressing the gripper base linearly, so the processes can be easily programmed with a robot.

The opening magnitude of the gripper can be controlled by the actuation force, so is the bending angle of both fingers. The gripping interaction is a result of the friction between the fingertip and the fabric ply, which can be achieved by applying a pressure perpendicular to the working surface. With the large variety of opening gestures, the gripper can obtain a firm gripping from inclined or curved surfaces. It was also shown possible to separate one fabric ply from a stack of fabric mats. By applying a moderate pressure perpendicular to the fabric surface while gripping, the gripper successfully picked up a single ply without causing any disturbance to the fabric underneath. Finally, the gripper can also be used for de-wrinkling by reversing the gripping motion. These processes are shown in Figure 5.25.

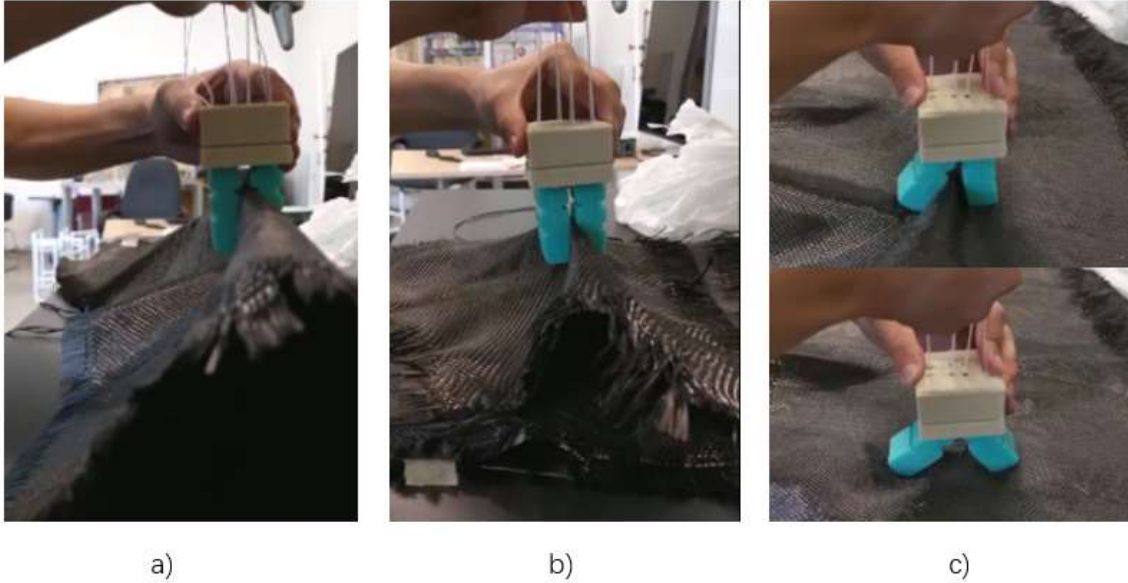


Figure 5.25 Manual tests

a. Picking up a single ply   b. Separating a ply from a stack   c. De-wrinkling

The force response during the actuation procedures were measured using a force gauge. Figure 5.26 shows the relation between the displacement of the string tip the driving force. the data was compared with the simulation data previously obtained to validate the FE model. It was also measured that it required approximately 31.36 N driving force to fully enclose the gripper.

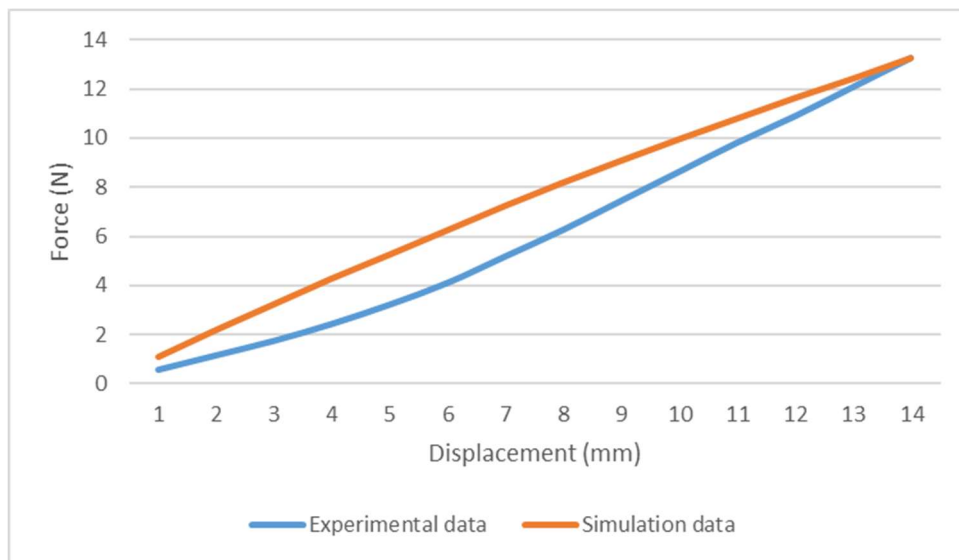


Figure 5.26 Comparison between experimental data and simulation data

The CC of the experimental data and the simulation data was calculated to be 0.9882. The simulation successfully predicted the overall behaviour of the gripper. It can be observed that there was relatively larger error at the initial stage, where the experimental data showed an accelerating trend that the simulation did not capture. This could be caused by imperfection of the hyperelastic material model used in the simulation. Other factors may also accumulate to the error, such as the shift between the U-shape tube and the inner surface of the elastomer, the elastic behavior of the string, the measurement error, etc.

With the data collected, a driving mechanism was designed as shown in Figure 5.27. The actuation power was achieved through a disc connected to a servo motor. Driving tendons were led through a separator and connected to the disc. The opening and gripping tendons were driven by different rotary directions respectively. The gripper base was connected to the motor box through a connector, so different gripper configurations can be fit to the same motor box.

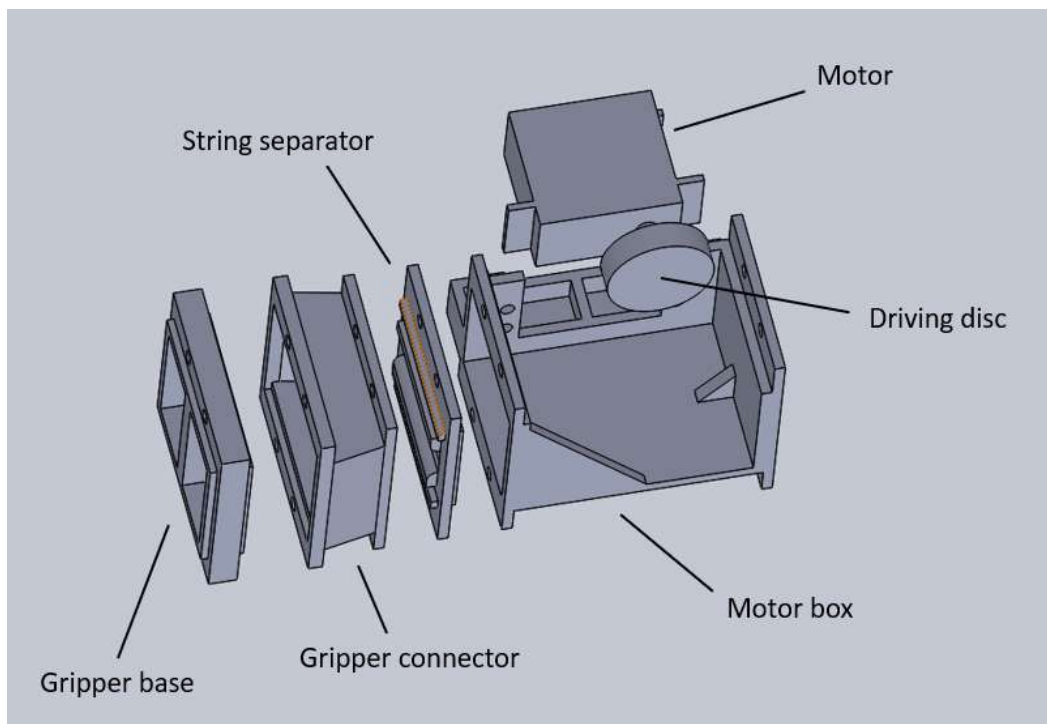


Figure 5.27 CAD design of the driving mechanism



The components were fabricated through FDM processes. A MG996R servo motor was selected for this prototype. Figure 5.28 shows the assembled prototype. Different gestures are shown in the following figures.

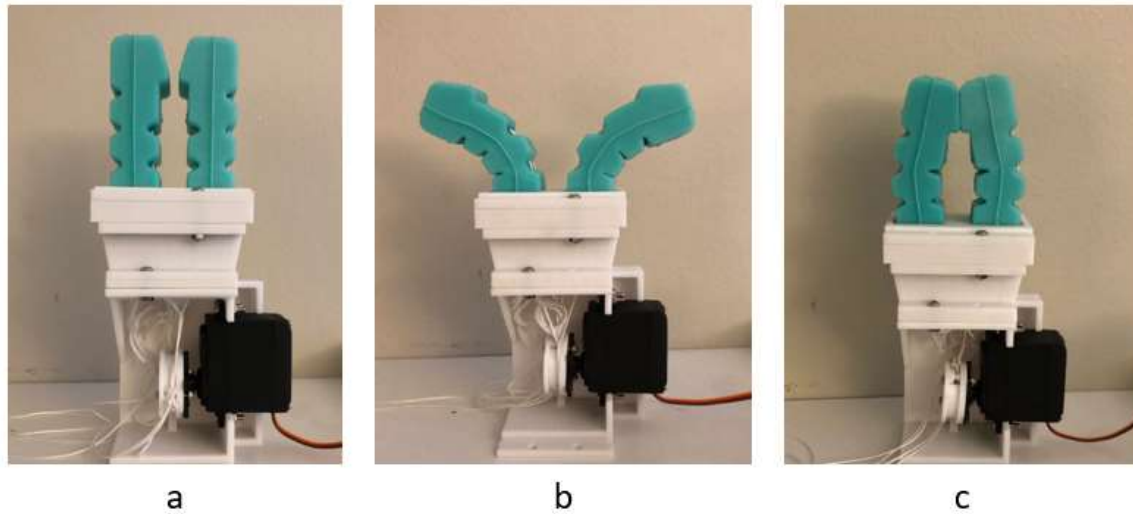


Figure 5.28 Gripper prototype with driving mechanism

a. Rest gesture   b. Opening   c. Gripping

## ***5.2 A Linkage-Based Gripper***

The elastomer-based gripper proved its capability for the objective operations of this project. One possible limitation of the gripper is that the elastomer fingers were relatively sensitive to environmental disturbances. This would be more obvious if the gripper configuration needs to be enlarged. The simulation for the elastomer structures was relatively complex due to the number of variables. In this section, a linkage-based underactuated gripper configuration is designed and assessed based on the insights previously obtained.

### ***5.2.1 Gripper Configuration and Simulation***

The working principle of a linkage-based underactuated gripper is mostly the same as the elastomer-based gripper. As mentioned in section 3.3, multiple hinge-connected linkages

that can freely rotate among each other were confined by an elastomer glove. An important property of the linkage-based gripper is that the motion would be based on the rotation of the rigid linkages, rather than the continuous deformation as for the elastomer finger. Because of the hinge connection, the motion of the linkages would also be confined onto a plane, making it more resistant to environmental disturbances. Since the magnitude of the rotary motions depends on the deformation of the elastomer material, the gripper would still be flexible and adjustable.

The configuration of the underactuated gripper is based on the elastomer gripper previously developed. Figure 5.29 shows the CAD model of an assembled finger, where the transparent component is the elastomer glove and the solid portion is the skeleton made of rigid linkages.

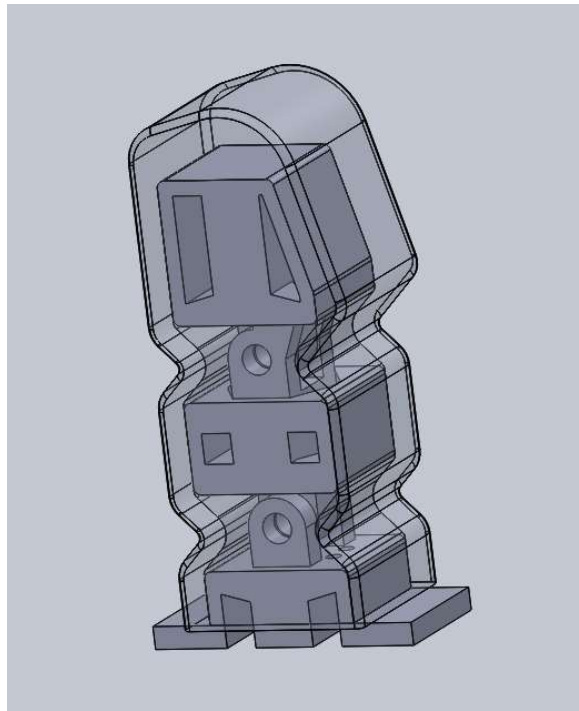


Figure 5.29 CAD model of the linkage-based finger

To simulate the behavior of the finger, a FE model was established as shown in Figure 5.30a. The elastomer component and the string were modelled the same way as in the previous section. Hinge connectors are used to build the rigid skeleton. Self-contact is



established on the external surface of the elastomer glove. Only half of the finger is modelled because of the geometrical symmetry.

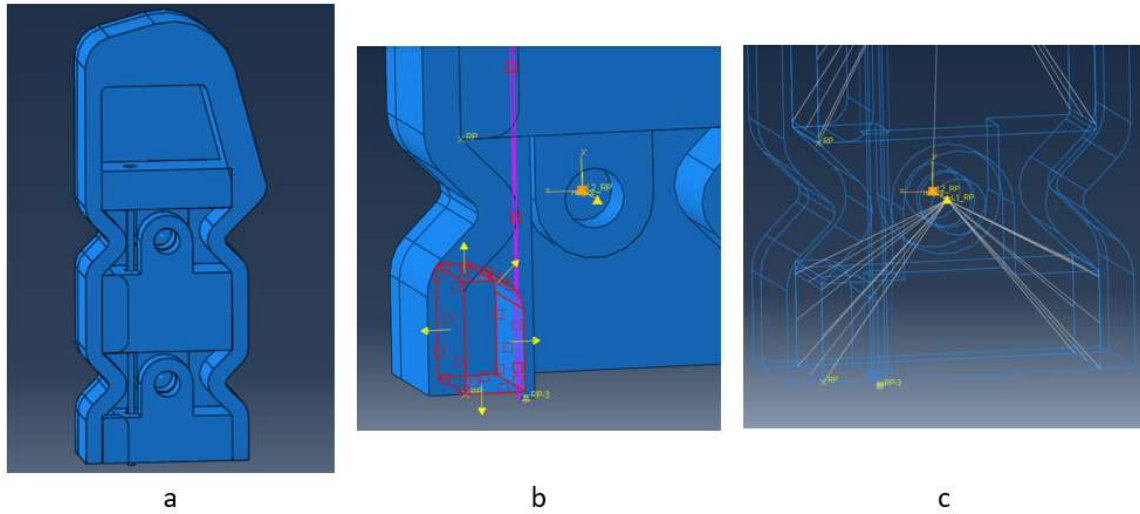


Figure 5.30 FE model of the linkage-based finger  
a. Assembly b. Contact pair c. Coupling constraint

One problem during the simulation is that the contact between the string and the rigid structures led to convergence problems. To solve the problem, the models of the linkages are treated only as display bodies and geometrical references. The contact between the string and the linkages are simulated by analytical rigid parts, as shown in Figure 5.30b. The rigid parts are coupling constrained to specific reference points so they would perform the same motion as the linkages. The cross-section of the string was changed to a square to simplify the model. The sliding between the inner surface of the glove and the linkages is very small due to its elasticity, so the contact among those regions is also simplified as coupling constraint to certain reference points (Figure 5.30c). The contact between the glove and the string is neglected.

A 7 mm displacement was applied at the bottom tip of the string. A reference point is created to record the motion of the fingertip. The model was run, and obtained deformation results are shown in Figure 5.31.

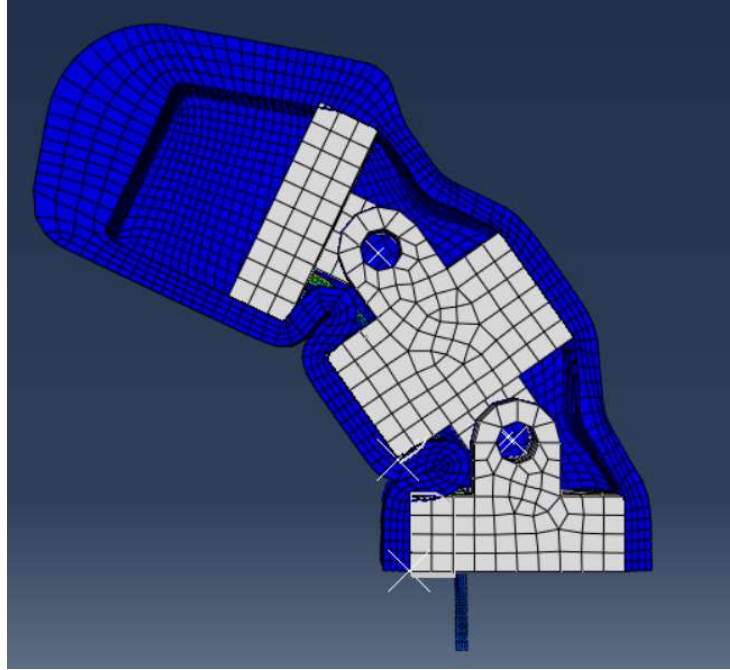


Figure 5.31 Deformation result

The force-displacement relation is obtained for both the string tip and the fingertip. Figure 5.32 shows the relation between the driving force and the displacement of the fingertip (force multiplied by four). Figure 5.33 shows the relationship between the driving force and the fingertip displacement on vertical direction. Figure 5.34 shows the trajectory of the fingertip.

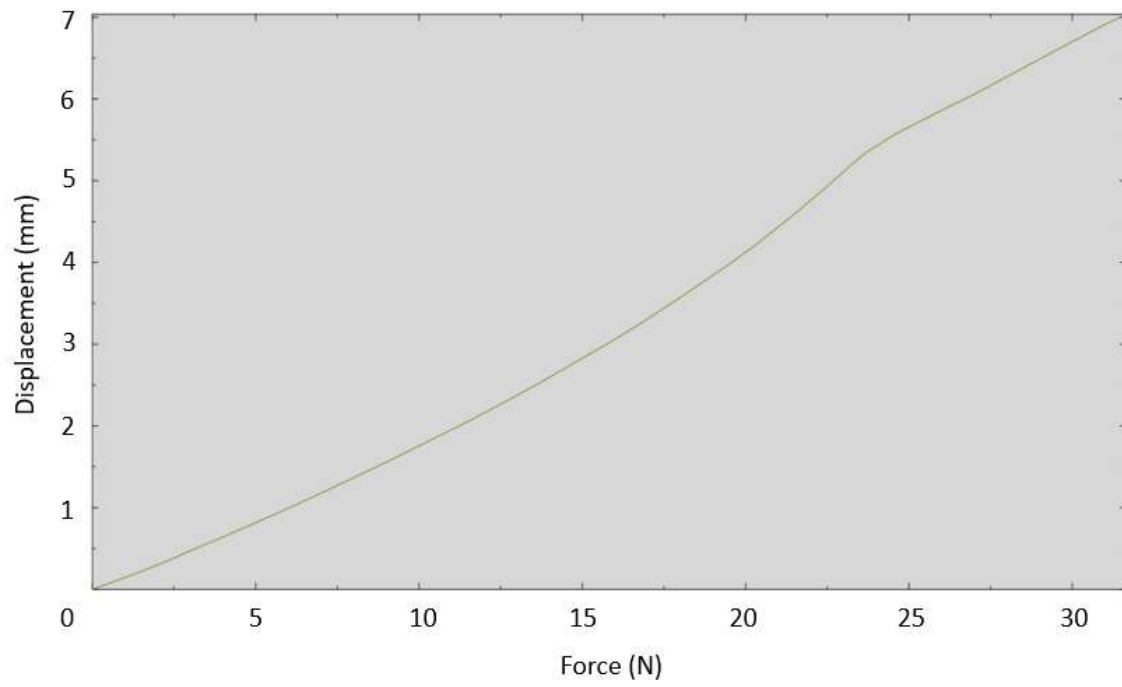


Figure 5.32 String tip displacement

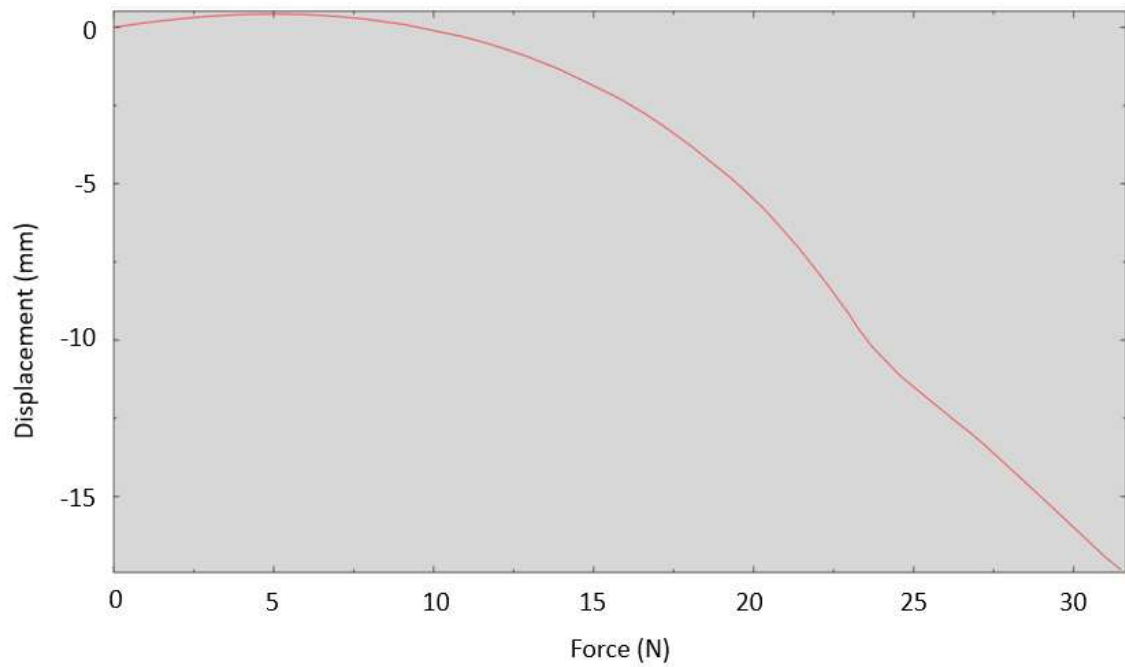


Figure 5.33 Fingertip displacement

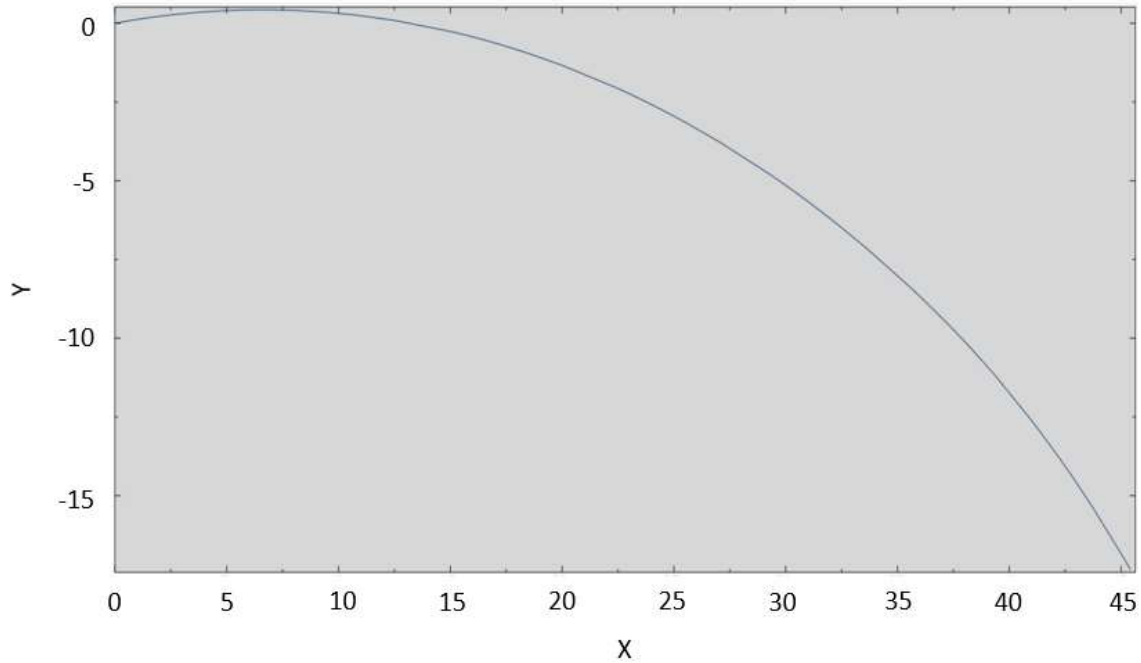


Figure 5.34 Fingertip trajectory

A similar model is built to simulate the gripping movement. It was found that the linkage-based gripper had different gripping behavior than the elastomer gripper previously investigated. Because the top section of the finger is supported by rigid structure, the rolling grip occurred with this two-gap configuration, as shown in Figure 5.35a.

One solution to solve this problem is to extend the top of the elastomer glove to make it compliant. This approach had been validated in the previous section and would not be further explored here. The other way to solve the problem is to introduce asymmetry of the finger assemble. If the top linkage of one finger was forbidden to rotate and the other finger is left free, the rolling grip can be avoided as the tip of the confined finger kept approximating the rolling tip during gripping. Simulation proves the feasibility of this solution, as shown in Figure 5.35b.

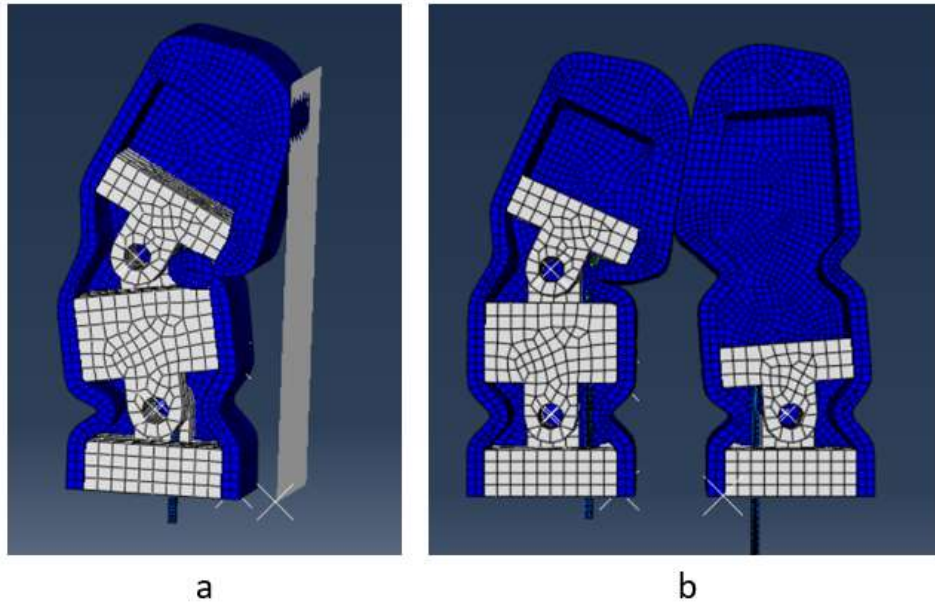


Figure 5.35 Gripping simulation

a. Rolling grip   b. Firm grip achieved by asymmetrical configuration

For the actual design, the prohibition of the rotation toward a certain direction can be achieved by the linkage geometry, as shown in Figure 5.36.

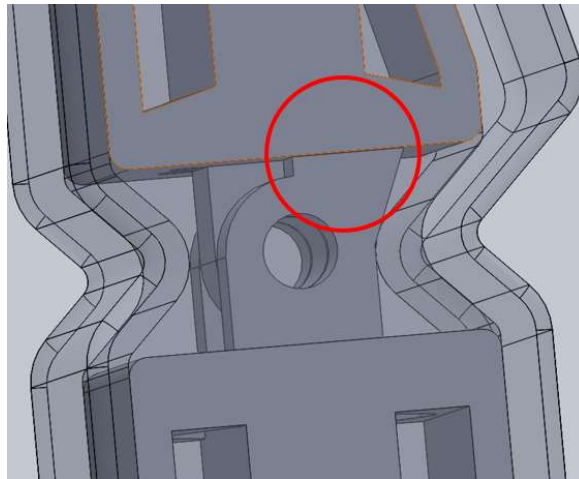


Figure 5.36 Structure to limit the rotary motion on certain direction

Because the working principle of this gripper is the same as the elastomer gripper previously developed, the gripping simulation and automation will not be redundantly

performed. The capability of this gripper is verified through prototyping and manual tests.

### ***5.2.2 Prototyping and Experiments***

A prototyping is fabricated using the similar methods as previously mentioned. The elastomer gloved is molded from a 3D printed mold set shown in Figure 5.37. The rigid linkages that form the skeleton can also be directly printed from CAD models. The linkages are connected by screw bolts.

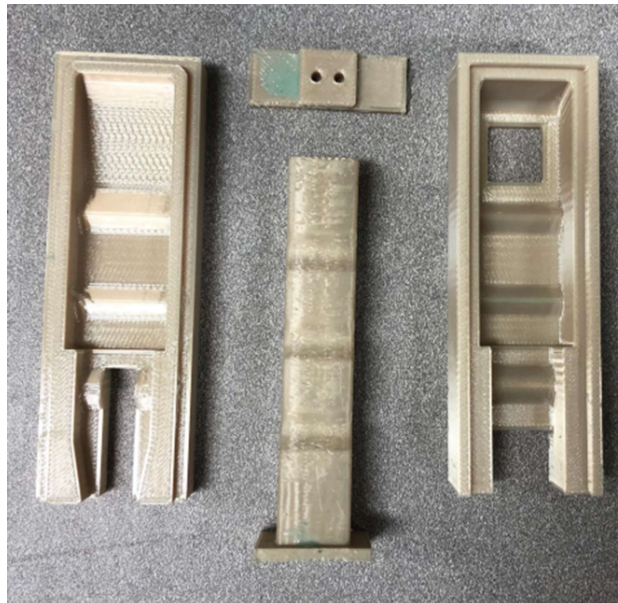


Figure 5.37 Mold set

After assembling, the final gripper is shown in Figure 5.38a. The following figures show the opening and gripping gestures respectively.

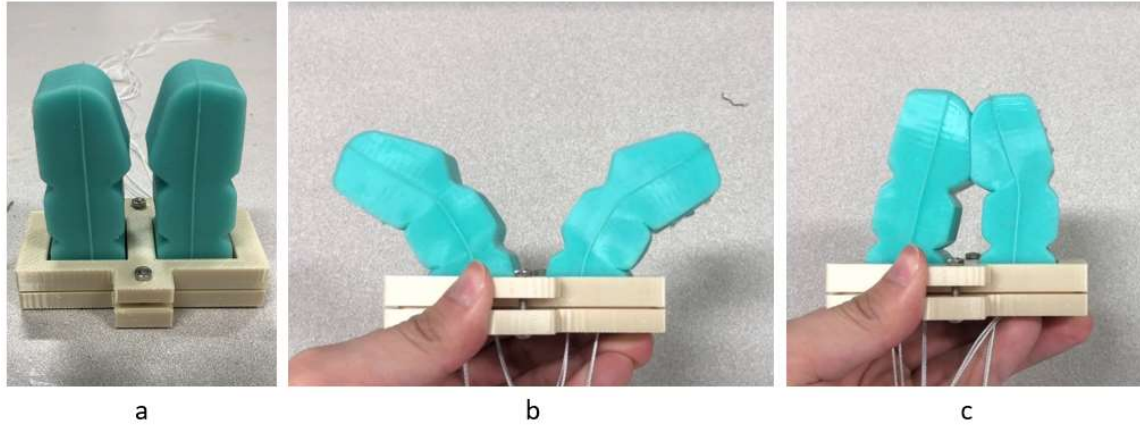


Figure 5.38 Gripper prototype

a. Rest gesture b. opening c. gripping

It took 4 hours and 26 minutes to print the mold set using ULT9085 and approximately an hour to remove the support material. Similarly, the time and effort spent on removing support material can be reduced with different materials. With the mold set prepared, it takes about an hour to mold one silicone glove. The rigid linkages and the gripper base together take 4 hours and 30 minutes to print and approximately 2 hours to remove the support material. The time consumption is summarized in Table 5.3. With the mold set prepared, it takes approximately 6 hours and 30 minutes to make one gripper prototype.

Table 5.3 Fabrication time

Reusable	Printing the mold set	4h26m
	Removing support material	1h
Molding silicone gloves		1h * 2
Printing the rigid components		1h15m * 2
Removing support material		2h
<b>Total</b>		11h56m (first time) / <b>6h30m</b>

The weight of the assembled gripper is 120 g. The size of this linkage-based gripper is shorter but wider than the elastomer-based gripper. The maximum contact area is measured to be approximately 500 mm<sup>2</sup>, much larger the elastomer-based gripper. Some important geometrical parameters are summarized in Table 5.4.



Table 5.4 Geometrical data

Size (mm)	Normal	Maximum open
	80 * 86 * 58	65 * 126 * 56
Weight (g)	120	
Maximum open angle (°)	180	
Maximum open length (mm)	126	
Maximum contact area (mm <sup>2</sup> )	500	

Likewise, this gripper prototype is tested using a force gauge. It requires approximately 31.36 N driving force to fully enclose the gripper. Figure 5.39 shows the relation between the displacement of the string tip and the driving force, comparing with the simulation data previously obtained from the FE model.

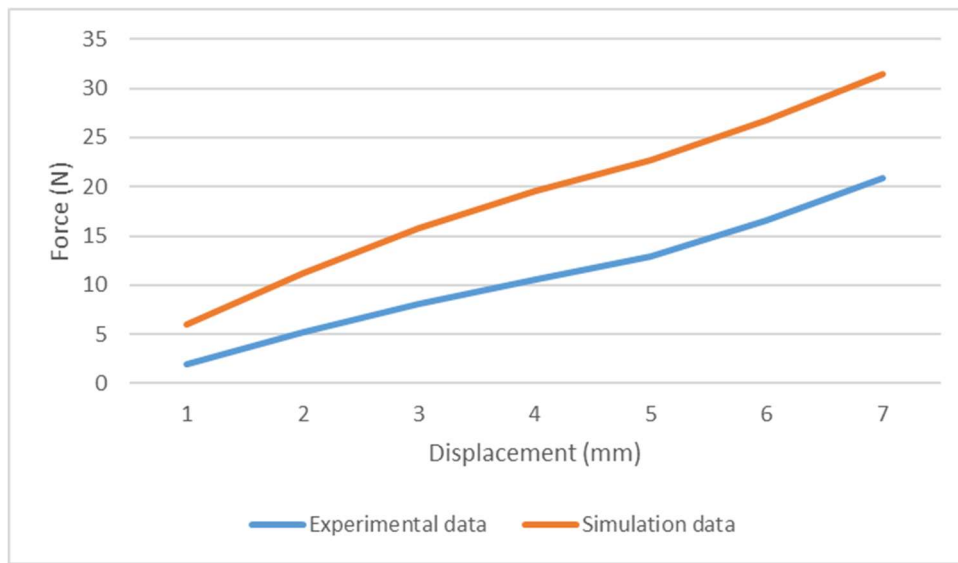


Figure 5.39 Comparison between experimental data and simulation data

The CC of the experimental data and the simulation data was calculated to be 0.9956. Though the FE model successfully simulated the motion pattern of the gripper, the force reaction is not as ideal as that of the elastomer-based gripper. The force response calculated from the simulation was larger than the experimental data, especially for higher deformation zone. This phenomenon could be caused by the multiple simplification strategies applied in the FE model.



As a conclusive discussion, this linkage-based underactuated gripper was proved to be a feasible solution for required tasks. The stiffness of this gripper was higher than the elastomer-based gripper, making it more resilient toward environmental disturbances. The FE model developed in this section can capture the motion patterns of this gripper configuration and can provide important insights for its structural design. However, more sophisticated modelling would be needed if detailed static or dynamic responses are desired.

## CHAPTER 6

### CONCLUSIONS AND FUTURE WORK

#### *6.1 Conclusions*

In this research, some characteristics of fabric handling operations using the clamping approach are quantitatively investigated. Three types of soft robotic grippers are designed, analyzed, and tested.

Experiments for fabric pick and place operations are performed with the YUMI ABB 14000 dual arm collaborative robot. The plain-woven carbon fiber fabric is selected as the specimen because of its wide range of applications in industry and its challenging properties regarding pick and place tasks.

The original rigid gripper showed its inability to reliably pick up the fabric mats. By reverse engineering the original gripper connected to the YUMI robot, a set of soft gloves made of silicone rubber are designed. When attached to the rigid gripper, the silicone gloves would serve as a compliant structure that can increase friction and prevent damage to the fabric ply. Experiments show that the silicone gloves can significantly improve the performance of the gripper by avoiding damage and reducing slippage. Furthermore, a second-generation silicone glove with a curved gripping tip is designed and tested. The curved gripping tip can increase the contact and provide a better result than the first-generation glove design.

Having been proved feasible, the grippers were applied in a more realistic pick and place experiment, which is using two grippers to pick up a rectangular fabric ply from a plain working surface and place it to a target area. The experiment characterizes general pick and place operation by the combination of the lifting, translating, rotating, and dropping movements. The performance of a picking strategy is evaluated by two criteria: the average displacement of multiple reference points on the fabric ply and the projected area after placement.

Through these experiments, it is shown that traditional rigid grippers with hard plastic surface cannot be used to pick up the workpiece without introducing large slippage or damaging the fabric. However, with the application of soft robotic grippers, it is proved feasible to reliably perform pick and place operation for fabric materials through a clamping approach. Therefore, this solution approach has practical implications.

It is discovered that various factors can affect the performance of a fabric handling solution, including gripping force, moving velocity, and toolpath planning. Lower gripping force and higher velocity lead to worse slippage and wrinkling results. While the slippage can be avoided by a firm gripping condition, the wrinkling magnitude after placement becomes more predictable but cannot be eliminated as the gripping condition is improved. Through appropriate picking positions and toolpath planning, accurate placement and the avoidance of wrinkling can be achieved. More research is required to explore this further.

As the experiments proved it feasible to perform basic fabric handling tasks using a simple 1-DOF gripper equipped with compliant structure, advanced movements such as picking up a fabric from a curved surface require a more flexible gripper configuration.

By mimicking the movements of the human hand when manually picking up fabric plies, two types of underactuated soft robotic grippers are developed. The first gripper design is based on elastomer fingers with gaps distributed on both sides of each finger. The elastomer finger is actuated by driving tendons inserted in pre-built slots that go through the gaps. When the tendons are pulled, the fingers bend toward the corresponding direction to either open or close the gripper. A driving mechanism is designed to actuate the tendons by a disc connected to a servo motor. The second gripper design is based on the principle of the elastomer-based gripper, but the finger is made of hinge-connected rigid linkages that are covered by an elastomer glove. The existence of the rigid skeleton can increase the stiffness of the linkage-based gripper and make it more resilient toward environmental disturbances. Both gripper configurations are simulated and prototyped.

The new technologies used here show great potentiality for relevant research. FEA

simulation is a crucial tool for the design of the soft robotic grippers. In this research, the simulation is performed in Abaqus. The most important parts are the simulation of the underactuated structure and the fabrics. The behavior of the underactuated structure, which is silicone rubber in this case, can be simulated using the hyperelastic material model. The simulation results can provide detailed insights regarding the force-deformation relationship and the influence of the gripper geometry, which can be used to develop or innovate the gripper configurations. The simulation of fabric material is also a challenging problem in relevant research. For the gripper design purpose, a simplified isotropic fabric model can be used to verify the functionality of a certain gripper configuration.

For both the prototyping and experiments, AM and overmolding processes are both important technologies. Through the FDM process, rigid components and molds can be directly printed from CAD models. With the mold set prepared, elastomer parts can be repeatedly fabricated by molding or overmolding.

To conclude, soft robotic grippers are proved to be a useful technology for the automation of fabric handling tasks. Sophisticated toolpath planning can ensure the performance of pick and place operations using the clamping approach. Advanced design and simulation tools, rapid prototyping technology, and collaborative robots provide new opportunities in relevant research.

## ***6.2 Limitations and Future Work***

There are several limitations and unfinished tasks in this research that should be further investigated in the future.

In this research, the study on the fabric behavior during pick and place operations only covers fundamental scenarios, and the methodology is limited to experimental research. Since the evaluation criteria developed in Chapter 4 has built a foundation for further studies, it is reasonable to expand the research domain to more complicated scenarios, i.e. fabric workpiece with complex geometry or challenging properties. Advanced tools such

as simulation and neural network or other machine learning approaches can be applied for sophisticated toolpath planning.

As for the soft robotic grippers, most of the FE models developed in this research are simplified in order to save computational costs. In some cases, the simplification strategies caused errors between the simulation results and experimental results. The most severe case is the force-deformation relationship of the linkage-based gripper, as described in Chapter 5. More accurate FE modelling strategies should be explored in the future. With the simulation model improved, the structure of the gripper can be further optimized. This will also provide insights for other similar research.

Finally, the automation and control of the gripper and the robot motions should be improved in the future. The control strategies developed in this research are open-looped. More intelligent control can be achieved by introducing contact sensors and proximity sensors. The improvement on automation will also make it available to perform experiments with the soft robotic gripper attached on the collaborative robot, which can provide helpful feedback for relevant research.

## REFERENCES

- [1] Shishoo, R. (Ed.). (2008). Textile advances in the automotive industry. Elsevier.
- [2] Fung, W., & Hardcastle, J. M. (2000). Textiles in automotive engineering (Vol. 13). Woodhead Publishing.
- [3] Heuss, R, Müller, N., Sintern, W., Starke, A., Tschiesner, A. (2012) Lightweight, heavy impact: How carbon fiber and other lightweight materials will develop across industries and specifically in automotive, Mckinsey & Company, editor.
- [4] Herrmann, A. S., Pabsch, A. R. N. O., & Kleineberg, M. A. R. K. U. S. (2001). SLI-RTM Fairings for Fairchild Dornier DO 328 Jet. In 22nd SAMPE Europe International Conference, Paris.
- [5] Strong, A. B. (2008). Fundamentals of composites manufacturing: materials, methods and applications. Society of Manufacturing Engineers.
- [6] Kordi, M. T., Husing, M., & Corves, B. (2007, September). Development of a multifunctional robot end-effector system for automated manufacture of textile preforms. In 2007 IEEE/ASME international conference on advanced intelligent mechatronics (pp. 1-6). IEEE.
- [7] Koustoumpardis, P. N., & Aspragathos, N. A. (2004). A review of gripping devices for fabric handling. *hand*, 19, 20.
- [8] Association of Workers' Compensation Boards of Canada (2016) Lost Time Claims in Canada, url: [http://awcbc.org/?page\\_id=14](http://awcbc.org/?page_id=14), viewed on 19 June 2018.
- [9] Hearle, J. W., Grosberg, P., & Backer, S. (1969). Structural mechanics of fibers, yarns, and fabrics.
- [10] Mazumdar, S., (2006) Composites Manufacturing (Materials, Product, and Process Engineering), CRC Press LLC, USA.
- [11] Miller, E. (1968). Textiles: properties and behaviour. Batsford.
- [12] Ceken, F., Kayacan, Ö., Özkurt, A., & Uğurlu, Ş. S. (2012). The electromagnetic shielding properties of some conductive knitted fabrics produced on single or double needle bed of a flat knitting machine. *Journal of the Textile Institute*, 103(9), 968-979.
- [13] Sölar, V., Öner, E., & Okur, A. (2013). Roughness and frictional properties of cotton and polyester woven fabrics.

- [14] Liao, X., Hu, J., Li, Y., Li, Q., & Wu, X. (2011). A review on fabric smoothness-roughness sensation studies. *Journal of Fiber Bioengineering & Informatics*, 4(2), 105-114.
- [15] Kawabata, G. (1982). The development of the objective measurement of fabric Handle, textile machinery society of Japan.
- [16] Mercier, A. A. (1930). Coefficient of friction of fabrics. *Bureau of Standards Journal of Research*, 5, 243-246.
- [17] Elder, H. M., & El-Tawashi, M. (1977). Some bending measurements on yarns.
- [18] Choudhary, A. K., & Bansal, P. (2017). Drape measurement technique using manikins with the help of image analysis. In *Manikins for Textile Evaluation* (pp. 173-195). Woodhead Publishing.
- [19] Kenkare, N., & May-Plumlee, T. (2005). Fabric drape measurement: A modified method using digital image processing. *Journal of Textile and Apparel, Technology and Management*, 4(3), 1-8.
- [20] Taylor, P. M., Wilkinson, A. J., Taylor, G. E., Gunner, M. B., & Palmer, G. S. (1990, August). Automated fabric handling problems and techniques. In *1990 IEEE International Conference on Systems Engineering* (pp. 367-370). IEEE.
- [21] Taylor, P. M. (1995). Presentation and gripping of flexible materials. *Assembly Automation*, 15(3), 33-35.
- [22] Muccilli, S. (2017). A Comparison of Force Demand Measurement Methods while operating a Lift-assist during Automotive Assembly.
- [23] Market available Cryo and Needle Grippers, [www.naiss.de](http://www.naiss.de), from NAISS GmbH Berlin.
- [24] Market available Needle Grippers, [www.eoat.net](http://www.eoat.net), from ATS Automation Technology Schwoppe Inc., Germany.
- [25] Market available Needle Grippers, [www.technosommer.com](http://www.technosommer.com), from Techno Sommer Automatic, USA.
- [26] Parker, J. K., Dubey, R., Paul, F. W., & Becker, R. J. (1983). Robotic fabric handling for automating garment manufacturing. *Journal of Engineering for Industry*, 105(1), 21-26.
- [27] Market available Vacuum and Needle Grippers, [www.polytex.ch](http://www.polytex.ch), from Polytex Switzerland.

- [28] Sarhadi, M., Nicholson, P. R., & Simmons, J. E. (1986). Advances in gripper technology for apparel manufacturing. *IMechE*, 372(86), 47-53.
- [29] Doulgeri, Z., Fahantidis, N., (2002) Picking up flexible pieces out of a bundle, *IEEE robotics & automation magazine*, 9/2: 919.
- [30] Ono, E., Ichijo, H., & Aisaka, N. (1992). Flexible robotic hand for handling fabric pieces in garment manufacture. *International Journal of Clothing Science and Technology*, 4(5), 16-23.
- [31] Ono, E., Okabe, H., Akami, H., & Aisaka, N. (1991). Robot hand with a sensor for cloth handling. *Journal of the textile machinery society of Japan*, 37(1), 14-24.
- [32] Seesselberg, H. A. (1990). A challenge to develop fully automated garment manufacturing. In *Sensory robotics for the handling of limp materials* (pp. 53-67). Springer, Berlin, Heidelberg.
- [33] Taylor, P. M., Pollett, D. M., & Griebner, M. T. (1996). Pinching grippers for the secure handling of fabric panels. *Assembly Automation*, 16(3), 16-21.
- [34] Market available Clamp Grippers (Walton Picker), [www.pickrobotics.com](http://www.pickrobotics.com), from PickRobotics Inc., USA.
- [35] Karakerezis, A., Ippolito, M., Doulgeri, Z., Rizzi, C., Cugini, C., & Petridis, V. (1994, October). Robotic handling for flat non-rigid materials. In *Proceedings of IEEE International Conference on Systems, Man and Cybernetics* (Vol. 1, pp. 937-946). IEEE.
- [36] Paul, F. W., & Dixon, M. W. (1992). Advanced automation for shirt-collar manufacturing. *International Journal of Clothing Science and Technology*, 4(2-3), 26-33.
- [37] Market available Clamp Grippers (Walton Picker), [www.pickrobotics.com](http://www.pickrobotics.com), from PickRobotics Inc., USA.
- [38] Le, T., Jilich, M., Landini, A., Zoppi, M., Zlatanov, D., Molfinio, R., (2013) On the development of a specialized flexible gripper for garment handling, *Journal of Automation and Control Engineering*, 1/3: 255-259.
- [39] Costo, S., G. Altamura, L. E. Bruzzzone, R. M. Molfinio, Zoppi, M. (2002) Design of a re-configurable gripper for the fast robotic picking and handling of limp sheets, *Proceedings of the 33rd International Symposium on Robotics*.



- [40] Kolluru, R., Valavanis, K. P., Steward, A., & Sonnier, M. J. (1995). A flat surface robotic gripper for handling limp material. *IEEE Robotics & Automation Magazine*, 2(3), 19-26.
- [41] Hebert, T. M., Valavanis, K. P., & Kolluru, R. (1997, April). A robotic gripper system for limp material manipulation: Hardware and software development and integration. In *Proceedings of International Conference on Robotics and Automation* (Vol. 1, pp. 15-21). IEEE.
- [42] Tsourveloudis, N. C., Kolluru, R., Valavanis, K. P., & Gracanin, D. (2000). Suction control of a robotic gripper: A neuro-fuzzy approach. *Journal of Intelligent and Robotic Systems*, 27(3), 215-235.
- [43] Kolluru, R., Valavanis, K. P., & Hebert, T. M. (1998). Modeling, analysis, and performance evaluation of a robotic gripper system for limp material handling. *IEEE Transactions on Systems, Man, and Cybernetics, Part B (Cybernetics)*, 28(3), 480-486.
- [44] Seliger, G., & Stephan, J. (1998). Flexible garment handling with adaptive control strategies. *Proceedings of the 29th ISR*, 4(27), 5.
- [45] Stephan, J., & Seliger, G. (1999). Handling with ice—the cryo-gripper, a new approach. *Assembly Automation*, 19(4), 332-337.
- [46] Ozcelik, B., & Erzincanli, F. (2002). A non-contact end-effector for the handling of garments. *Robotica*, 20(4), 447-450.
- [47] Ozcelik, B., Erzincanli, F., & Findik, F. (2003). Evaluation of handling results of various materials using a non-contact end-effector. *Industrial Robot: An International Journal*, 30(4), 363-369.
- [48] Monkman, G. J. (1992). Compliant robotic devices, and electroadhesion. *Robotica*, 10(2), 183-185.
- [49] Monkman, G. J., Taylor, P. M., & Farnworth, G. J. (1989). Principles of electroadhesion in clothing robotics. *International Journal of Clothing Science and Technology*, 1(3), 14-20.
- [50] Taylor, P. M., Monkman, G. J., & Taylor, G. E. (1988, April). Electrostatic grippers for fabric handling. In *Proceedings. 1988 IEEE International Conference on Robotics and Automation* (pp. 431-433). IEEE.
- [51] Fleischer, J., Ochs, A., Förster, F., (2013) Gripping Technology for Carbon Fibre Material. *CIRP International conference on competitive manufacturing*, 65-71.

- [52] Fleischer, J., Förster, F. & Crispieri, N. (2014) Intelligent gripper technology for the handling of carbon fiber material, *Production Engineering*, 8: 691.
- [53] Koustoumpardis, P., Nastos, K., Aspragathos, N. (2014) Underactuated 3-finger robotic gripper for grasping fabrics, *Robotics in Alpe-Adria-Danube Region*, 23rd International Conference, 1-8.
- [54] Murakami, K., & Hasegawa, T. (2004). Novel fingertip equipped with soft skin and hard nail for dexterous multi-fingered robotic manipulation. *Journal of the Robotics Society of Japan*, 22(5), 616-624.
- [55] Costo, S., G. Altamura, L. E. Bruzzone, R. M. Molfino, Zoppi, M. (2002) Design of a re-configurable gripper for the fast robotic picking and handling of limp sheets, *Proceedings of the 33rd International Symposium on Robotics*.
- [56] Ragunathan, S., L. Karunamoorthy, (2008) Modular reconfigurable robotic gripper for limp material handling in garment industries, *International journal of robotics & automation*, 23/4: 213.
- [57] Zimmer, P., (1977) Flat stencil for imprinting textile fabrics, U.S. Patent 4,023,488, issued May 17, 1977.
- [58] Flixeder, S., Tobias G., Kug, A., (2017) Force-based cooperative handling and lay-up of deformable materials: Mechatronic design, modeling, and control of a demonstrator, *Mechatronics* 47: 246-261.
- [59] Kordi, M., Tarsha, M. Husing, Corves, B., (2007) Development of a multifunctional robot end-effector system for automated manufacture of textile preforms, In conference on Advanced intelligent mechatronics, 2007 IEEE/ASME, 1-6.
- [60] Rus, D., & Tolley, M. T. (2015). Design, fabrication and control of soft robots. *Nature*, 521(7553), 467-475.
- [61] Trivedi, D., Rahn, C. D., Kier, W. M., & Walker, I. D. (2008). Soft robotics: Biological inspiration, state of the art, and future research. *Applied bionics and biomechanics*, 5(3), 99-117.
- [62] Kim, S., Laschi, C., & Trimmer, B. (2013). Soft robotics: a bioinspired evolution in robotics. *Trends in biotechnology*, 31(5), 287-294.
- [63] Laschi, C., & Cianchetti, M. (2014). Soft robotics: new perspectives for robot bodyware and control. *Frontiers in bioengineering and biotechnology*, 2, 3.

- [64] Birglen, L., Gosselin, C., & Laliberté, T. (2008). Underactuated robotic hands(Vol. 40, p. 13). Berlin: Springer.
- [65] Shintake, J., Cacucciolo, V., Floreano, D., & Shea, H. (2018). Soft robotic grippers. *Advanced Materials*, 30(29), 1707035.
- [66] Manti, M., Hassan, T., Passetti, G., D'Elia, N., Laschi, C., & Cianchetti, M. (2015). A bioinspired soft robotic gripper for adaptable and effective grasping. *Soft Robotics*, 2(3), 107-116.
- [67] Nagase, J. Y., Wakimoto, S., Satoh, T., Saga, N., & Suzumori, K. (2011). Design of a variable-stiffness robotic hand using pneumatic soft rubber actuators. *Smart Materials and Structures*, 20(10), 105015.
- [68] Rateni, G., Cianchetti, M., Ciuti, G., Mencias, A., & Laschi, C. (2015). Design and development of a soft robotic gripper for manipulation in minimally invasive surgery: a proof of concept. *Meccanica*, 50(11), 2855-2863.
- [69] Ilievski, F., Mazzeo, A. D., Shepherd, R. F., Chen, X., & Whitesides, G. M. (2011). Soft robotics for chemists. *Angewandte Chemie International Edition*, 50(8), 1890-1895.
- [70] Yap, H. K., Ng, H. Y., & Yeow, C. H. (2016). High-force soft printable pneumatics for soft robotic applications. *Soft Robotics*, 3(3), 144-158.
- [71] Hao, Y., Wang, T., Ren, Z., Gong, Z., Wang, H., Yang, X., ... & Wen, L. (2017). Modeling and experiments of a soft robotic gripper in amphibious environments. *International Journal of Advanced Robotic Systems*, 14(3), 1729881417707148.
- [72] Brown, E., Rodenberg, N., Amend, J., Mozeika, A., Steltz, E., Zakin, M. R., ... & Jaeger, H. M. (2010). Universal robotic gripper based on the jamming of granular material. *Proceedings of the National Academy of Sciences*, 107(44), 18809-18814.
- [73] Rogers, J. A., Someya, T., & Huang, Y. (2010). Materials and mechanics for stretchable electronics. *science*, 327(5973), 1603-1607.
- [74] Hammock, M. L., Chortos, A., Tee, B. C. K., Tok, J. B. H., & Bao, Z. (2013). 25th anniversary article: the evolution of electronic skin (e-skin): a brief history, design considerations, and recent progress. *Advanced materials*, 25(42), 5997-6038.

- [75] Kaltenbrunner, M., Sekitani, T., Reeder, J., Yokota, T., Kuribara, K., Tokuhara, T., ... & Bauer, S. (2013). An ultra-lightweight design for imperceptible plastic electronics. *Nature*, 499(7459), 458-463.
- [76] Ballier, F. J. (2019). Systematic Gripper Arrangement for a Handling Device in Lightweight Production Processes. Shaker.
- [77] Alebooyeh, M., Wang, B., Urbanic, R. J., Djuric, A., & Kalami, H. (2019). Investigating Collaborative Robot Gripper Configurations for Simple Fabric Pick and Place Tasks (No. 2019-01-0699). SAE Technical Paper.
- [78] Askin, R. G., & Standridge, C. R. (1993). Modeling and analysis of manufacturing systems. John Wiley & Sons Inc.
- [79] Peshkin M., Edward J. C., CoBots (1999) *Industrial Robot*, 26/5: 335-341.
- [80] Anvaripour, M., Saif, M., & Ahmadi, M. (2016, July). A novel approach to provide safe indoor industrial environment. In 2016 International Conference on High Performance Computing & Simulation (HPCS) (pp. 544-548). IEEE.
- [81] Djuric, A. M., Urbanic, R. J., & Rickli, J. L. (2016). A framework for collaborative robot (CoBot) integration in advanced manufacturing systems. *SAE International Journal of Materials and Manufacturing*, 9(2), 457-464.
- [82] Cho, K. J., Koh, J. S., Kim, S., Chu, W. S., Hong, Y., & Ahn, S. H. (2009). Review of manufacturing processes for soft biomimetic robots. *International Journal of Precision Engineering and Manufacturing*, 10(3), 171-181.
- [83] Fabricated, L. H., & Kurman, M. (2013). The New World of 3D Printing.
- [84] Cham, J. G., Bailey, S. A., Clark, J. E., Full, R. J., & Cutkosky, M. R. (2002). Fast and robust: Hexapedal robots via shape deposition manufacturing. *The International Journal of Robotics Research*, 21(10-11), 869-882.
- [85] Xia, Y., & Whitesides, G. M. (1998). Soft lithography. *Annual review of materials science*, 28(1), 153-184.
- [86] Khayat, A., Urbanic, R. J., Farias, A., Schuelke-Leech, B. A., (2018), Development of Reconfigurable Thoracentesis Training Mannequins, CAD and A, in-press
- [87] Kalami, H., Urbanic, R. J., (2018), A Hybrid Manufacturing Approach for Fabrication of Low Volume High Temperature Thermoplastic/Thermoset Material Molds, Proceedings of The Canadian Society for Mechanical Engineering International Congress 2018

- [88] Mooney, M. (1940) A theory of large elastic deformation. *J. Appl. Phys.* 11, 582–592.
- [89] Rivlin, R. S. (1948) Large elastic deformations of isotropic materials. iv: Further developments of the general theory. *Philos. Trans. R. Soc. Lond.* A241, 379.
- [90] Ogden, R. W. (1984) *Non-Linear Elastic Deformations*. Dover Publications Inc., Mineola, NY, USA.
- [91] Holzapfel, G. A. (2000) *Nonlinear Solid Mechanics*. John Wiley and Sons, New York.
- [92] Veronda, D. R. and Westmann, R. A. (1970) Mechanical characterization of skin-finite deformations. *J. Biomech.* 3, 111–124.
- [93] Fung, Y. C. (1993) *BIOMECHANICS – Mechanical Properties of Living Tissues*, 2nd edn. Springer-Verlag Inc., New York.
- [94] Martins, P. A. L. S., Natal Jorge, R. M., & Ferreira, A. J. M. (2006). A comparative study of several material models for prediction of hyperelastic properties: Application to silicone - rubber and soft tissues. *Strain*, 42(3), 135-147.
- [95] Korochkina, T. V., Jewell, E. H., Claypole, T. C., & Gethin, D. T. (2008). Experimental and numerical investigation into nonlinear deformation of silicone rubber pads during ink transfer process. *Polymer Testing*, 27(6), 778-791.
- [96] Monkman, G. J. (1995). Robot grippers for use with fibrous materials. *The International journal of robotics research*, 14(2), 144-151.
- [97] Gent, A. N. (2012). *Engineering with rubber: how to design rubber components*. Carl Hanser Verlag GmbH Co KG.
- [98] Jauffrès, D., Sherwood, J. A., Morris, C. D., & Chen, J. (2010). Discrete mesoscopic modeling for the simulation of woven-fabric reinforcement forming. *International journal of material forming*, 3(2), 1205-1216.
- [99] Nasri, M., Garnier, C., Abbassi, F., Labanieh, A. R., Dalverny, O., & Zghal, A. (2019). Hybrid approach for woven fabric modelling based on discrete hypoelastic behaviour and experimental validation. *Composite Structures*, 209, 992-1004.
- [100] Diehl, T., Dixon, R. D., Lamontia, M. A., & Hanks, J. A. (2003). The development and use of a robust modeling approach for predicting structural

- performance of woven fabric using ABAQUS. In 2003 ABAQUS Users' Conference.
- [101] Eischen, J. W., Deng, S., & Clapp, T. G. (1996). Finite-element modeling and control of flexible fabric parts. *IEEE Computer Graphics and Applications*, 16(5), 71-80.
- [102] Kang, S., & Im, S. (1997). Finite element analysis of wrinkling membranes.
- [103] Sun, B., & Zhang, X. (2019, August). A New Electrostatic Gripper for Flexible Handling of Fabrics in Automated Garment Manufacturing. In 2019 IEEE 15th International Conference on Automation Science and Engineering (CASE) (pp. 879-884). IEEE.
- [104] Rachik, M., Schmidtt, F., Reuge, N., Le Maoult, Y., & Abbeé, F. (2001). Elastomer biaxial characterization using bubble inflation technique. II: Numerical investigation of some constitutive models. *Polymer Engineering & Science*, 41(3), 532-541.

## APPENDICES

### *Appendix A: Engineering Drawing of the YUMI Robot Arm*

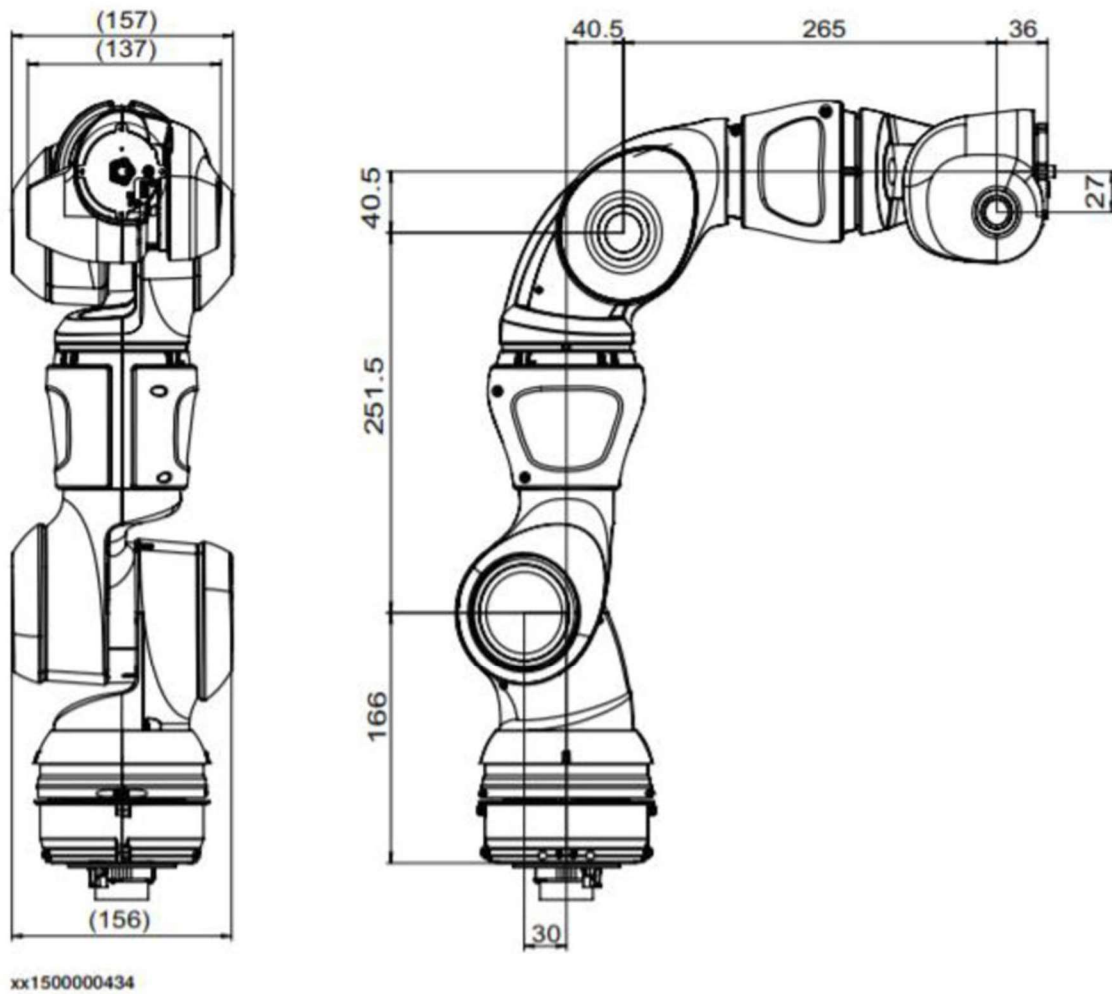


Figure A.1 Engineering drawing of the YUMI robot arm

## Appendix B: Experimental Data for Pick and Place Tests

The original test data is the coordinates of reference points after every placement. The displacement and projection area are calculated from the coordinates.

Table B.1 Data for plain picking

			test 1		test 2		test 3		average
			X	Y	X	Y	X	Y	
One arm	coordinates of the projected polygon	point 1	32.2	33.4	17.4	26.2	19.4	32.0	
		point 2	61.6	35.4	34.2	30.2	35.8	32.0	
		point 3	67.8	27.8	39.0	25.6	41.4	26.8	
		point 4	36.8	3.4	52.4	32.2	50.5	28.8	
		point 5	16.7	23.2	62.0	26.8	60.2	23.4	
		point 6			35.4	3.0	47.8	7.2	
		point 7					25.8	4.0	
	projection area		895.0		619.0		767.5		760.5
Dual arm plain	coordinates of the projected polygon	point 1	11.3	33.8	10.4	34.2	12.8	30.8	
		point 2	65.8	35.0	64.6	36.4	15.4	32.2	
		point 3	64.2	19.7	66.2	20.6	44.8	34.2	
		point 4	47.4	12.0	19.6	7.8	64.7	25.2	
		point 5	19.8	7.4	13.0	12.2	67.2	9.1	
		point 6	30.6	11.6			14.5	7.2	
		point 7					12.8	8.4	
	projection area		961.0		1170.8		1249.1		1127.0
	coordinates of the location reference points	point 1 BR	64.2	19.7	66.2	20.6	67.2	9.1	
		point 2 BL	14.2	6.2	13.6	5.8	12.8	7.0	
		point 3 TR	65.8	35.0	64.6	36.4	64.7	25.2	
		point 4 TL	11.3	33.8	10.4	34.2	12.8	32.0	
	displacements of the location reference points	point 1		13.2		13.8		2.3	
		point 2		2.2		1.6		1.3	
		point 3		0.5		1.7		10.4	
		point 4		1.0		1.2		3.1	
	average		4.2		4.6		4.3		4.4



Table B.2 Data for pre folded picking

			test 1		test 2		test 3		average
			X	Y	X	Y	X	Y	
1 mm pre-folding	coordinates of the projected polygon	point 1	11.8	33.6	11.4	33.6	11.8	34.8	
		point 2	65.5	34.6	65.2	34.8	65.8	34.6	
		point 3	66.6	8.2	65.6	8.4	65.5	8.0	
		point 4	14.8	7.2	23.0	7.0	34.0	7.2	
		point 5	12.2	9.4	12.2	12.0	11.8	11.2	
	projection area		1425.6		1399.7		1423.7		1416.3
	coordinates of the location reference points	point 1 BR	66.6	8.2	65.6	8.4	65.5	8.0	
		point 2 BL	12.4	7.0	12.4	5.8	11.8	11.2	
		point 3 TR	65.5	34.6	65.2	34.8	65.8	34.6	
		point 4 TL	11.8	33.6	11.4	33.6	11.8	34.8	
	displacements of the location reference points	point 1	1.5		2.1		1.9		
		point 2	1.1		0.4		5.2		
		point 3	1.0		1.1		0.9		
		point 4	1.3		1.2		0.4		
	average		1.2		1.2		2.1		1.5
2 mm pre-folding	coordinates of the projected polygon	point 1	12.4	34.2	12.0	33.4	11.6	33.5	
		point 2	65.8	34.5	65.4	34.4	65.5	34.4	
		point 3	66.8	8.6	65.8	7.8	65.8	7.8	
		point 4	12.6	7.0	12.4	7.2	12.0	7.5	
	projection area		1429.0		1410.1		1416.5		1418.5
	coordinates of the location reference points	point 1 BR	66.8	8.6	65.8	7.8	65.8	7.8	
		point 2 BL	12.6	7.0	12.4	7.2	12.0	7.5	
		point 3 TR	65.8	34.5	65.4	34.4	65.5	34.4	
		point 4 TL	12.4	34.2	12.0	33.4	11.6	33.5	
	displacements of the location reference points	point 1	1.8		1.6		1.6		
		point 2	1.2		1.3		1.5		
		point 3	1.0		1.3		1.2		
		point 4	1.2		1.5		1.3		
	average		1.3		1.4		1.4		1.4
	3 mm pre-folding	coordinates of the projected polygon	point 1	13.0	33.5	13.0	33.5	13.0	33.4
point 2			64.8	34.2	65.2	35.0	65.6	35.0	
point 3			65.4	7.3	65.8	8.0	65.7	7.8	
point 4			13.0	7.8	13.5	8.0	13.0	7.8	
projection area		1370.3		1372.0		1389.9		1377.4	
coordinates of the location reference points		point 1 BR	65.4	7.3	65.8	8.0	65.7	7.8	
		point 2 BL	13.0	7.8	13.5	8.0	13.0	7.8	
		point 3 TR	64.8	34.2	65.2	35.0	65.6	35.0	
		point 4 TL	13.0	33.5	13.0	33.5	13.0	33.4	
displacements of the location reference points		point 1	1.7		1.7		1.6		
		point 2	2.1		2.5		2.1		
		point 3	1.8		0.9		0.6		
		point 4	2.1		2.1		2.1		
average		1.9		1.8		1.6		1.8	

Table B.3 Data for auto-jammed picking

			test 1		test 2		test 3		average
			X	Y	X	Y	X	Y	
1 mm auto-jamming	coordinates of the projected polygon	point 1	10.8	34.4	11.8	34.0	11.8	34.0	
		point 2	65.4	34.6	65.6	34.2	65.8	34.5	
		point 3	67.2	8.2	67.6	7.7	68.2	8.2	
		point 4	12.0	7.4	12.4	7.4	12.4	7.0	
	projection area		1466.6		1447.3		1464.4		1459.4
	coordinates of the location reference points	point 1 BR	67.2	8.2	67.6	7.7	68.2	8.2	
		point 2 BL	12.0	7.4	12.4	7.4	12.4	7.0	
		point 3 TR	65.4	34.6	65.6	34.2	65.8	34.5	
		point 4 TL	10.8	34.4	11.8	34.0	11.8	34.0	
	displacements of the location reference points	point 1	1.4		1.1		1.8		
		point 2	1.4		1.5		1.1		
		point 3	1.1		1.4		1.0		
		point 4	0.7		0.9		0.9		
		average	1.2		1.2		1.2		1.2
2 mm auto-jamming	coordinates of the projected polygon	point 1	11.6	34.0	11.6	34.0	11.4	34.0	
		point 2	65.8	34.4	65.8	34.4	65.6	34.4	
		point 3	67.0	8.0	66.2	8.0	66.4	8.4	
		point 4	12.6	7.2	11.8	7.3	12.2	7.4	
	projection area		1445.0		1441.8		1426.0		1437.6
	coordinates of the location reference points	point 1 BR	67.0	8.0	66.2	8.0	66.4	8.4	
		point 2 BL	12.6	7.2	11.8	7.3	12.2	7.4	
		point 3 TR	65.8	34.4	65.8	34.4	65.6	34.4	
		point 4 TL	11.6	34.0	11.6	34.0	11.4	34.0	
	displacements of the location reference points	point 1	1.2		1.4		1.7		
		point 2	1.3		1.3		1.4		
		point 3	1.1		1.1		1.2		
		point 4	0.8		0.8		0.8		
		average	1.1		1.2		1.3		1.2
3 mm auto-jamming	coordinates of the projected polygon	point 1	11.6	34.0	11.4	34.0	11.4	33.8	
		point 2	65.6	34.8	65.5	34.5	65.8	34.4	
		point 3	66.2	8.4	66.5	8.6	66.5	8.4	
		point 4	11.9	7.4	11.8	7.2	11.8	7.5	
	projection area		1435.4		1434.1		1426.9		1432.1
	coordinates of the location reference points	point 1 BR	66.2	8.4	66.5	8.6	66.5	8.4	
		point 2 BL	11.9	7.4	11.8	7.2	11.8	7.5	
		point 3 TR	65.6	34.8	65.5	34.5	65.8	34.4	
		point 4 TL	11.6	34.0	11.4	34.0	11.4	33.8	
	displacements of the location reference points	point 1	1.8		1.9		1.7		
		point 2	1.4		1.2		1.5		
		point 3	0.8		1.1		1.1		
		point 4	0.8		0.8		1.0		
		average	1.2		1.3		1.3		1.3

Table B.4 Data for pick and place operations with spatial transferring

			test 1		test 2		test 3		average
			X	Y	X	Y	X	Y	
2 mm auto-jamming	coordinates of the projected polygon	point 1	10.8	33.5	11.6	33.4	12.0	34.0	
		point 2	65.2	34.2	65.6	34.0	43.0	34.5	
		point 3	66.6	9.0	67.1	8.5	65.8	30.4	
		point 4	12.4	7.2	12.9	7.0	67.0	8.0	
		point 5					12.5	6.8	
	projection area		1400.1		1405.4		1411.2		1405.6
	coordinates of the location reference points	point 1 BR	66.6	9.0	67.1	8.5	67.0	8.0	
		point 2 BL	12.4	7.2	12.9	7.0	12.5	6.8	
		point 3 TR	65.2	34.2	65.6	34.0	65.8	30.4	
		point 4 TL	10.8	33.5	11.6	33.4	12.0	34.0	
	displacements of the location reference points	point 1	2.2		1.7		1.2		
		point 2	1.3		1.3		0.9		
		point 3	1.5		1.6		5.1		
		point 4	1.4		1.4		1.0		
		average	1.6		1.5		2.1		
10 mm auto-jamming	coordinates of the projected polygon	point 1	11.2	33.0	11.4	34.0	12.0	33.2	
		point 2	65.5	34.0	66.2	34.2	65.8	33.8	
		point 3	67.5	8.5	66.2	8.2	67.5	9.4	
		point 4	13.0	7.2	39.0	7.0	13.2	7.6	
		point 5			12.5	14.2			
	projection area		1397.5		1354.6		1353.0		1368.4
	coordinates of the location reference points	point 1 BR	67.5	8.5	66.2	8.2	67.5	9.4	
		point 2 BL	13.0	7.2	12.5	14.2	13.2	7.6	
		point 3 TR	65.5	34.0	66.2	34.2	65.8	33.8	
		point 4 TL	11.2	33.0	11.4	34.0	12.0	33.2	
	displacements of the location reference points	point 1	1.8		1.6		2.6		
		point 2	1.6		8.2		2.0		
		point 3	1.6		1.3		1.7		
		point 4	1.8		0.8		1.7		
		average	1.7		3.0		2.0		
Side picking	coordinates of the projected polygon	point 1	12.4	34.4	11.8	34.4	12.0	34.4	
		point 2	65.4	34.7	65.8	35.0	66.0	35.5	
		point 3	67.0	6.3	66.8	6.4	67.0	6.8	
		point 4	12.4	6.0	12.4	6.0	12.6	5.8	
	projection area		1528.2		1545.1		1553.7		1542.3
	coordinates of the location reference points	point 1 BR	67.0	6.3	66.8	6.4	67.0	6.8	
		point 2 BL	12.4	6.0	12.4	6.0	12.6	5.8	
		point 3 TR	65.4	34.7	65.8	35.0	66.0	35.5	
		point 4 TL	12.4	34.4	11.8	34.4	12.0	34.4	
	displacements of the location reference points	point 1	0.5		0.4		0.0		
		point 2	0.4		0.4		0.6		
		point 3	1.0		0.5		0.0		
		point 4	1.1		0.6		0.7		
		average	0.7		0.5		0.3		

## VITA AUCTORIS

NAME: Bowen Wang

PLACE OF BIRTH: Ankang, Shaanxi, China

YEAR OF BIRTH: 1994

EDUCATION: Central South University, B.Sc., Changsha, China, 2013-2017

University of Windsor, M.A.Sc., Windsor, ON, 2017-2020